

Fig 2



## OAR-901 SATELLITE THERMAL TEST

N. C. Latture

ARO, Inc.

October 1971

Approved for public release; distribution unlimited.

**VON KÁRMÁN GAS DYNAMICS FACILITY  
ARNOLD ENGINEERING DEVELOPMENT CENTER  
AIR FORCE SYSTEMS COMMAND  
ARNOLD AIR FORCE STATION, TENNESSEE**

PROPERTY OF U.S. AIR FORCE  
AEDC LIBRARY  
F40600-72-C-0003

# ***NOTICES***

When U. S. Government drawings specifications, or other data are used for any purpose other than a definitely related Government procurement operation, the Government thereby incurs no responsibility nor any obligation whatsoever, and the fact that the Government may have formulated, furnished, or in any way supplied the said drawings, specifications, or other data, is not to be regarded by implication or otherwise, or in any manner licensing the holder or any other person or corporation, or conveying any rights or permission to manufacture, use, or sell any patented invention that may in any way be related thereto.

Qualified users may obtain copies of this report from the Defense Documentation Center.

References to named commercial products in this report are not to be considered in any sense as an endorsement of the product by the United States Air Force or the Government.

OAR-901 SATELLITE THERMAL TEST

N. C. Latture  
ARO, Inc.

Approved for public release; distribution unlimited.

## FOREWORD

The work reported herein was done at the request of the Air Force Cambridge Research Laboratory (AFCRL), Air Force Systems Command (AFSC), under Program Element 63404F. The satellite was designed and fabricated by AFCRL.

The results presented were obtained by ARO, Inc. (a subsidiary of Sverdrup & Parcel and Associates, Inc.), contract operator of the Arnold Engineering Development Center (AEDC), AFSC, Arnold Air Force Station, Tennessee, under Contract F40600-72-C-0003. The tests were conducted from April 20 through 22, 1971, under ARO Project No. VR0172, and the manuscript was submitted for publication on July 9, 1971.

This technical report has been reviewed and is approved.

Emmett A. Niblack, Jr.  
Lt Colonel, USAF  
AF Representative, VKF  
Directorate of Test

Joseph R. Henry  
Colonel, USAF  
Director of Test

**ABSTRACT**

The OAR-901 satellite flight is part of the continuing upper atmosphere experimental program. The satellite was tested in a vacuum chamber to establish equilibrium temperatures for three different orientations. Tests were successfully completed for two fixed orientations and with the satellite rotating  $\pm 270$  deg at 0.5 rpm. Solar simulation cycling was also performed to simulate earth shadowing. Simulated flight performances were accomplished satisfactorily. All facility equipment functioned satisfactorily throughout the test.

## CONTENTS

	<u>Page</u>
ABSTRACT . . . . .	iii
I. INTRODUCTION . . . . .	1
II. APPARATUS . . . . .	1
III. PROCEDURE . . . . .	3
IV. RESULTS AND DISCUSSION . . . . .	4
V. CONCLUDING REMARKS. . . . .	6

## APPENDIXES

### I. ILLUSTRATIONS

#### Figure

1. OAR-901 Satellite . . . . .	9
2. Top Half 1-in. -Thick Bronze Hemisphere . . . . .	10
3. Bottom Half 1-in. -Thick Bronze Hemisphere. . . . .	11
4. Satellite Instrumentation Section . . . . .	12
5. Aerospace Research Chamber (12V). . . . .	13
6. Satellite Chamber Installation . . . . .	15
7. Drive System for Satellite Rotation . . . . .	17
8. Drive Shaft for Satellite Rotation . . . . .	18
9. Satellite System Checkout . . . . .	19
10. Satellite Checkout with Solar Simulator On . . . . .	22
11. Cryosystem Thermocouple Locations . . . . .	23
12. Test Stand Thermocouple Locations . . . . .	24
13. Plot of Solar Source Intensity Relative Distribution over Test Area.. . . .	25
14. Solar Source Intensity . . . . .	26
15. Satellite Temperatures. . . . .	27
16. Primary Temperatures of Interest . . . . .	103
17. Temperatures Related to Conduction through the Belly Band . . . . .	106

<u>Figure</u>	<u>Page</u>
18. Conduction through +Y Mounting Block . . . . .	108
19. Conduction through -Y Mounting Block . . . . .	110
20. Temperatures of North Deck Boxes . . . . .	112
21. Temperatures of South Deck Boxes . . . . .	114

## II. TABLES

I. LN <sub>2</sub> Cryowall Temperatures. . . . .	116
II. Test Stand Temperatures . . . . .	117
III. Satellite Temperatures . . . . .	118

## SECTION I INTRODUCTION

The OAR-901 satellite was tested in Aerospace Research Chamber (12V) to determine the equilibrium temperatures of the satellite and to enable observation of simulated flight performance after achieving equilibrium. Equilibrium was achieved for three different satellite orientations. Two static test orientations, +X axis and +Z axis facing the solar source, were performed. A rotational test at 0.5 rpm was also conducted with full solar simulation and with solar source cycling to simulate earth shadowing. The satellite was rotated about the Y axis. Forty temperatures were monitored throughout all the testing.

## SECTION II APPARATUS

### 2.1 TEST SATELLITE

The OAR-901 satellite is shown in Fig. 1, Appendix I. The satellite is an 800-lb, 26-in. -diam sphere composed of two less-than-180-deg, 1-in. -thick, bronze hemispheres (Figs. 2 and 3) connected by a 2-in. -wide aluminum "belly band." Approximately 120 lb of instrumentation (Fig. 4) thermally isolated from the body is contained within the sphere. Maximum power dissipated by this instrumentation is 100 w. The sphere is completely covered with solar cells with the exception of the connecting band and two 5-in. -diam pole caps which are symmetrical about the Z axis.

### 2.2 TEST CHAMBER

Chamber 12V is a stainless steel vacuum chamber, 12 ft in diameter and 35 ft high (Fig. 5). The lower portion of the chamber is lined with 380 ft<sup>2</sup> of liquid-nitrogen (LN<sub>2</sub>)-cooled cryosurface which shields 120 ft<sup>2</sup> of gaseous-helium (GHe)-cooled surface that can be used to pump condensable gases. The top portion of the chamber houses the collimating mirror and entrance window for the off-axis solar simulator. The chamber vacuum pumping system consists of a 750-cfm roughing pump, a 140-cfm forepump, a 750-cfm blower, and a 50,000-liter/sec oil diffusion pump. For this test an LN<sub>2</sub>-cooled cryoshield was installed in the top of the chamber, thereby reducing the view which the satellite had to the uncooled top portion of the chamber.

The solar simulator<sup>1</sup> used to irradiate the satellite is an off-axis system consisting of three basic components: a source lamp array, an optical integrating lens system, and a collimating mirror. The source is an array of seven 20-kw xenon compact arc lamps in elliptical reflectors. The radiation from the lamps passes through a quartz integrating lens unit in the chamber wall to a 10-ft-diam aluminized collimating mirror. A shutter mounted at the entrance window is used to interrupt the solar simulator output. The mirror directs the beam down into the test volume. This system provides a beam of relatively uniform intensity ( $\pm 4$  percent) over the test volume. The measured beam decollimation is 1.84 deg.

The satellite installation in the chamber is shown in Fig. 6. The stand shown in Fig. 6b was insulated from the cryofloor and had strip heaters attached to control the stand temperature near the satellite to reduce conductive heat transfer. Rotation of the satellite was provided by the drive system shown in Fig. 7 mounted outside the chamber. A drive shaft utilizing a vacuum feedthrough connected the drive system to the satellite inside the test chamber (Fig. 8). The satellite was rotated through  $\pm 270$  deg at 0.5 rpm. Figure 6 shows the satellite in one position during system checkout, and Fig. 9 shows other positions as the satellite was rotated.

Figure 10 shows the satellite mounted in the chamber with the solar simulator turned on for a final check just before the chamber door was closed for pumpdown.

## 2.3 INSTRUMENTATION

The temperatures of the satellite and test chamber components were monitored throughout the tests. Figures 11 and 12 show the locations of the thermocouples used to measure the cryowall temperatures and test stand temperatures, respectively. The locations of the satellite thermocouples are tabulated in Table III (Appendix II).

The solar simulator output was measured by two water-cooled total radiometers (Figs. 10 and 12). For the solar simulator calibration, one of the radiometers was positioned throughout the solar beam. The results of this calibration are presented in Fig. 13.

---

<sup>1</sup>R. M. Warner. "Description and Performance of the 8-ft-diam Solar Simulation System at AEDC." AEDC-TR-67-219 (AD821819), October 1967.

The pressure in the chamber was measured by two ionization gages located in the test volume.

### SECTION III PROCEDURE

The satellite and instrumentation trailer were delivered to AEDC, and the power interface from the trailer to the chamber and outside support instrumentation was completed. The satellite was uncrated and reassembled in the model buildup area. Initial checkouts were performed and then the satellite was moved to the chamber area for final checkout with the instrumentation trailer.

The satellite was installed in the chamber as shown in Fig. 6 and mounted in the test stand. Instrumentation was connected from the satellite to the data system. The rotation of the satellite and cabling handling mechanism was checked as shown in Fig. 9. A final checkout of all facility systems was performed.

The chamber preoperational procedures were then performed, the chamber door was closed, and chamber evacuation was initiated. The chamber was evacuated to  $10^{-4}$  torr, and cooldown was started. The satellite was oriented in a static position with the +X axis facing the solar source. The chamber walls, floor, and top shield were cooled to LN<sub>2</sub> temperatures, and the satellite was allowed to cool to approximately -10 to 50°F which was below the predicted stabilization temperature of 53°F. The solar simulator was then turned on and set at one solar constant ( $1400 \text{ w/m}^2$ ). The satellite temperatures were allowed to stabilize (approximately 2.5 hr) with cold background and solar simulation. A complete subsystem check was then performed (approximately 3.5 hr).

The satellite was then rotated to the next static test position with the +Z axis (North) facing the solar source and allowed to stabilize (approximately 2.5 hr). Next, the satellite was rotated  $\pm 270$  deg at 0.5 rpm with the solar simulation on and allowed to stabilize at this condition. The last test run was with the satellite rotating and the solar simulation cycled on 63 min and off 42 min. After completion of this test the chamber was warmed up and repressurized with nitrogen to 200 torr and returned to atmospheric pressure with air. The satellite was inspected, removed from the chamber and packaged for shipment.

## SECTION IV RESULTS AND DISCUSSION

### 4.1 RESULTS

Table I is a complete listing of all cryowall, cryofloor, and cryo-shield temperatures for the test. The solar simulator mirror temperature is also shown in this table. Table II lists all the test stand temperatures as well as solar intensity and chamber pressure. Table III is a complete list of all satellite temperatures. Each cryo-shield and test stand temperature reading has been assigned a data point number from 1 through 45. The solar intensity is number 46, and chamber pressure is 48. Satellite temperatures are data points 51 through 83. The numbers in parentheses, e. g., (61) after data point 7, refer to the channel number on the computer-generated figures (Figs. 15 through 21).

The time 19:05 in the tables is when the satellite temperatures were stabilized with the +X axis facing the solar source, and 01:27 was the corresponding time with the +Z axis facing the solar source. The stabilized temperature of the satellite rotating  $\pm 270$  deg about the Y axis at 0.5 rpm with one solar constant continuous solar simulation input was attained at time 04:03. The readings at times 11:05 and 11:46 were made at the beginning and end of a 42-min solar simulator off period, respectively. The 14:00 reading was at the end of the test after the solar simulator had been on continuously for 2 hr and 13 min. Figure 14 is a plot of solar intensity measured during the test period.

Figures 15a through s are plots that cover a 30-hr test period from cooldown through all tests and chamber warmup. For clarity only two temperatures are plotted per figure. The numbers assigned to the curves refer to the data point numbers in parentheses in Tables I, II, and III, revealing the thermocouple locations. The figures that concern a specific test are discussed later under the appropriate heading. The plots start at 144 min which was approximately 2.5 hr after the start of pumpdown and data taking, but at the beginning of chamber cooldown. The solar simulation was first introduced into the chamber at 16:36, which corresponds to time 420 min on the plots.

#### 4.1.1 Static Test, +X North Axis toward Solar Source (Test 1)

This test was conducted with the satellite +X axis facing the solar source. Table III is a tabulation of the satellite temperatures. Data points 58, 59, 61, 76, 78, 79, and 80 for time 19:05 are directly

applicable to this test. They illustrate that the temperature change across the +X side was from 70°F, outside, to 64°F, inside; similarly, for the -X side the change was from 9°F, outside, to 20°F, inside. Figure 16a is a plot of the seven data channels mentioned above. The plots cover the period from the time the solar simulator was turned on until the temperatures had stabilized.

#### **4.1.2 Static Test, +Z North Axis toward Solar Source (Test 2)**

Subsystem checks which required internal power generation were performed from 19:05 until 22:42. The satellite was then rotated about the Y axis until the +Z axis was facing the solar source. Data points 58, 59, 61, 62, 63, 69, and 70 for time 01:27 are directly applicable for this test. The +Z outside temperature was 93°F and the inside temperature was 106°F, indicating that the internal power dissipated was having an effect on that temperature. The -Z outside temperature was 26°F and the inside temperature was 40°F, as expected since this side faces the LN<sub>2</sub>-cooled floor during this test. Figure 16b is a plot of the seven data points and covers the time period from 22:42 until satellite stabilization at 01:27.

#### **4.1.3 Rotating, Full Solar Simulation, and Shadowing (Test 3)**

This test was conducted with the satellite rotating at 0.5 rpm  $\pm 270$  deg about the Y axis. The five data points of most interest are numbers 58, 59, 61, 62, and 69 which are shown in Table III. The data at time 04:03 were recorded after the satellite had stabilized with a full solar constant impinging on it continuously. The data at time 11:05 were recorded after the solar simulator had been on and off several times, but had just completed a full 63-min on cycle. The data at 11:46 were taken after a full 42-min off cycle had been completed. The data at time 14:00 were recorded at the completion of the test and the solar simulator had been on continuously for 2 hr 13 min. Figure 16c is a plot of the five primary data points for Test 3.

#### **4.1.4 Conduction through Belly Band (Tests No. 2 and 3)**

Figure 17 is a plot of data points 68, 75, 76, and 77, for Tests 2 and 3. This is to illustrate conduction through the belly band, center section of the satellite. The first portion of Fig. 17 for the time between 780 and 950 min with the +Z axis facing the solar source shows that data point 25(+Z) (facing solar source) and data point 34 (-Z) (facing cold LN<sub>2</sub> floor) have a temperature spread of approximately 50°F as a result of poor conduction through the belly band section. During the remaining time period of Fig. 17, with the satellite rotating so that all

sides receive solar energy, the effect of poor conduction through the belly band is essentially eliminated and the temperature spread between +Z and -Z is reduced to approximately 4°F.

#### 4.1.5 Temperature Plots for All Tests

Figure 18 is a plot of data points 81, 41, 42, and 45 for all tests. This is to show the effect of conduction through the +Y mounting block. Figure 19 is a plot of data points 82, 43, and 44 and shows the effect of conduction through the -Y mounting block. Figure 20 is a plot of data points 52, 53, 55, 56, 57, and 58 showing some of the internal temperatures throughout the test for the north deck. Figure 21 is a plot of data points 51, 54, 59, and 61 which shows some of the internal temperatures for the south deck.

### SECTION V CONCLUDING REMARKS

Three thermal vacuum tests were successfully completed on the OAR-901 satellite. Temperature stabilization conditions were obtained for two static positions with the +X and +Z axes facing the solar source. A temperature stabilization test was conducted with the satellite rotating  $\pm 270$  deg at 0.5 rpm about the Y axis, while subjected to one solar constant ( $1400 \text{ w/m}^2$ ). Earth shadowing was also simulated by performing five cycles of solar source on (63 min) and off (42 min). The satellite was operated during the test and all systems performed satisfactorily, as did all test facility equipment.

**APPENDIXES**  
**I. ILLUSTRATIONS**  
**II. TABLES**



Fig. 1 OAR-901 Satellite

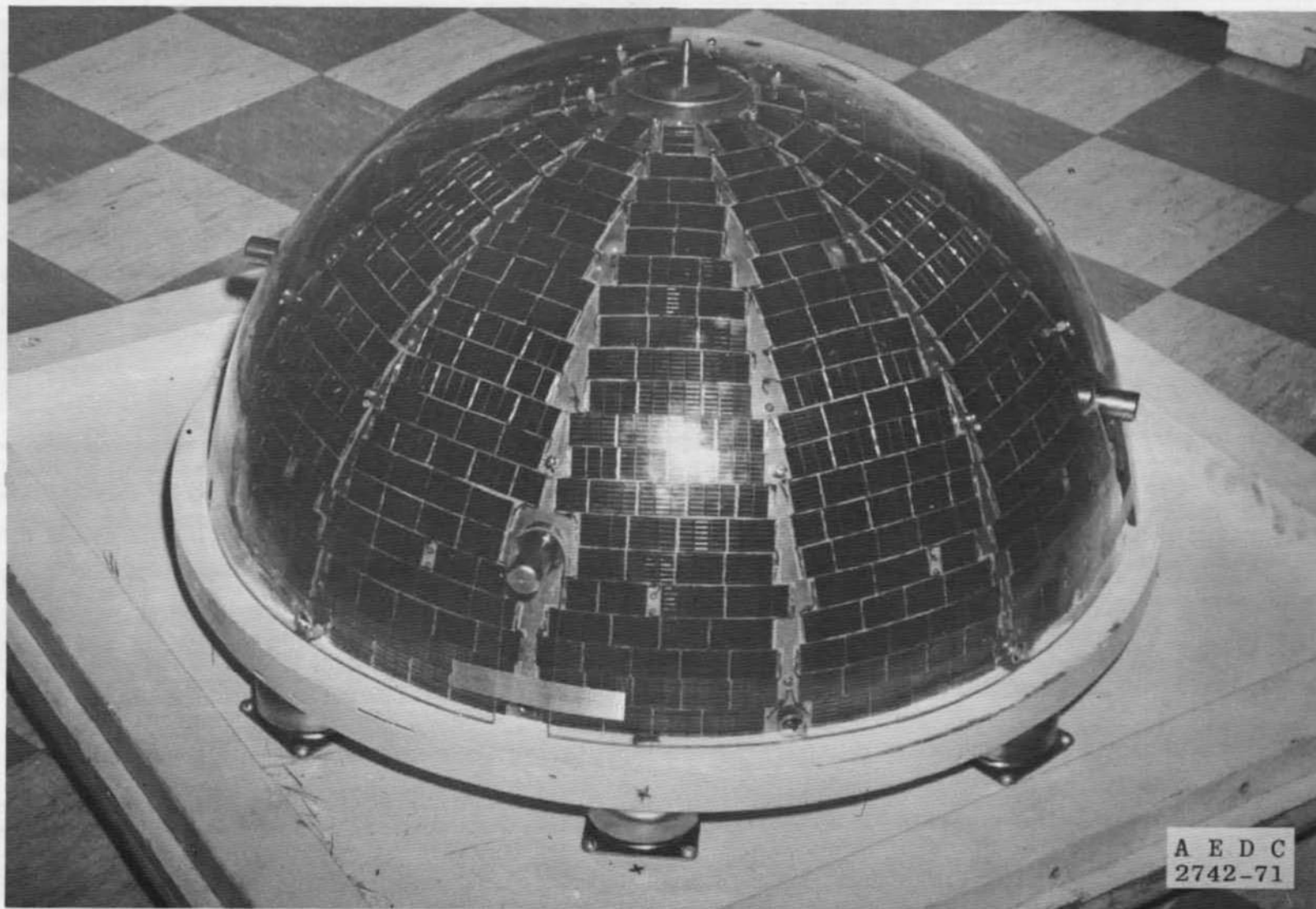


Fig. 2 Top Half 1-in.-Thick Bronze Hemisphere

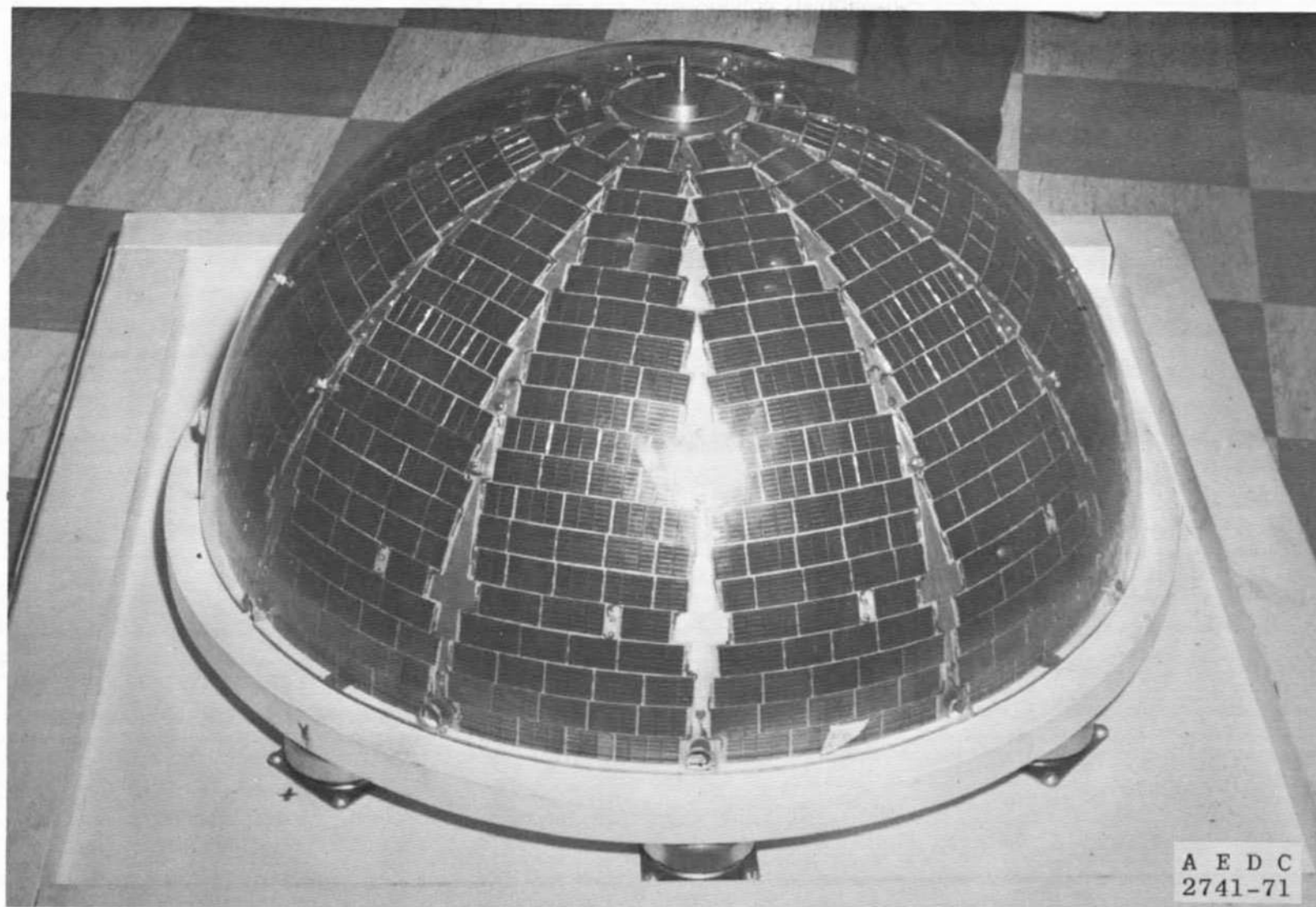


Fig. 3 Bottom Half 1-in.-Thick Bronze Hemisphere

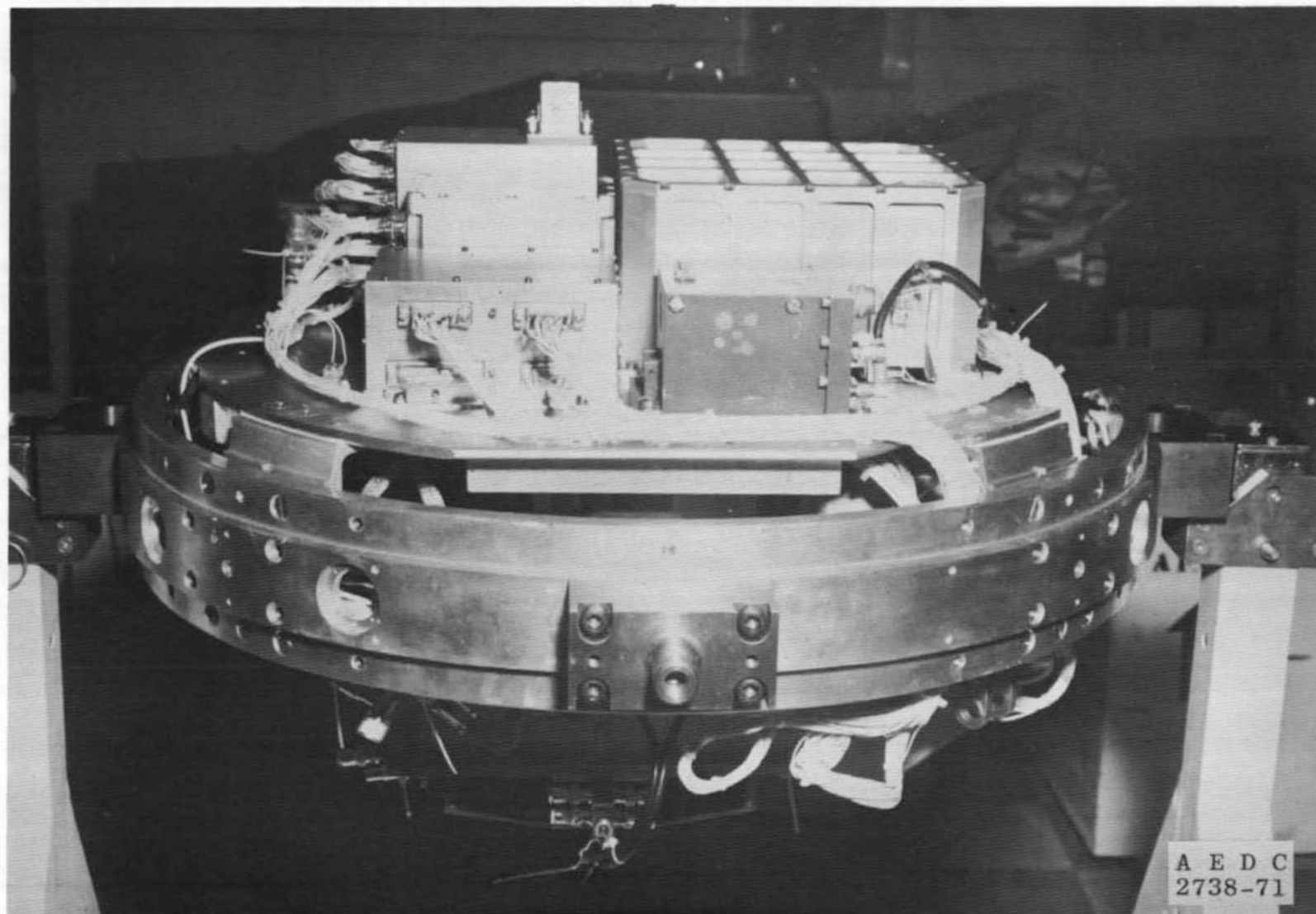
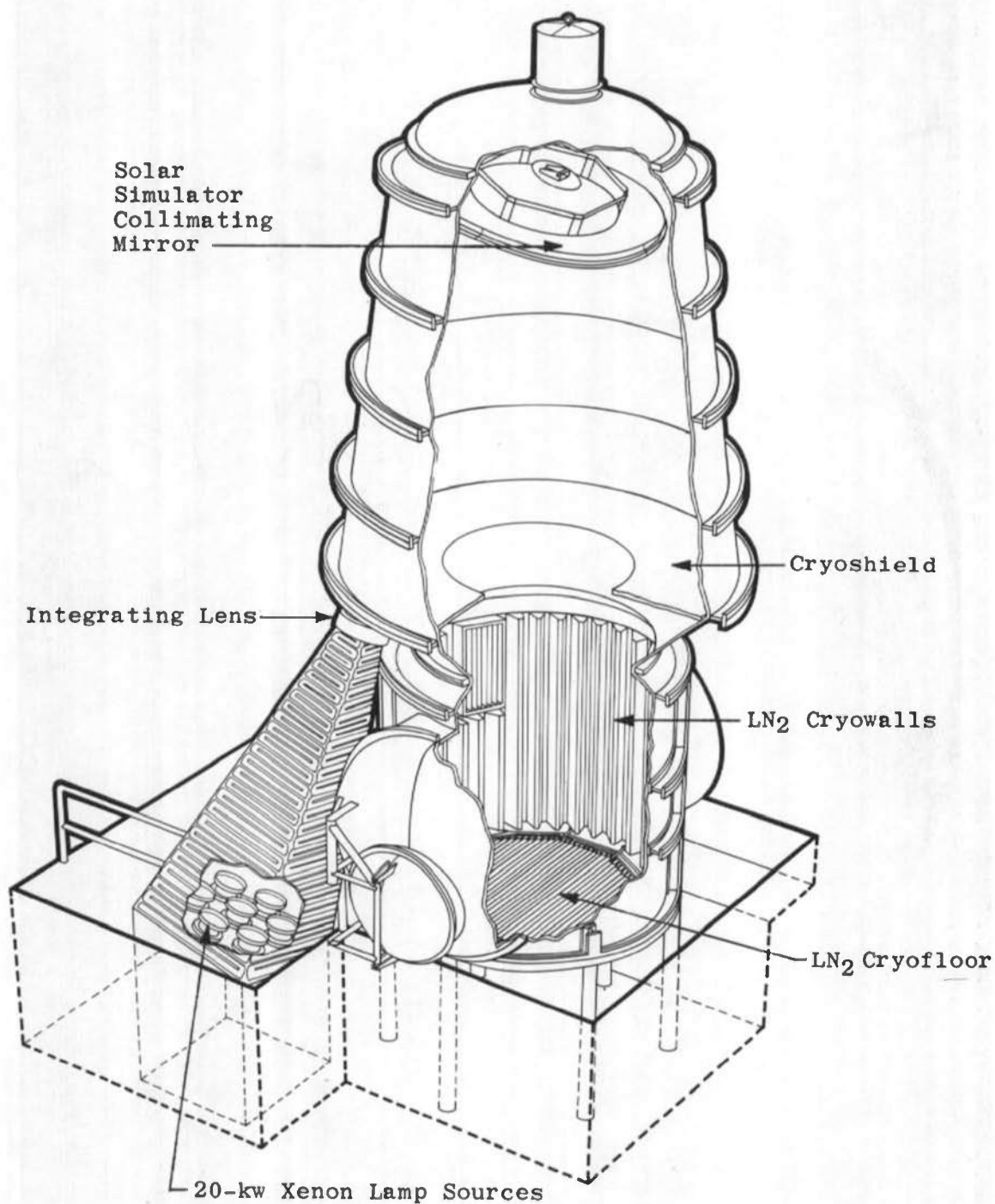


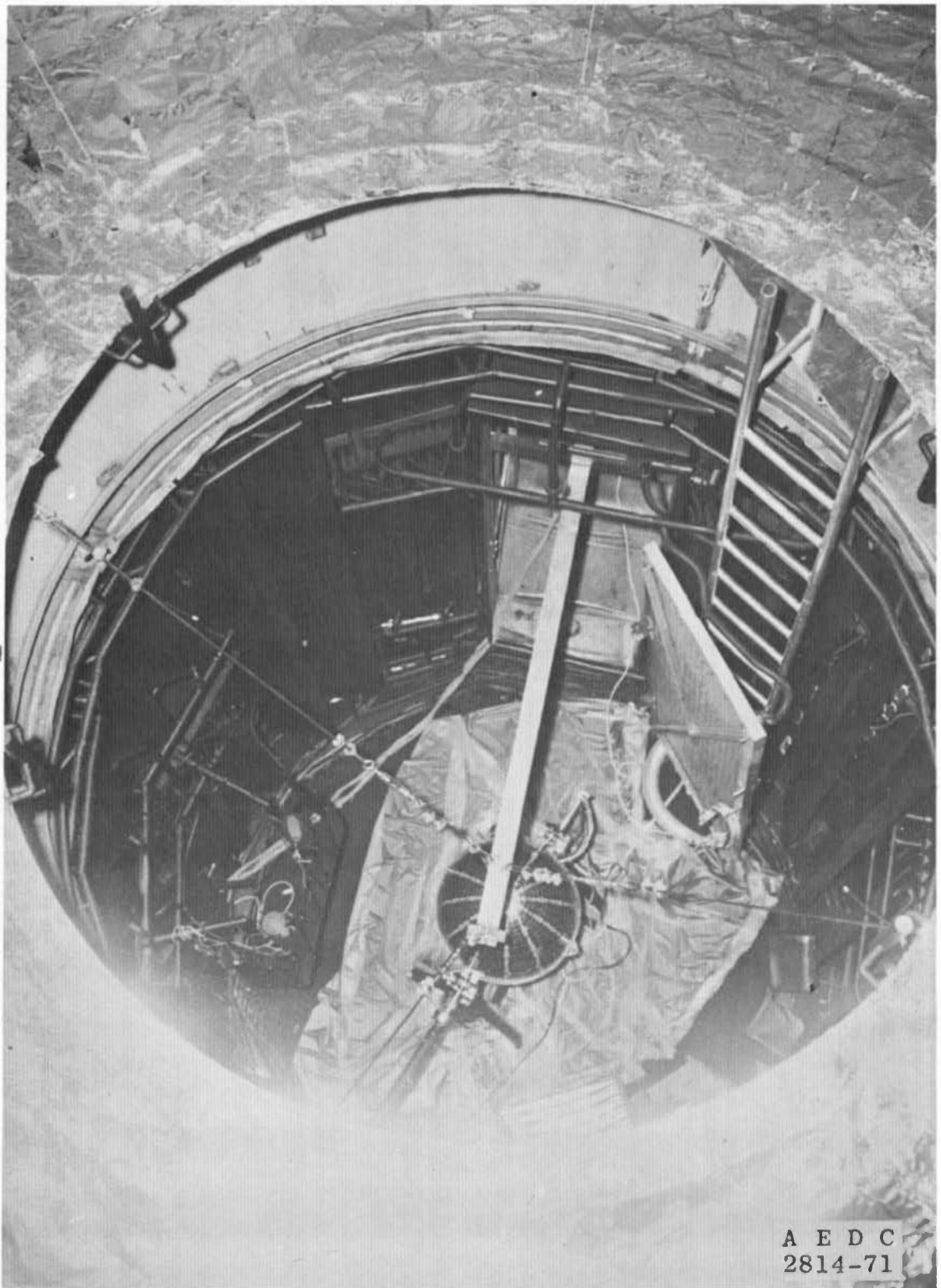
Fig. 4 Satellite Instrumentation Section



a. Photograph  
Fig. 5 Aerospace Research Chamber (12V)



b. Cutaway View  
Fig. 5 Concluded



a. Lowering Satellite onto Support Stand  
Fig. 6 Satellite Chamber Installation



b. Satellite Mounted in Chamber Support Stand at 270-deg Position  
Fig. 6 Concluded

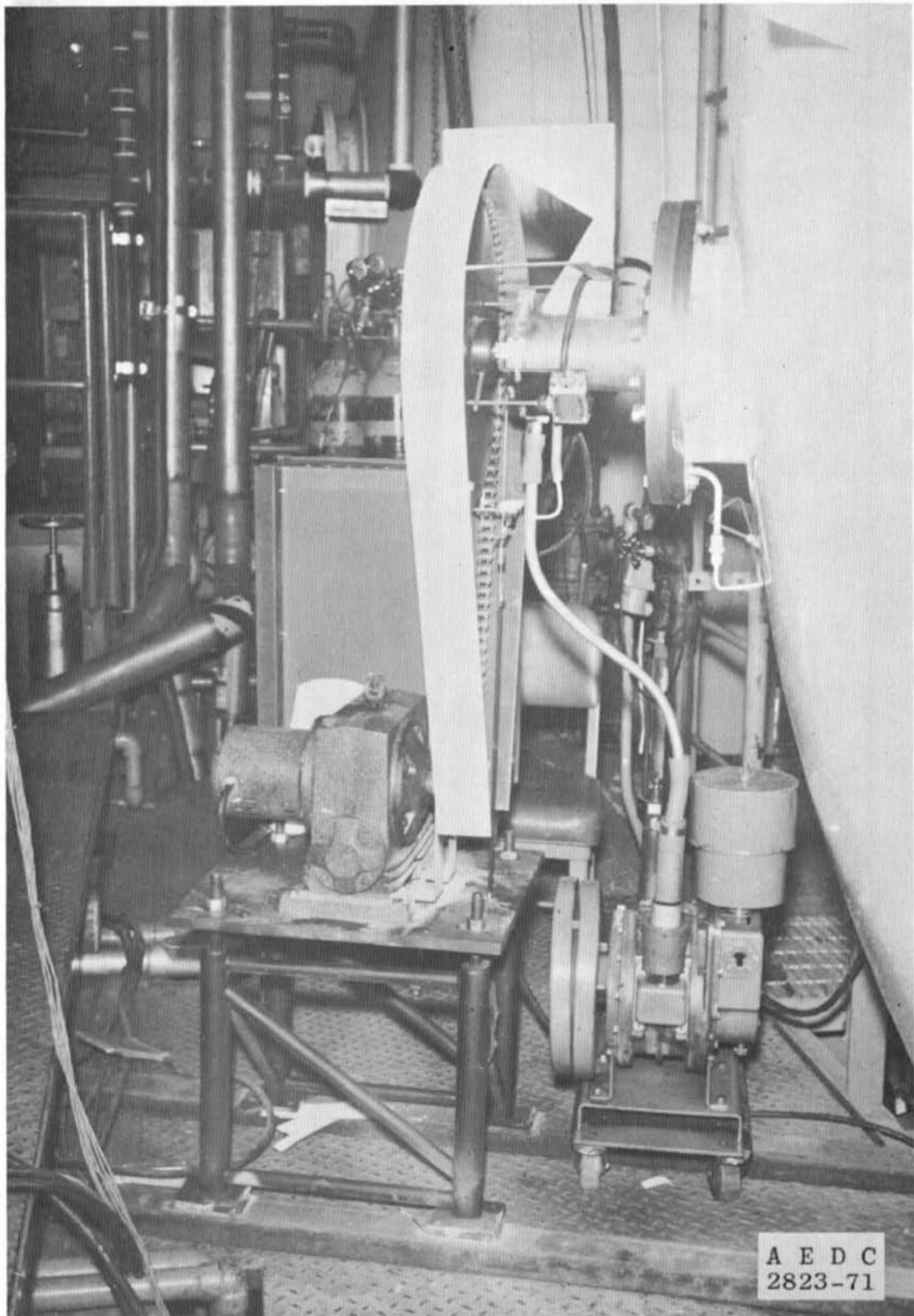


Fig. 7 Drive System for Satellite Rotation

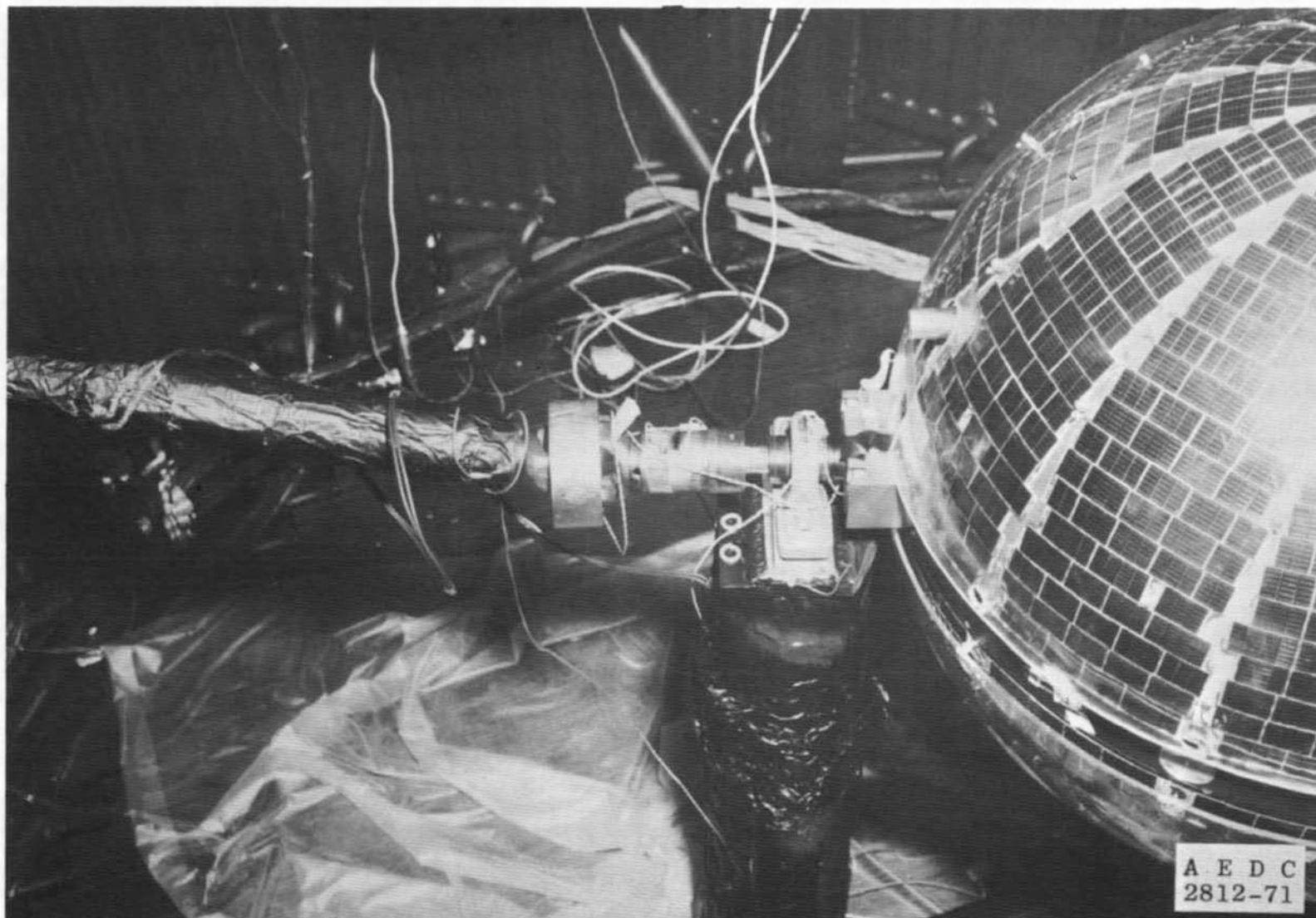
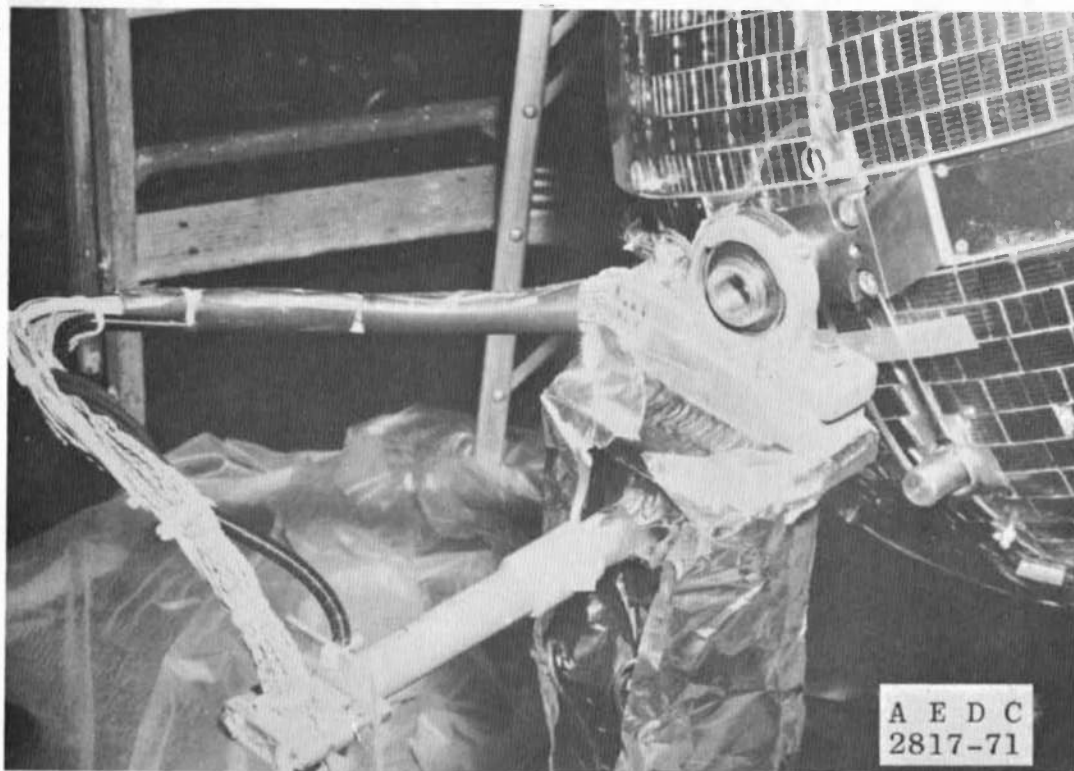
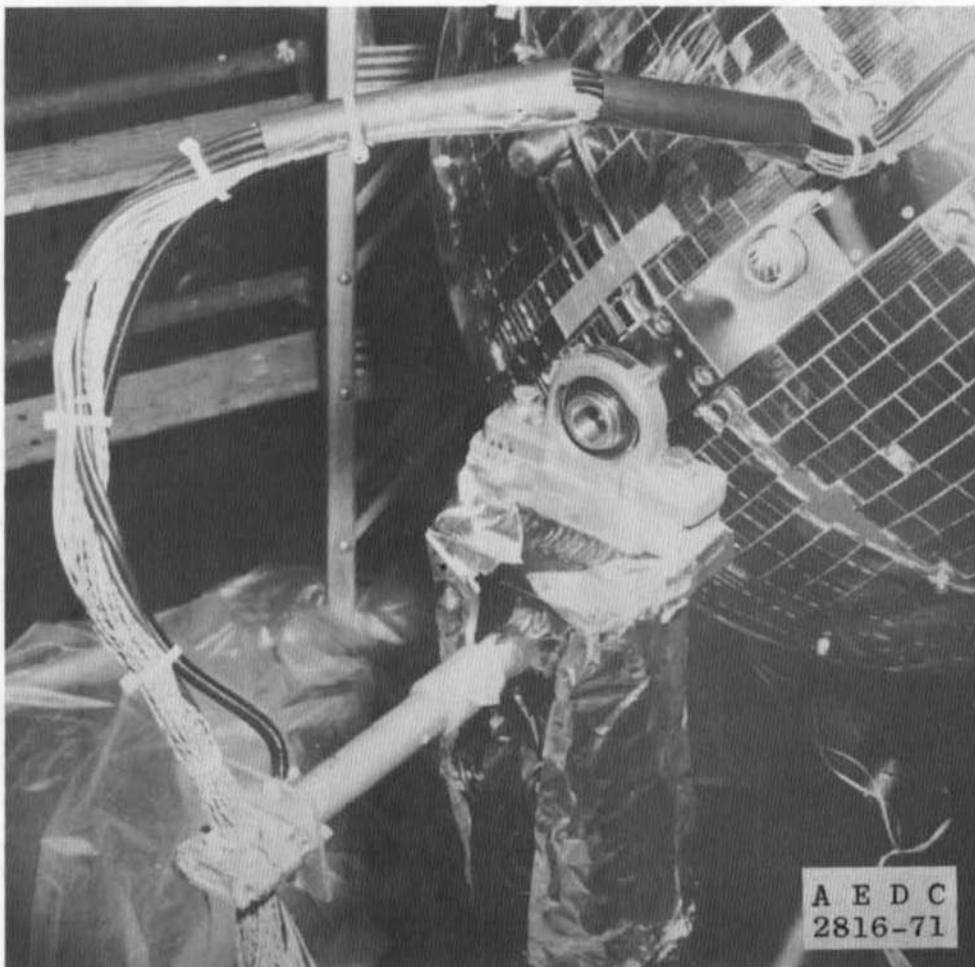


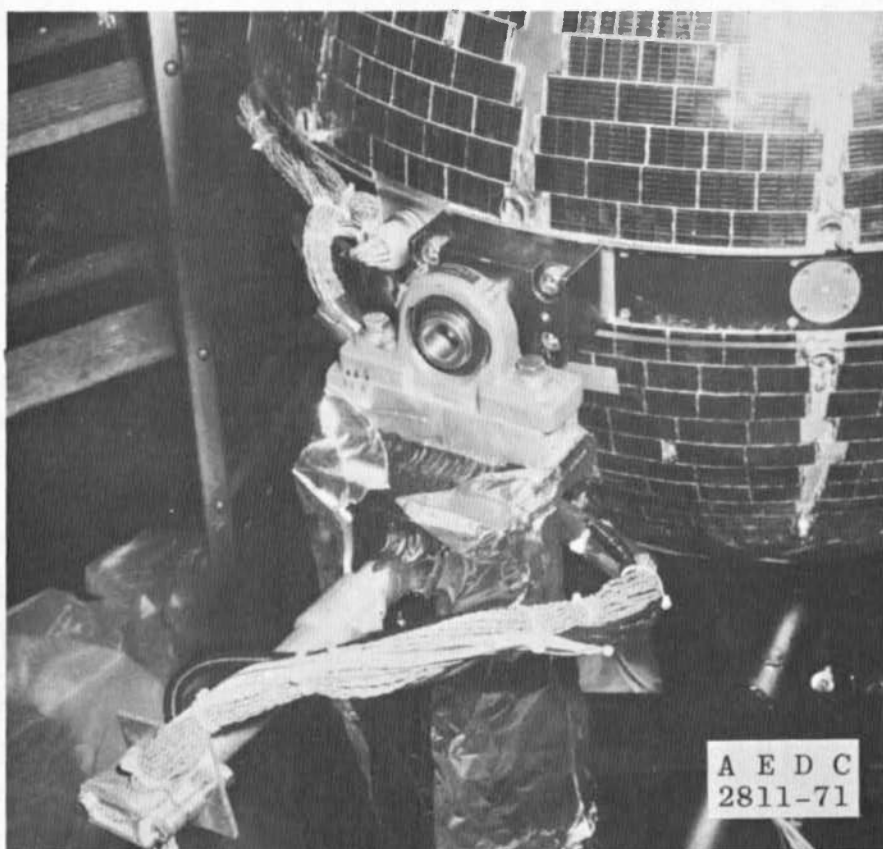
Fig. 8 Drive Shaft for Satellite Rotation



a. 100-deg Position  
Fig. 9 Satellite System Checkout



b. -30-deg Position  
Fig. 9 Continued



c. -270-deg Position  
Fig. 9 Concluded

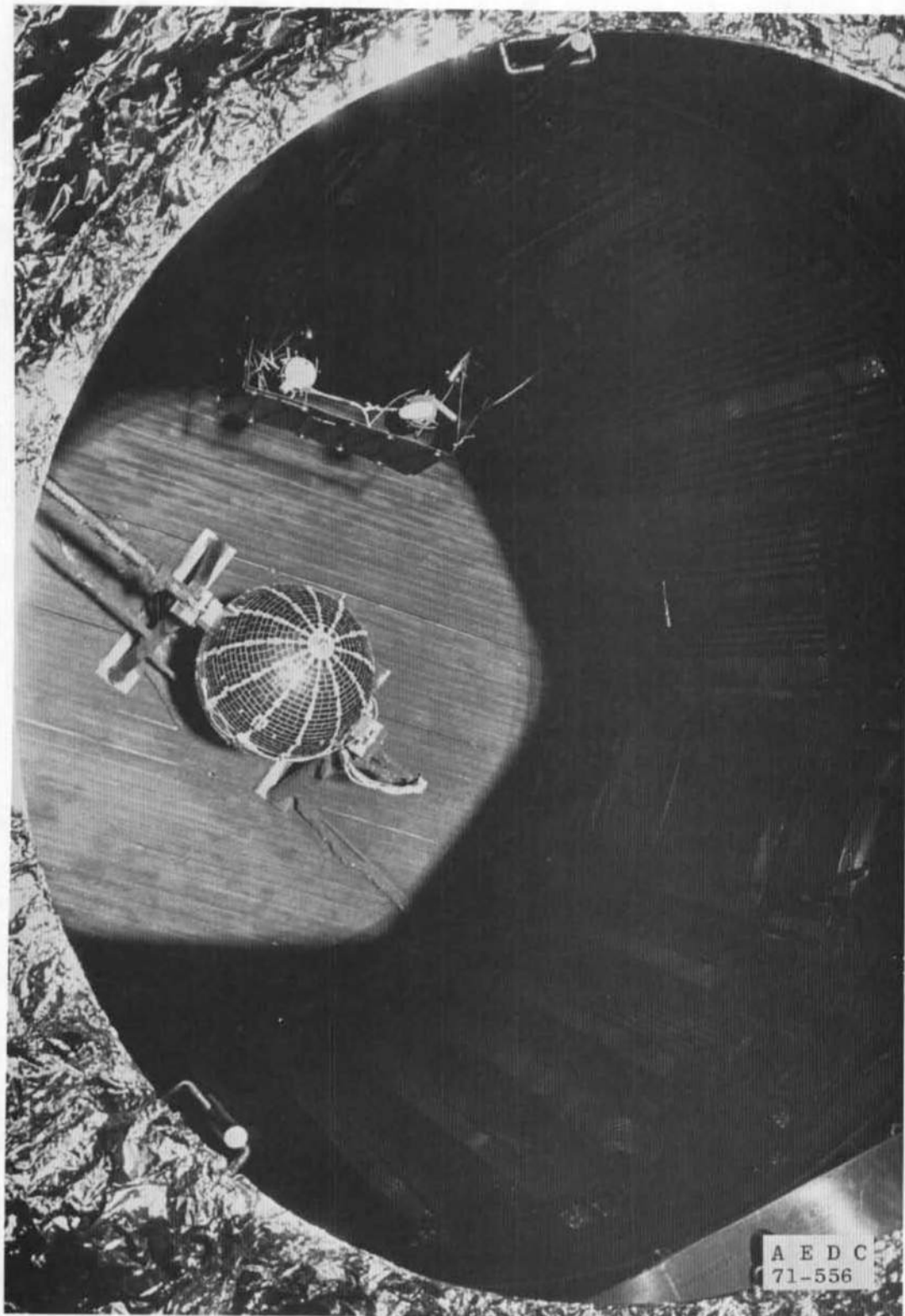


Fig. 10 Satellite Checkout with Solar Simulator On

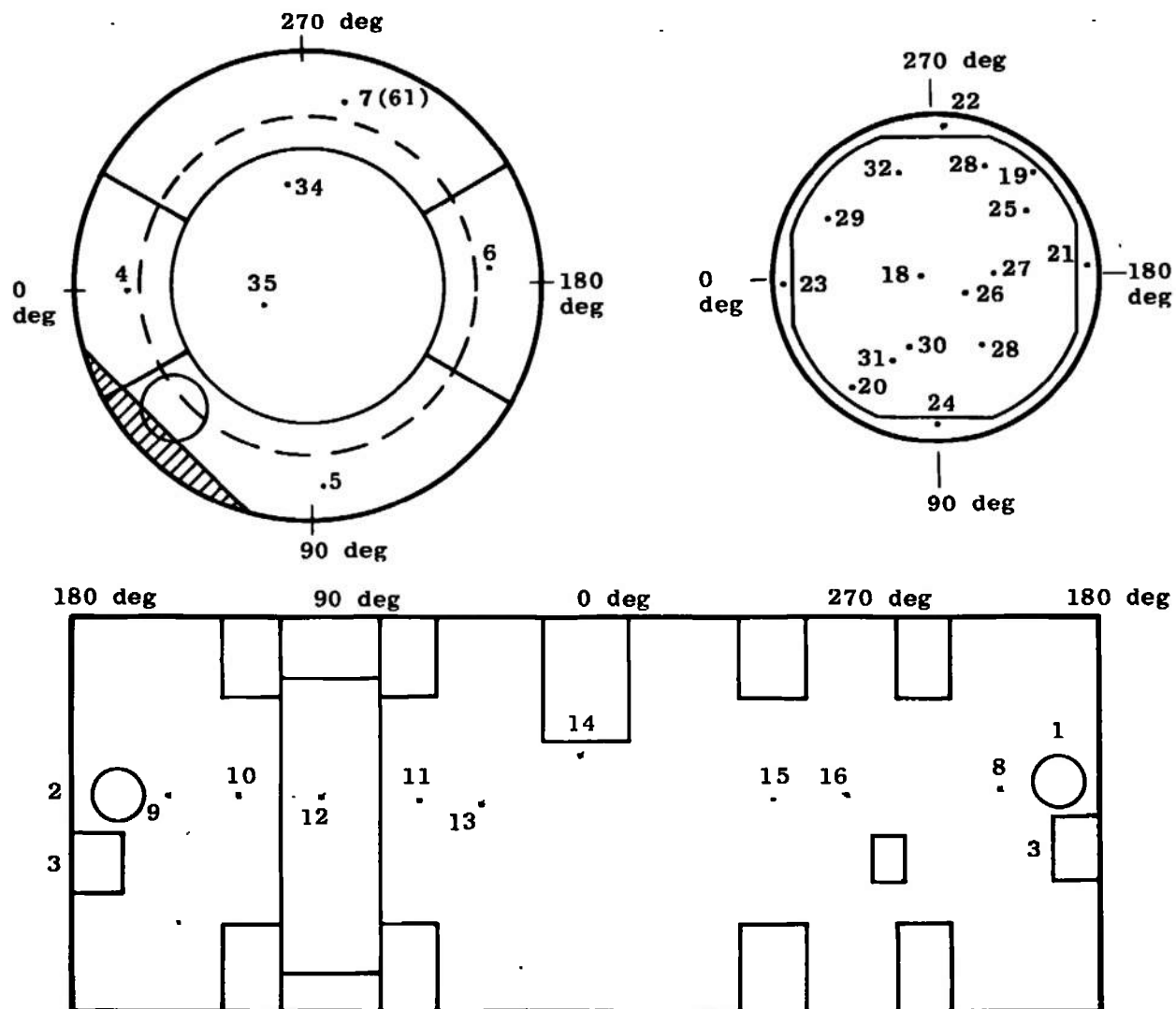


Fig. 11 Cryosystem Thermocouple Locations

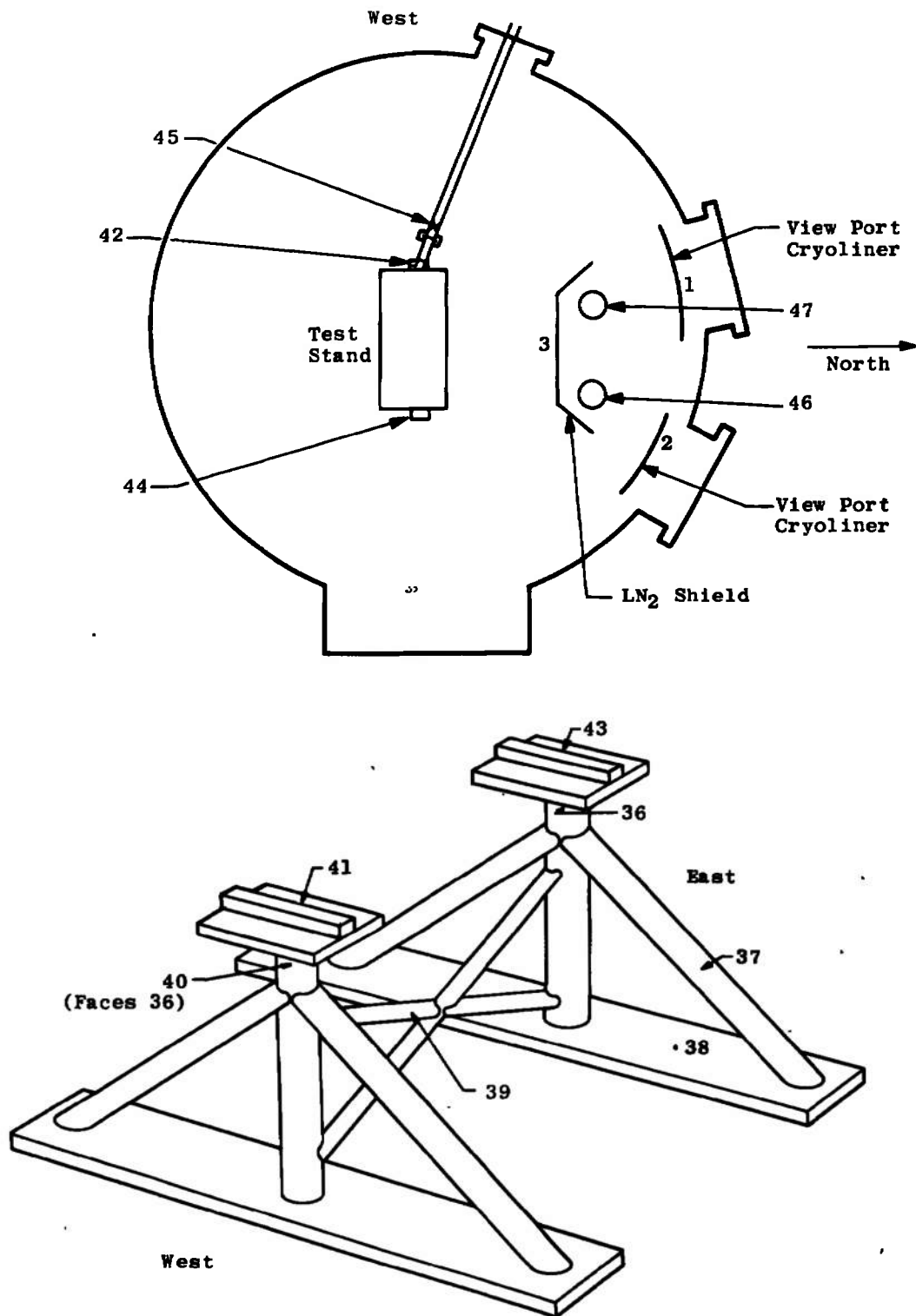
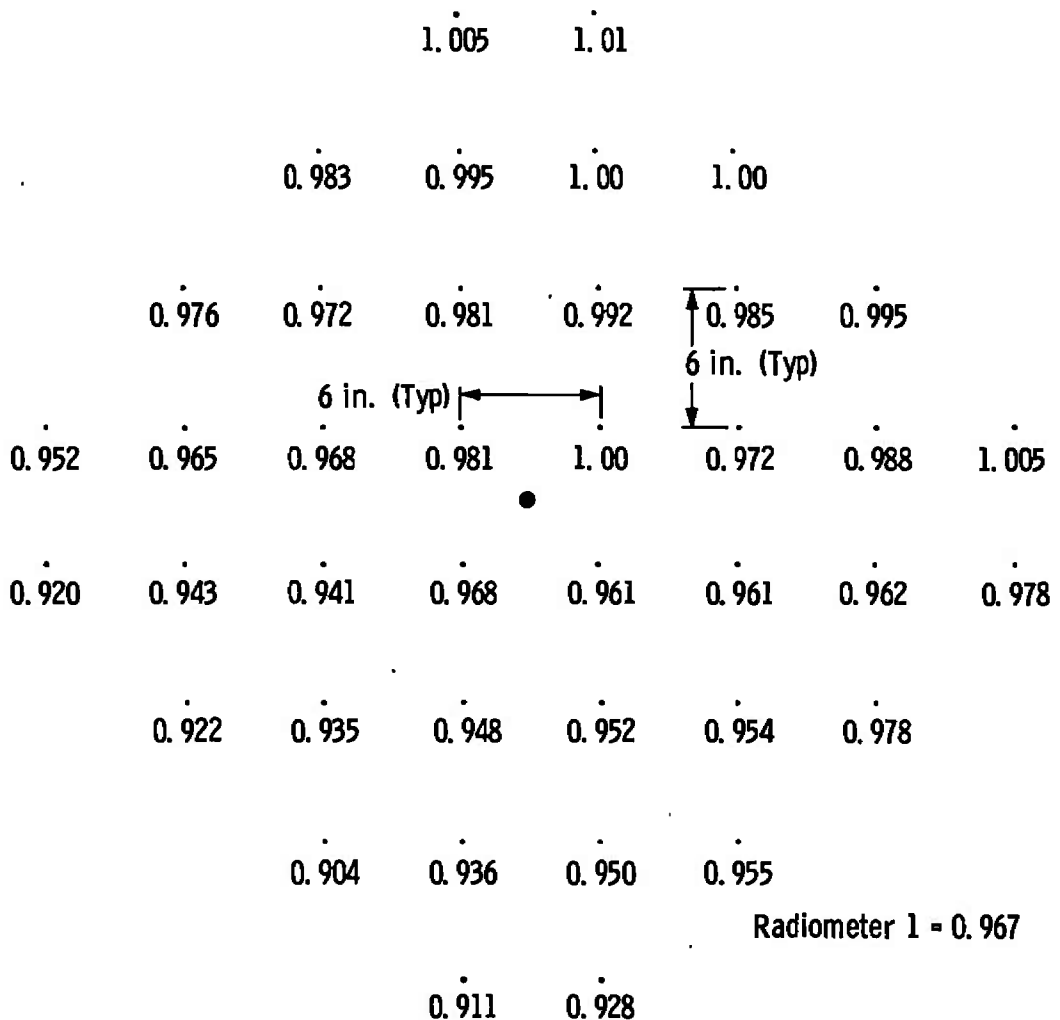


Fig. 12 Test Stand Thermocouple Locations

Inner Circle Range = 0.935 to 1.00  
 Inner Circle Average = 0.967 = 1352 w/m<sup>2</sup>  
 Radiometer 1 = 0.967 = 1352 w/m<sup>2</sup>  
 One Solar Constant = 1.00 = 1400 w/m<sup>2</sup>

Time	Inner Circle Average	Reading, w/m <sup>2</sup>
19:05	0.995	1392
01:27	1.005	1407
04:03	1.027	1439
11:05	0.960	1344
14:00	0.988	1383



Inner Circle = 27-in. Diameter  
 Outer Circle = 36-in. Diameter

Fig. 13 Plot of Solar Source Intensity Relative Distribution over Test Area

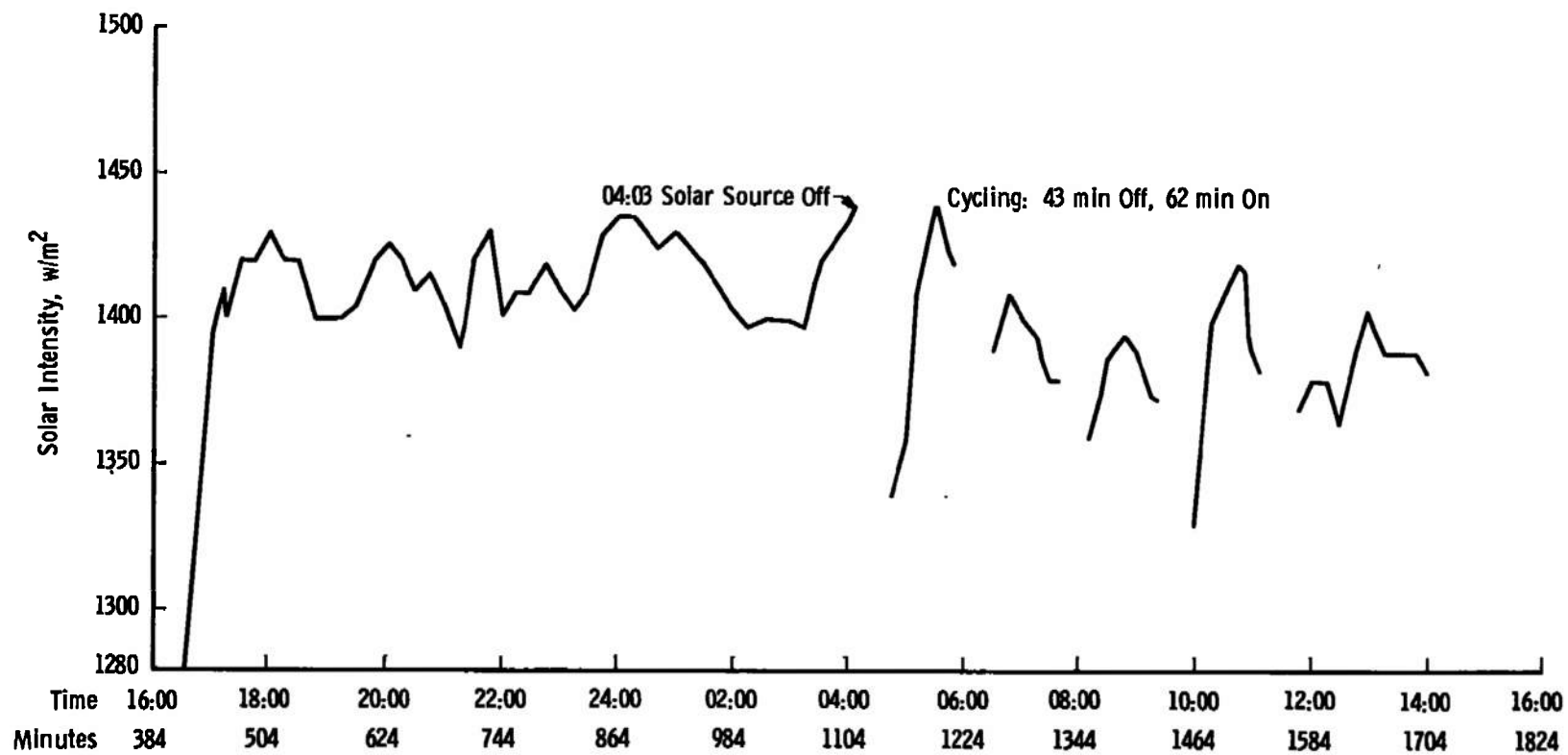
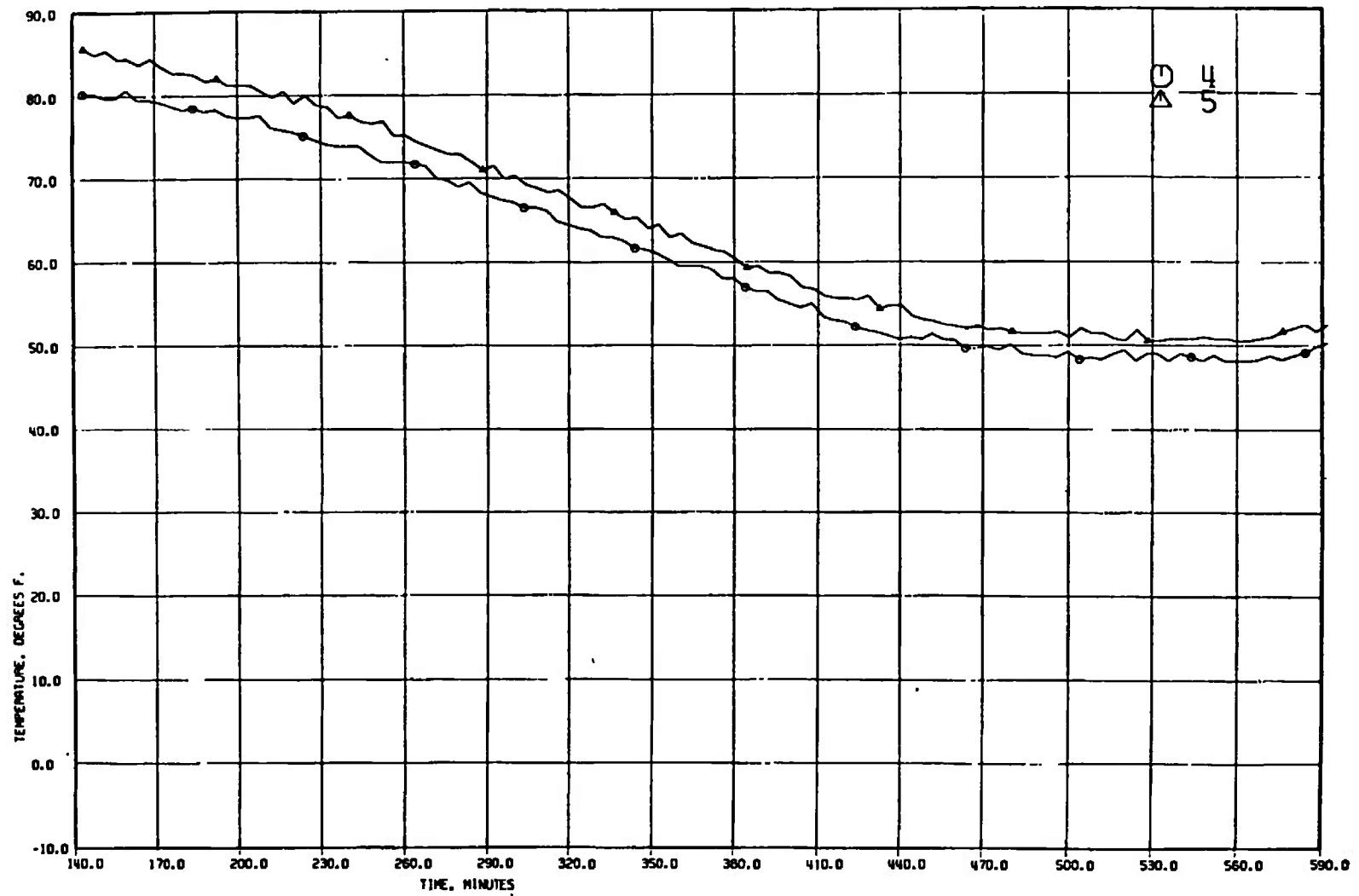
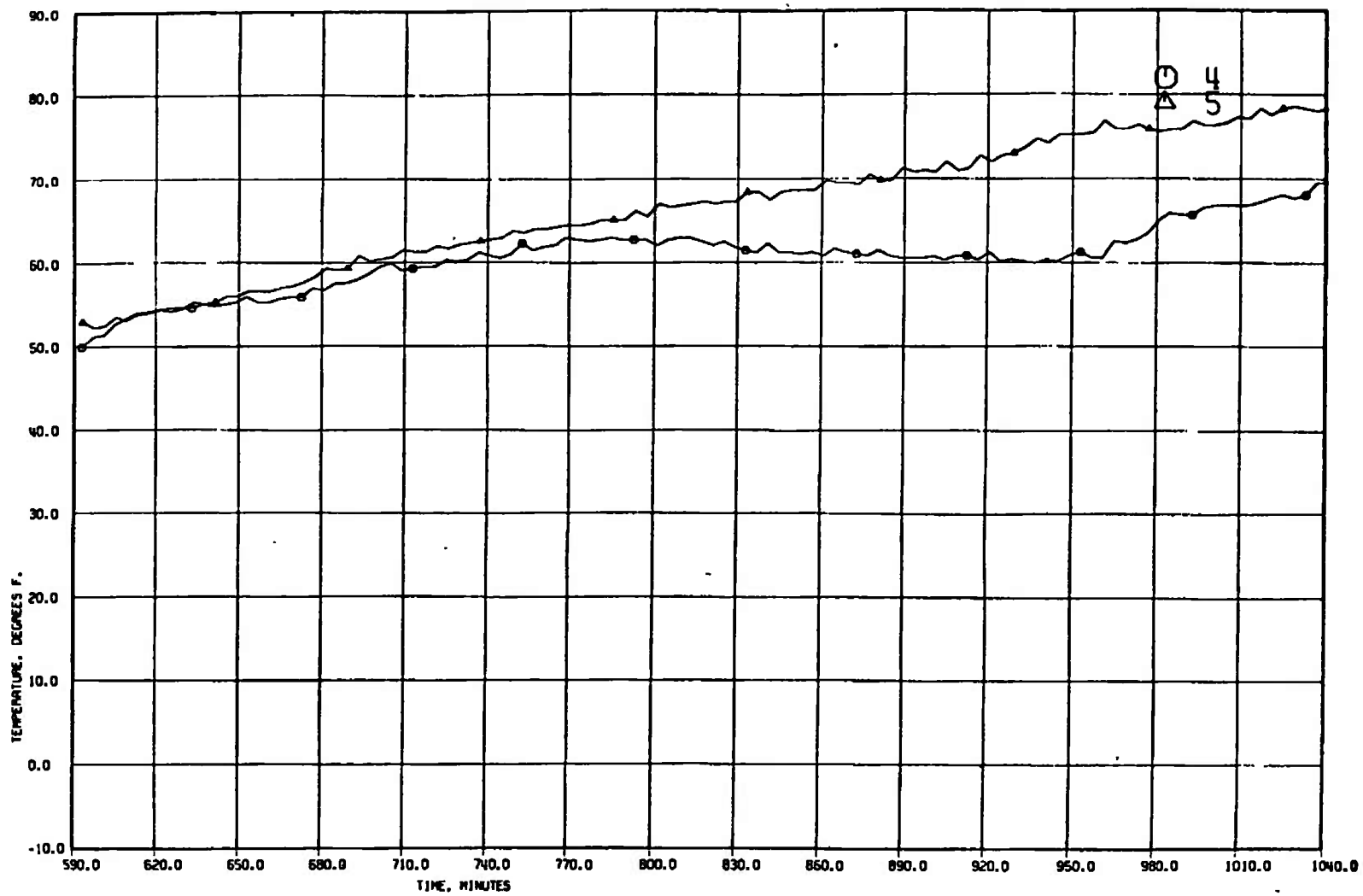


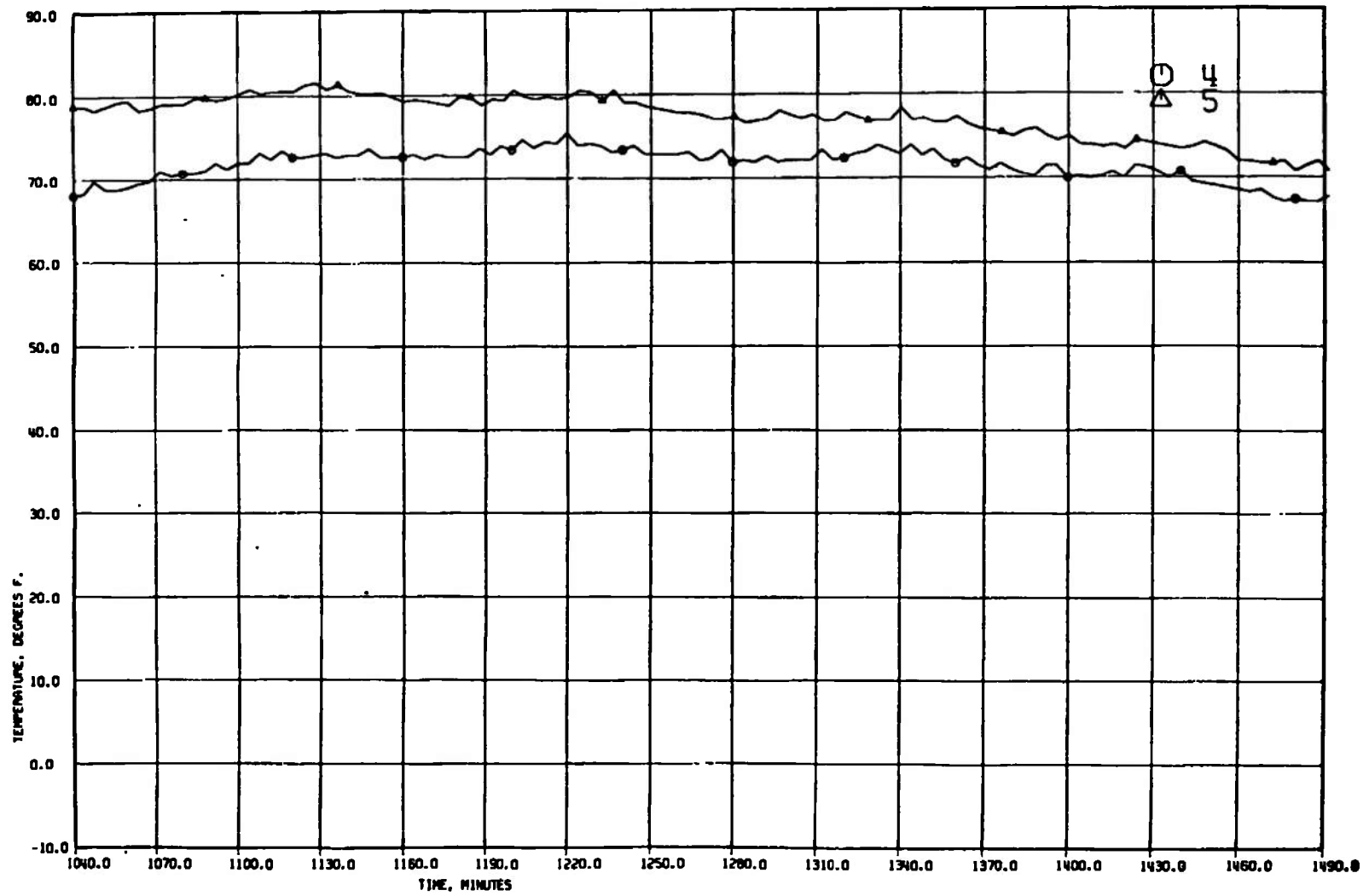
Fig. 14 Solar Source Intensity



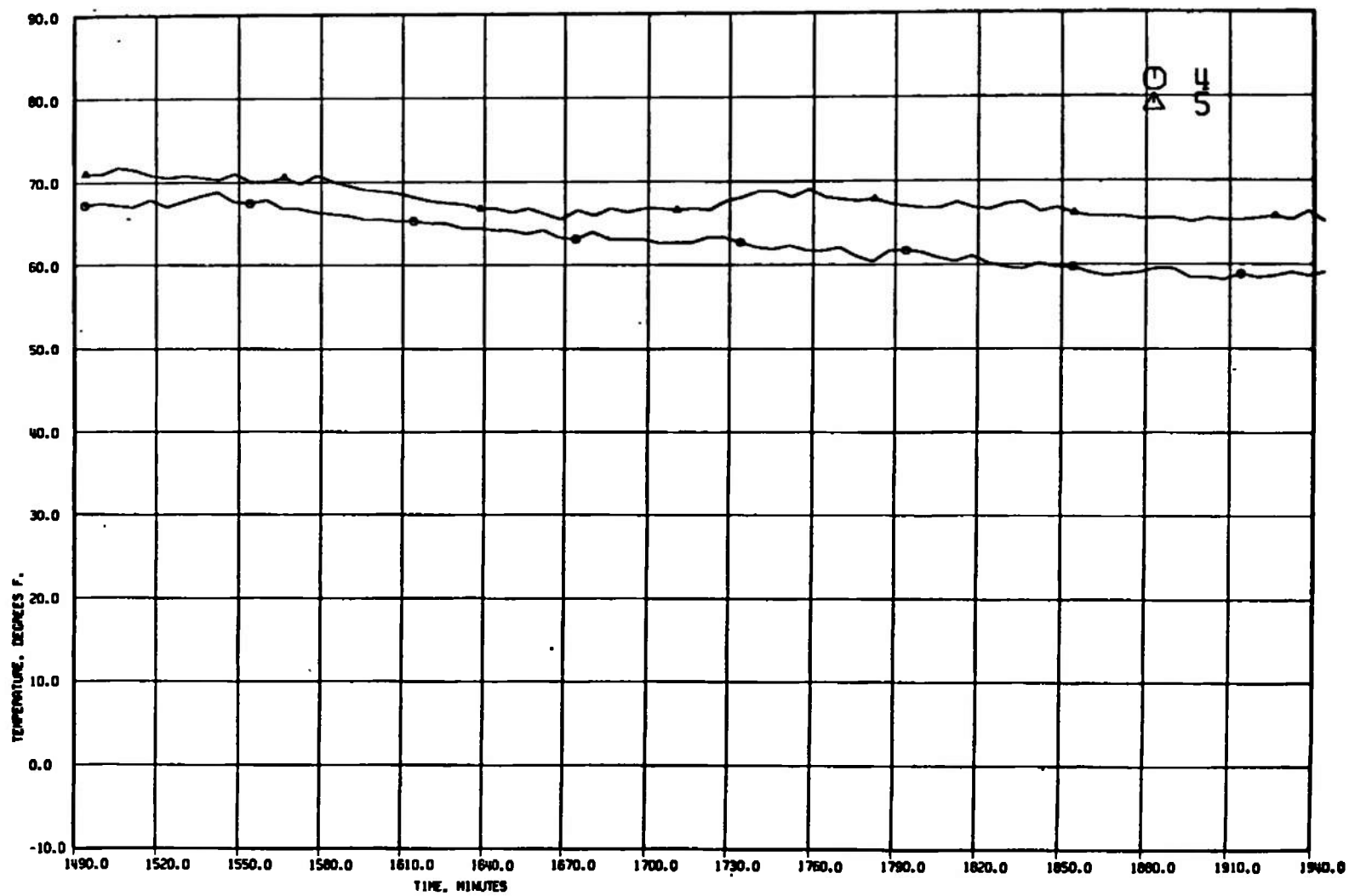
a. T/C 4 and 5  
Fig. 15 Satellite Temperatures



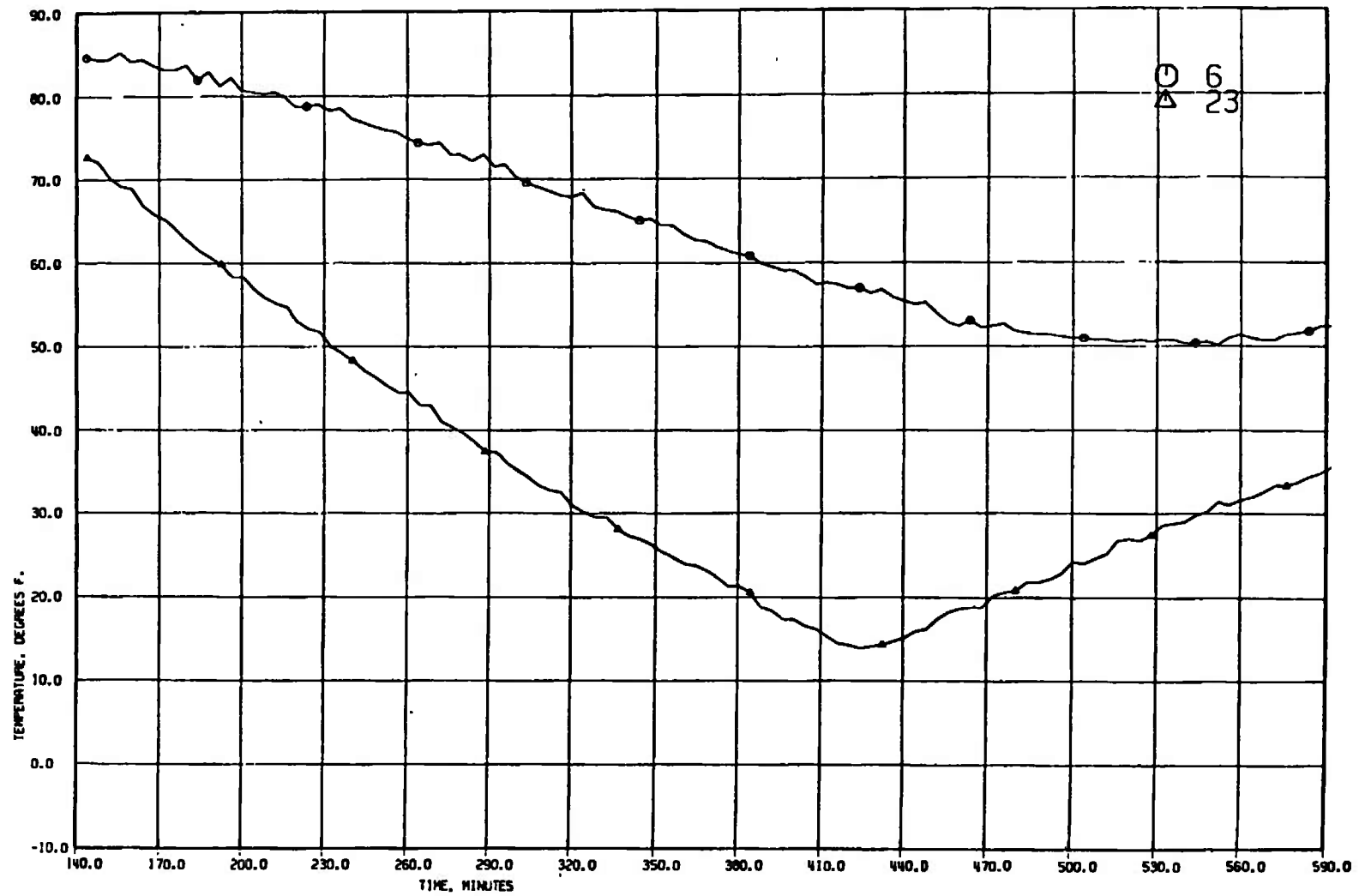
a. Continued  
Fig. 15 Continued



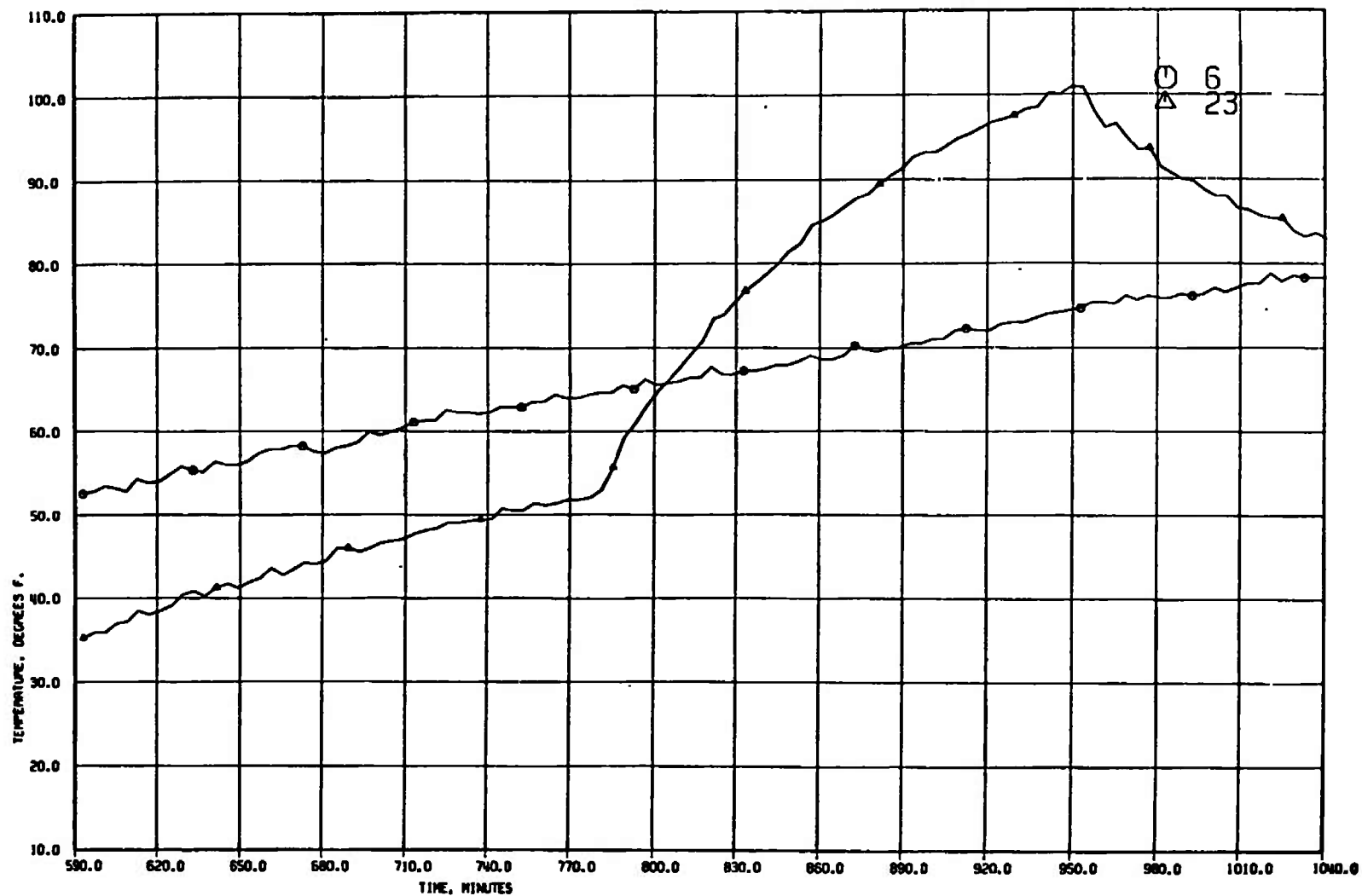
a. Continued  
Fig. 15 Continued



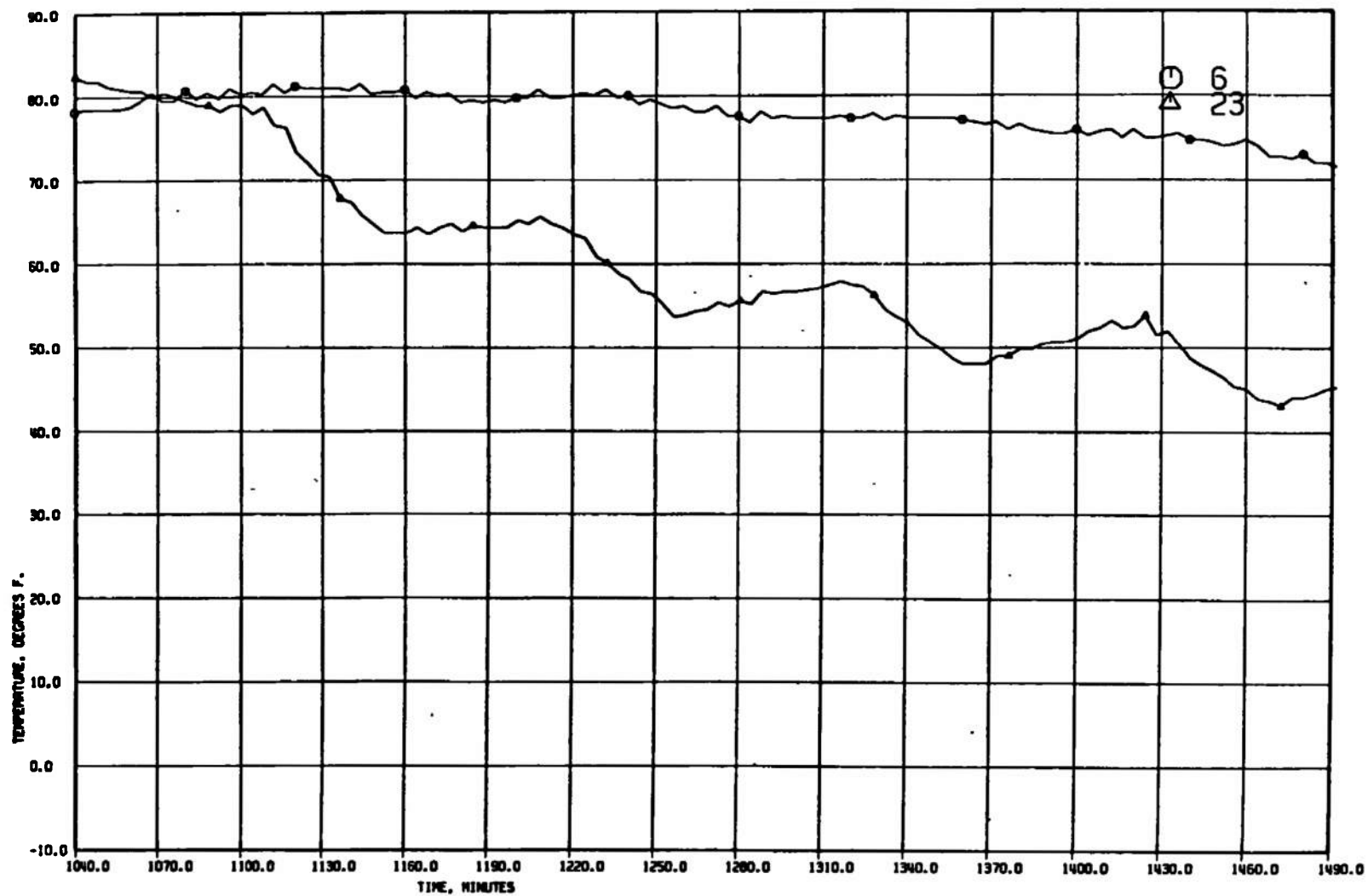
a. Concluded  
Fig. 15 Continued



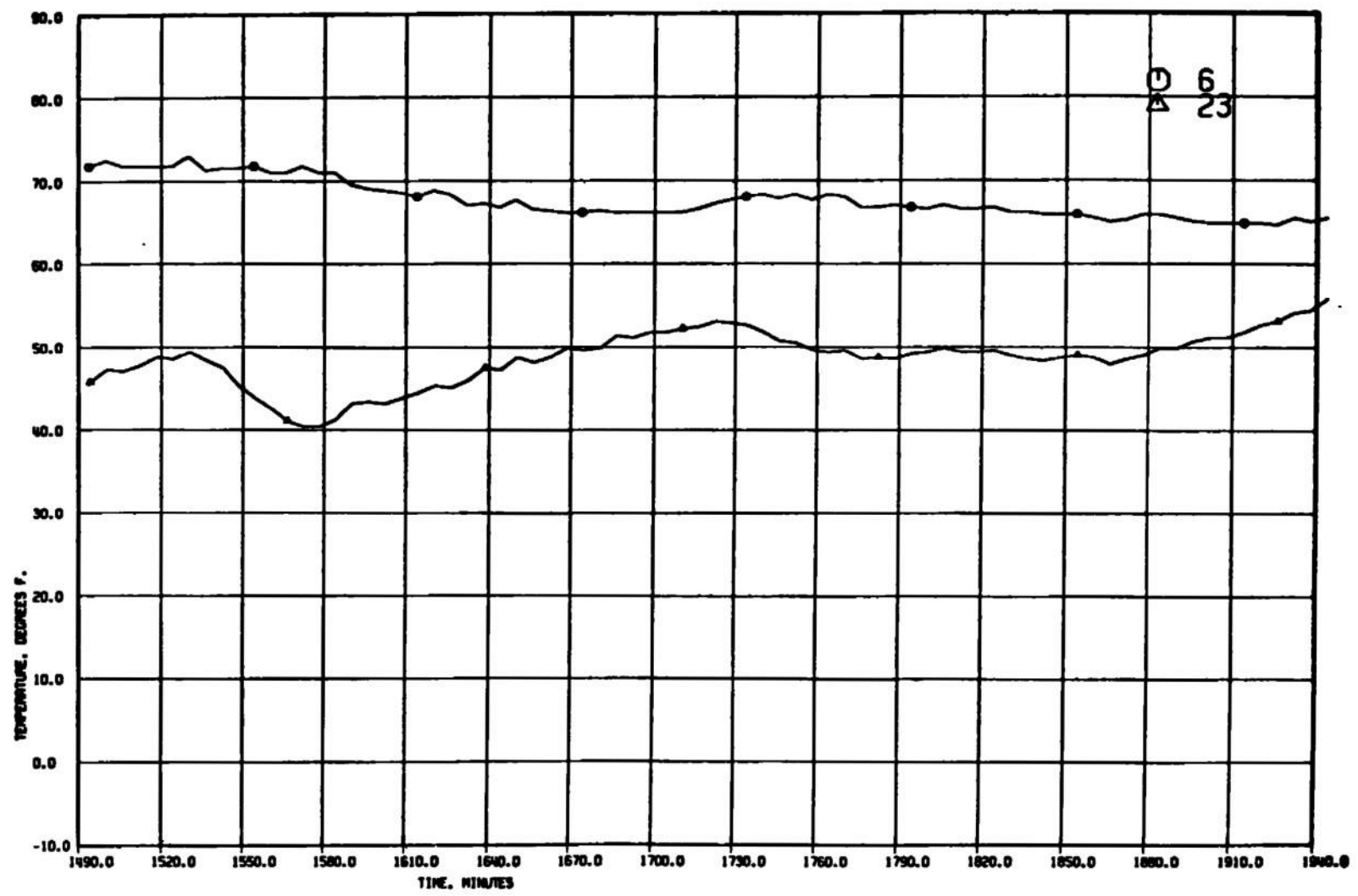
b. T/C 6 and 23  
Fig. 15 Continued



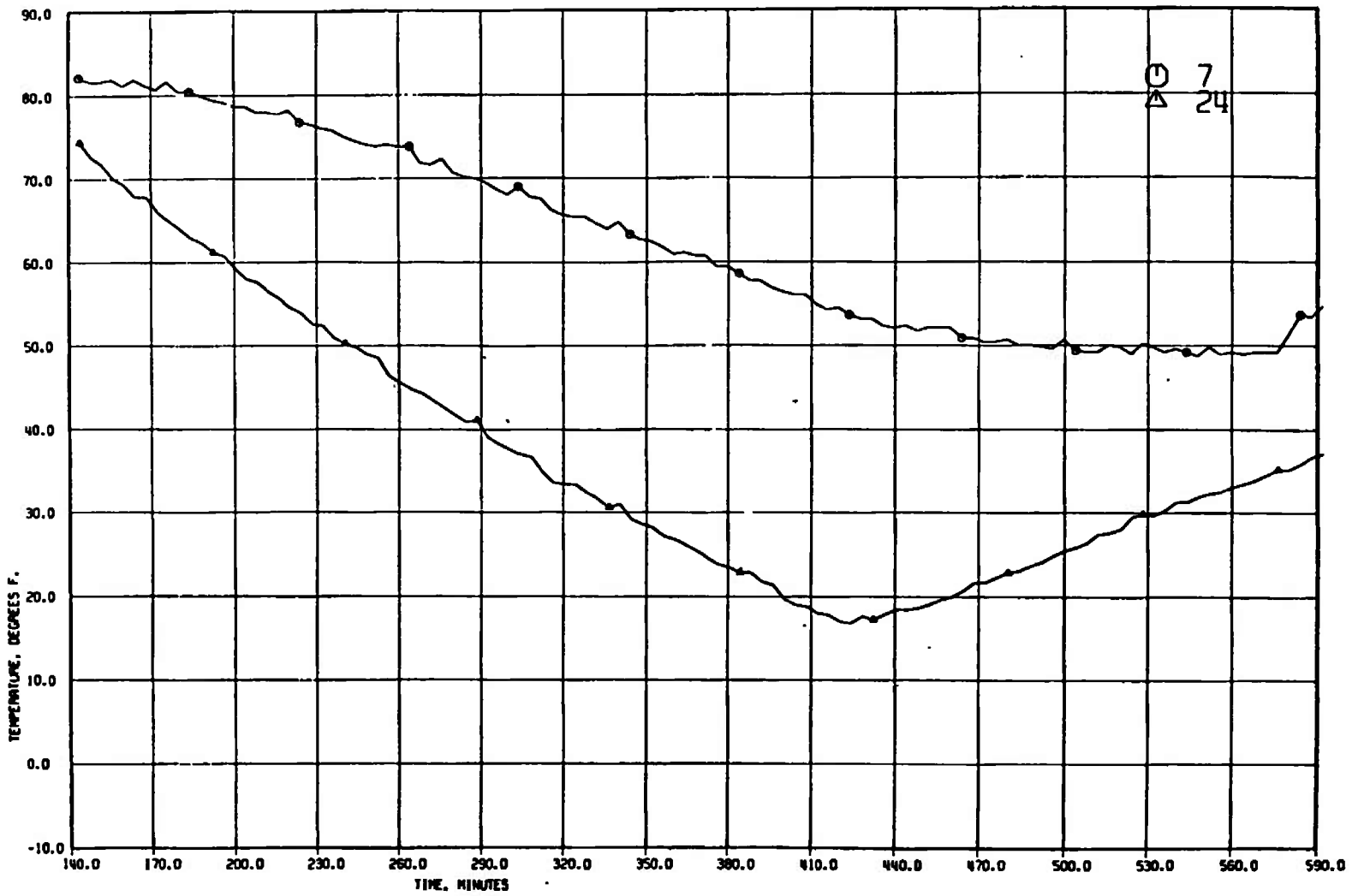
b. Continued  
Fig. 15 Continued



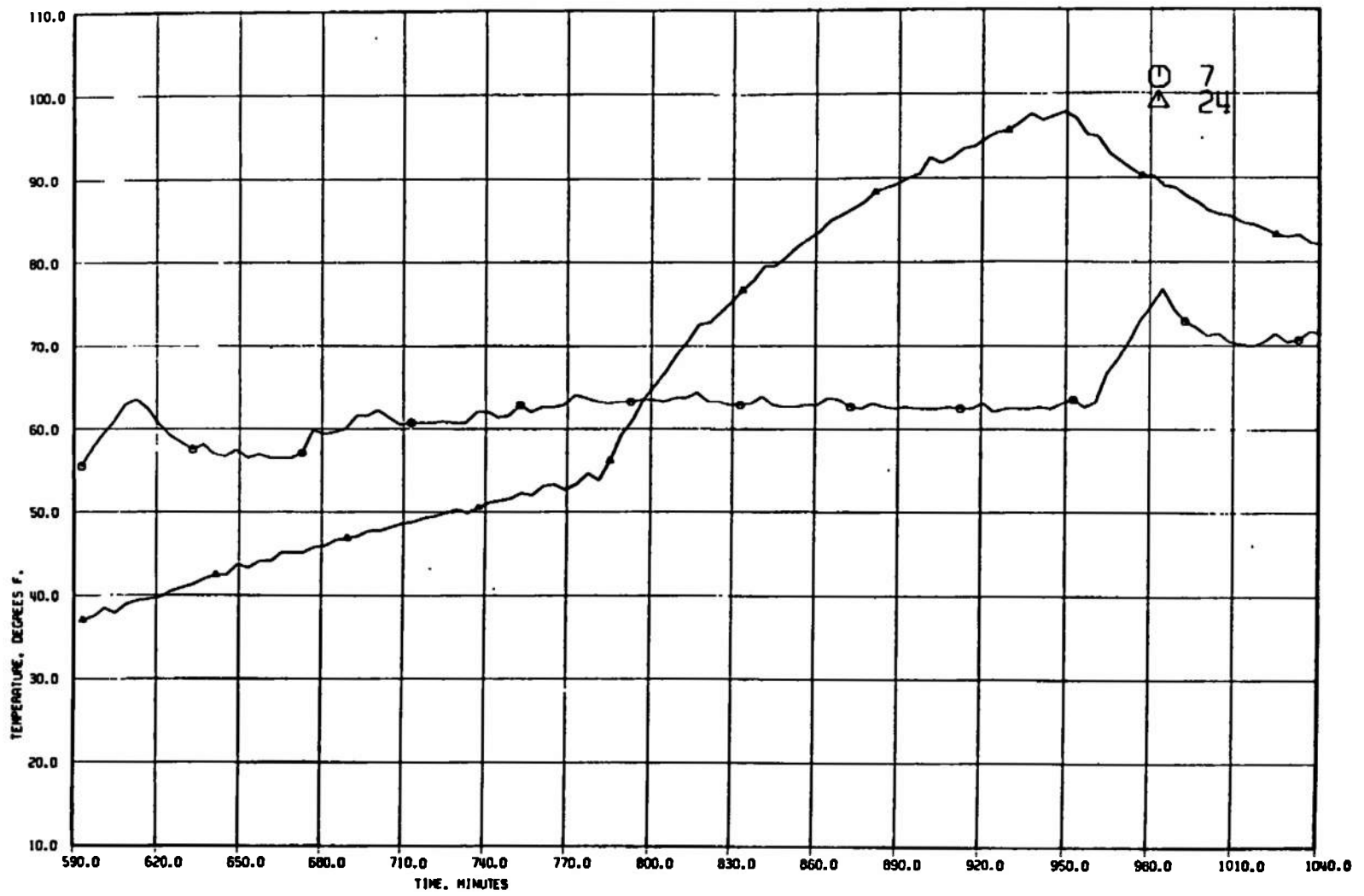
b. Continued  
Fig. 15 Continued



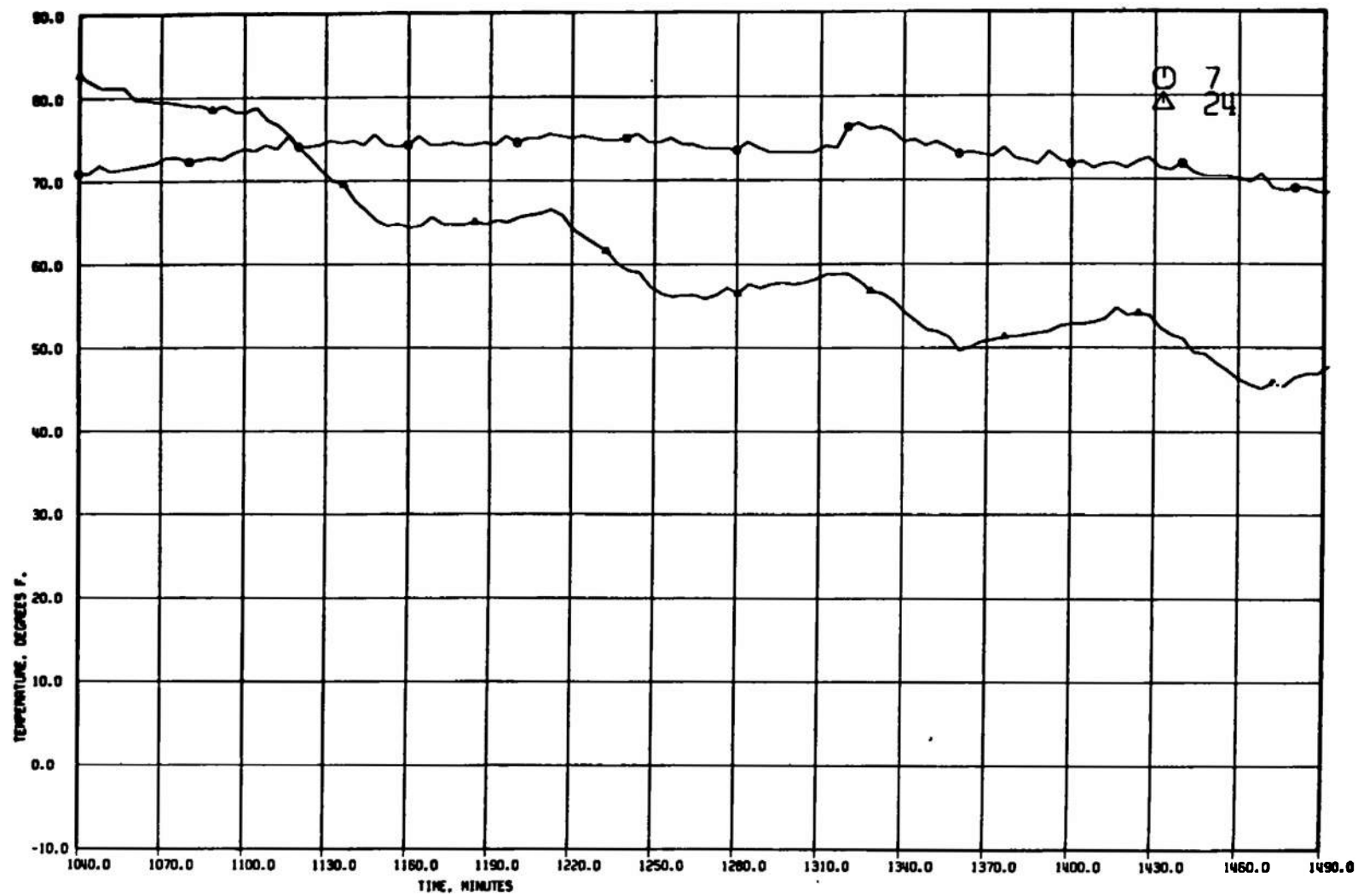
b. Concluded  
Fig. 15 Continued



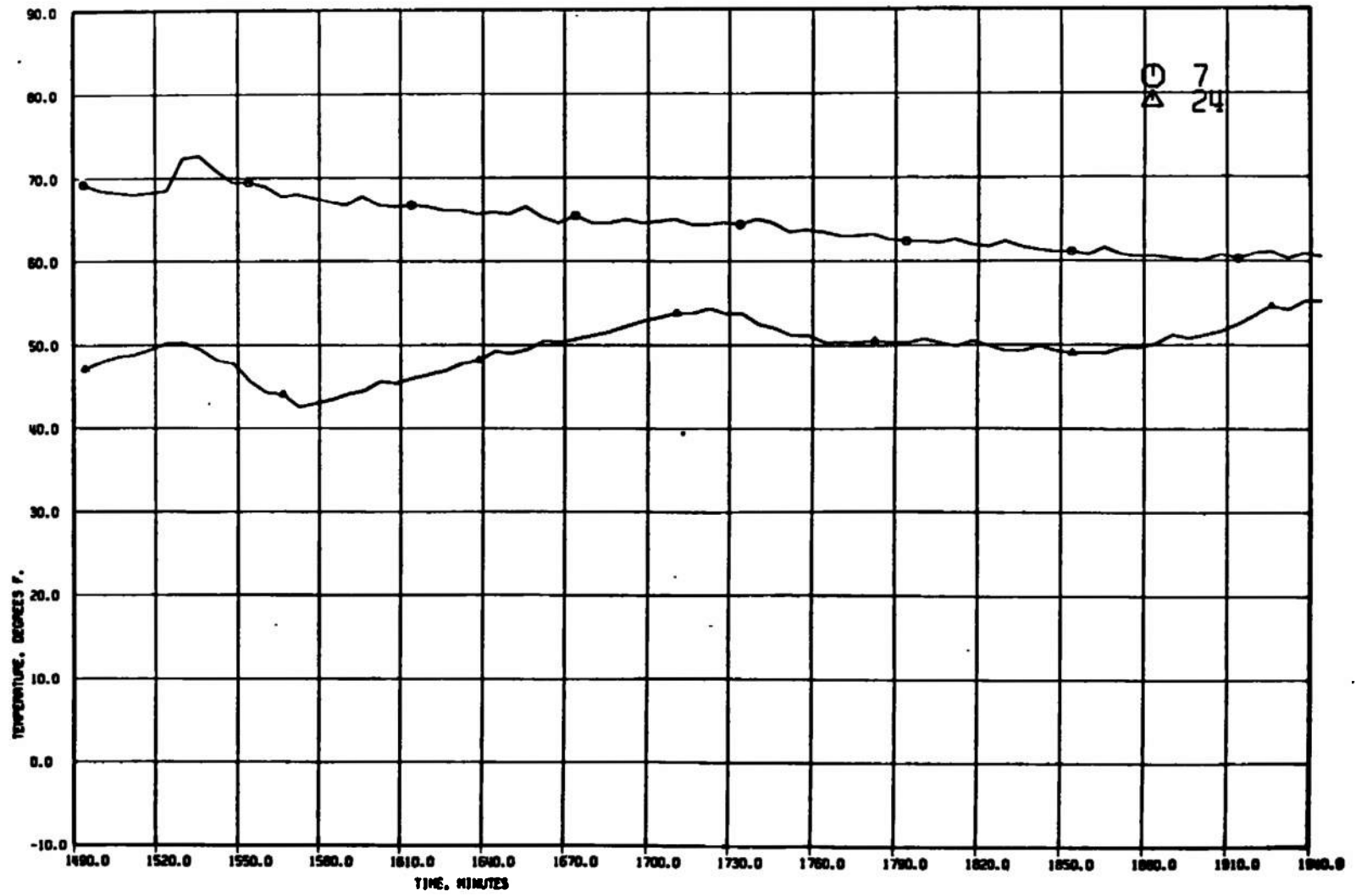
c. T/C 7 and 24  
Fig. 15 Continued



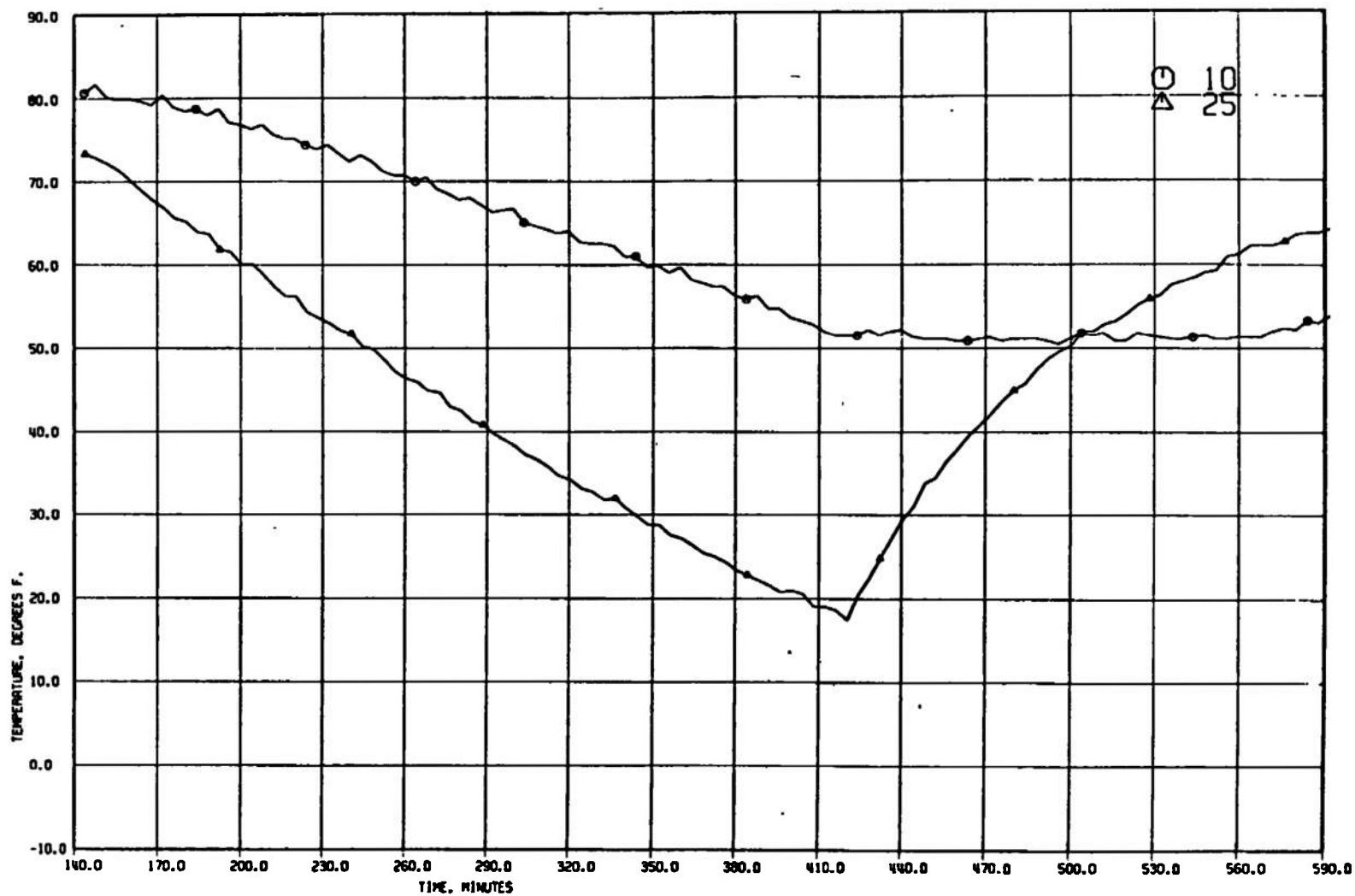
c. Continued  
Fig. 15 Continued



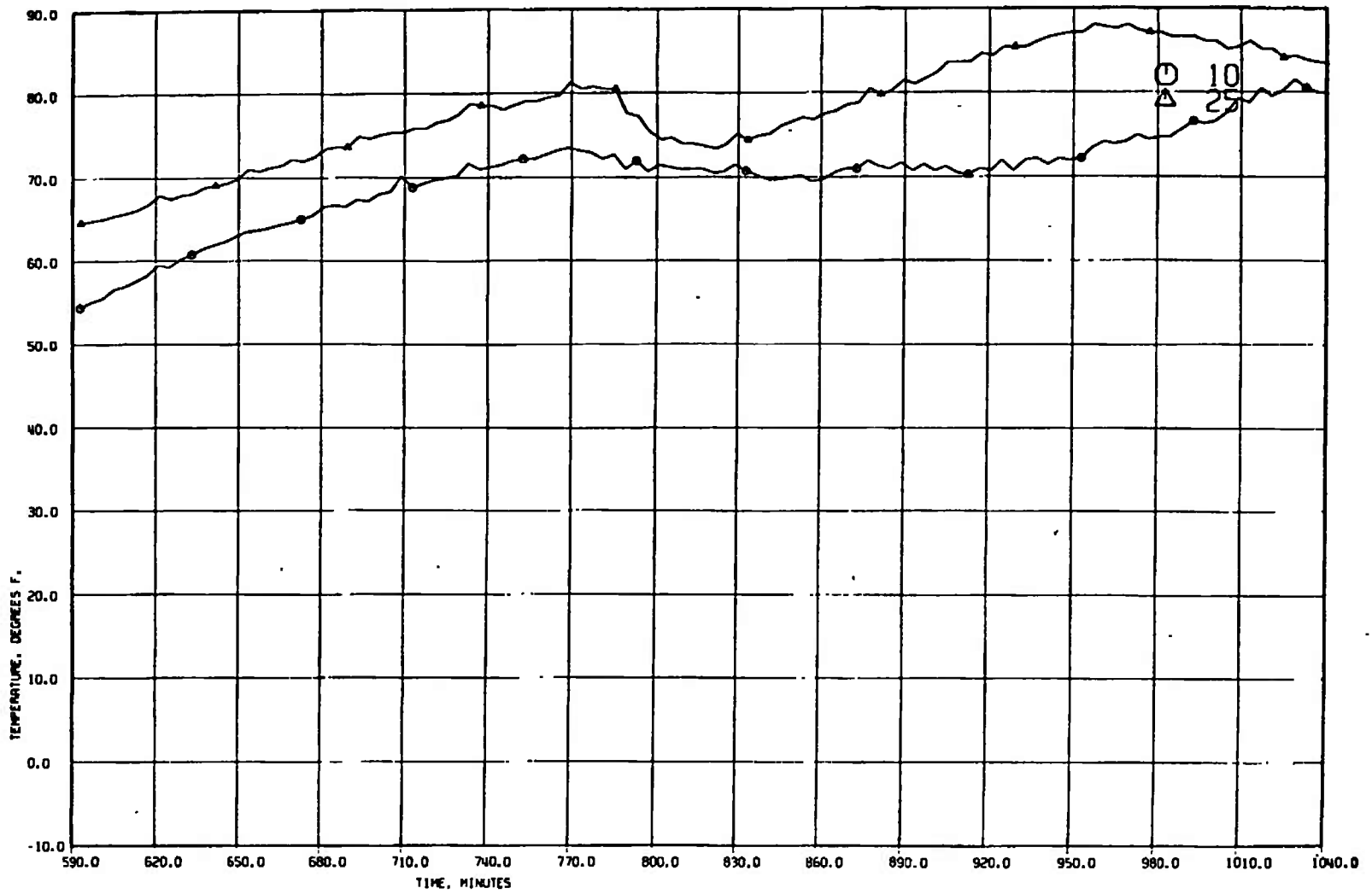
c. Continued  
Fig. 15 Continued



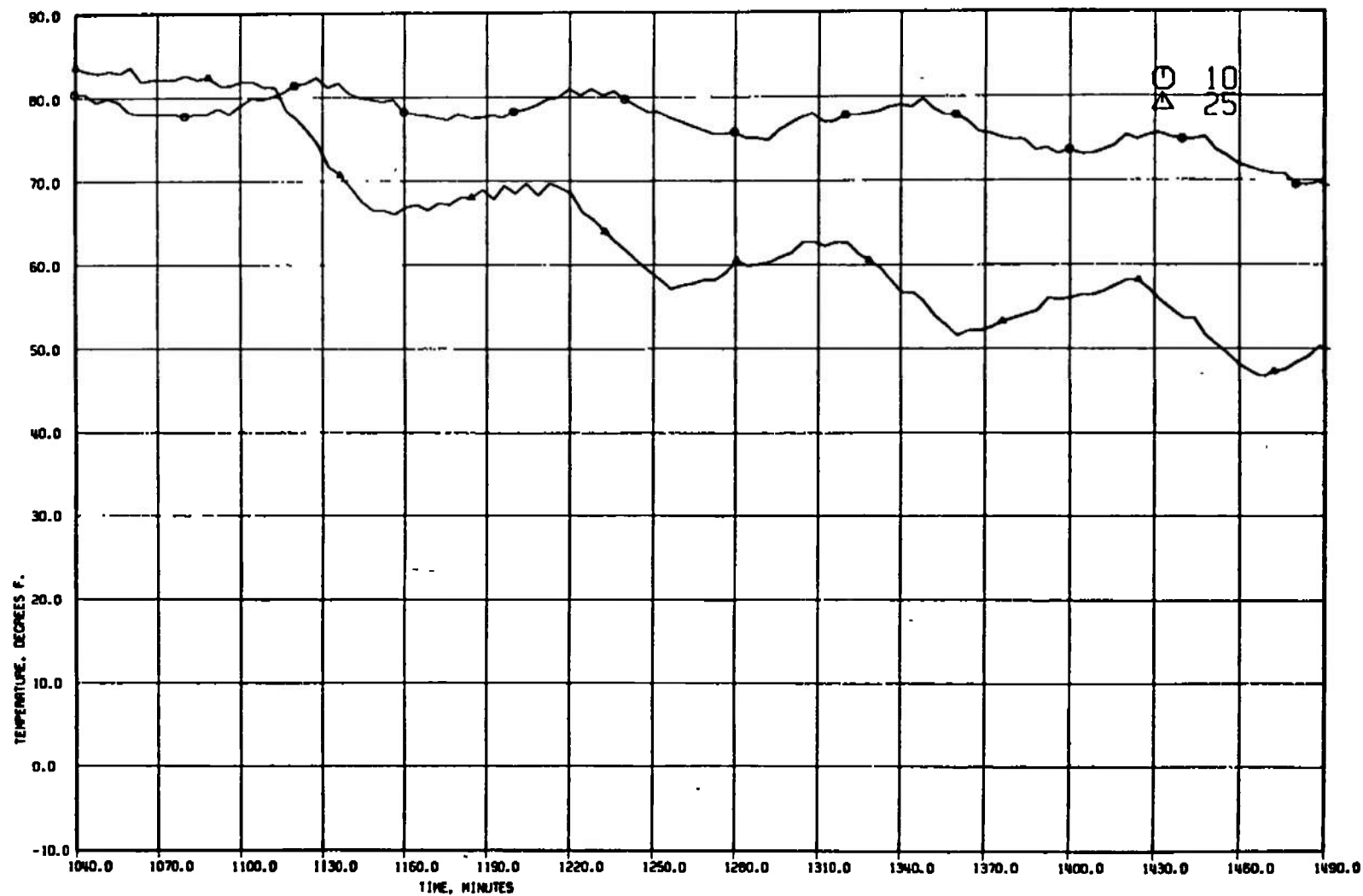
c. Concluded  
Fig. 15 Continued



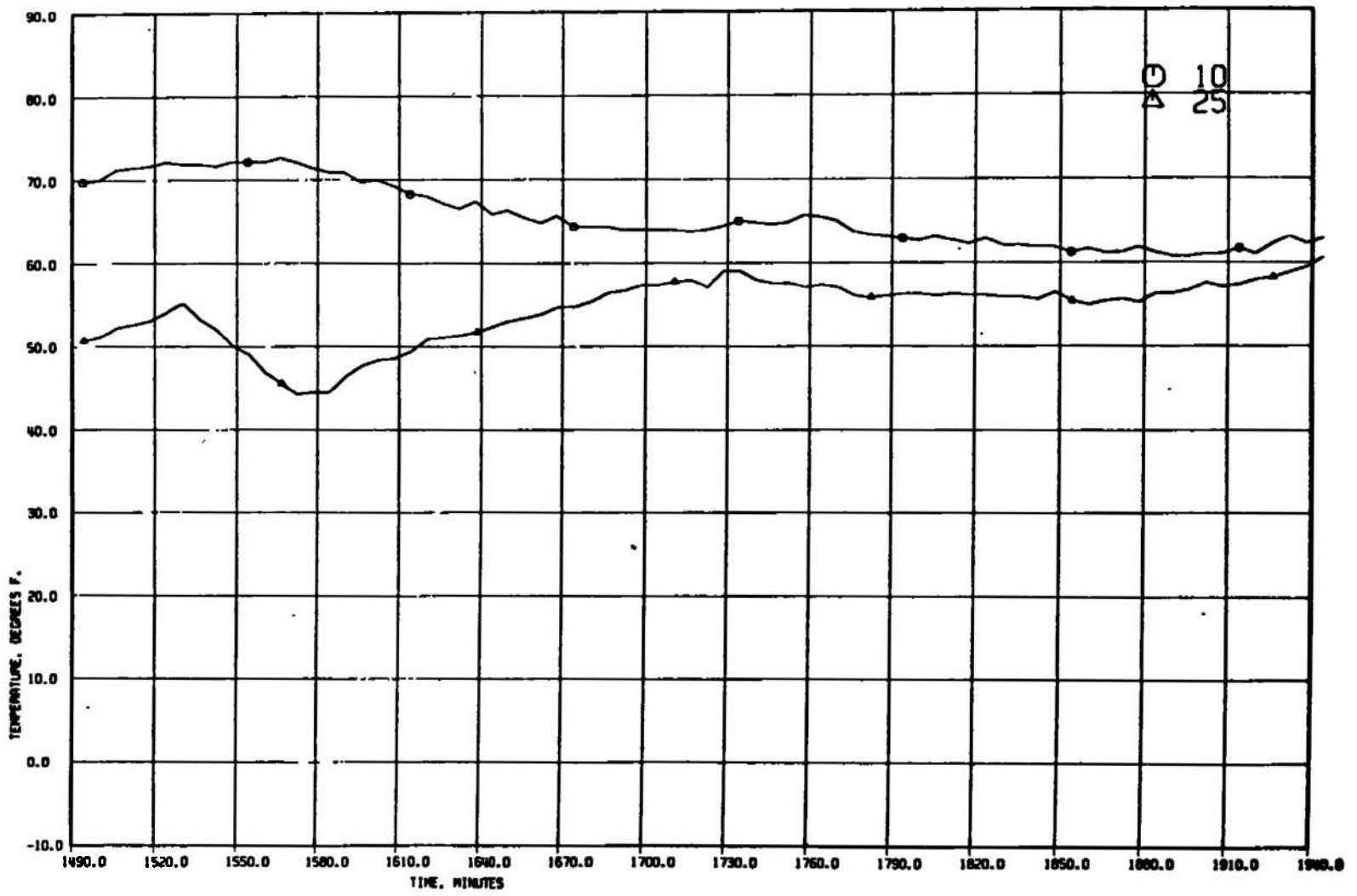
d. T/C 10 and 25  
Fig. 15 Continued



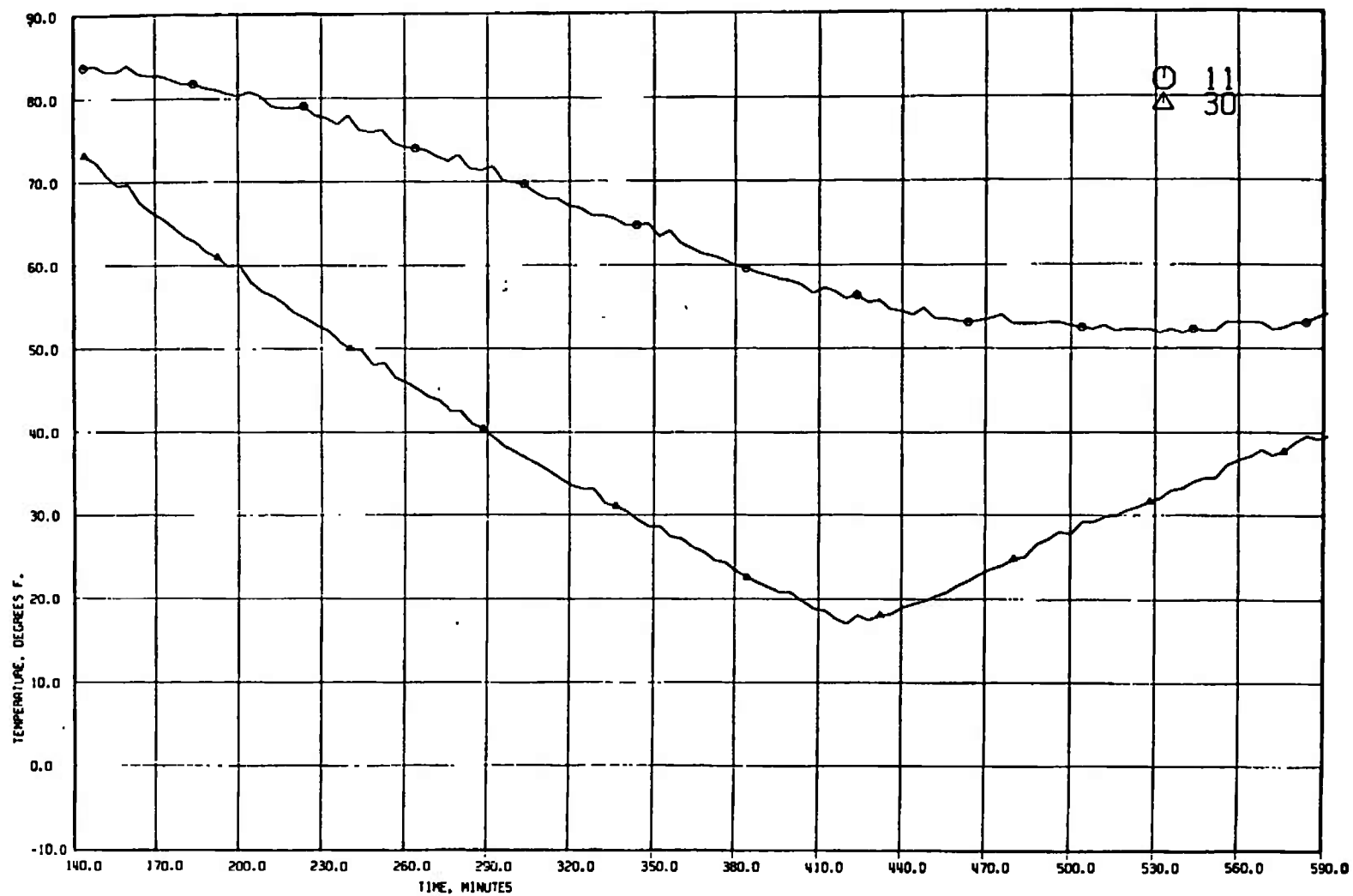
d. Continued  
Fig. 15 Continued



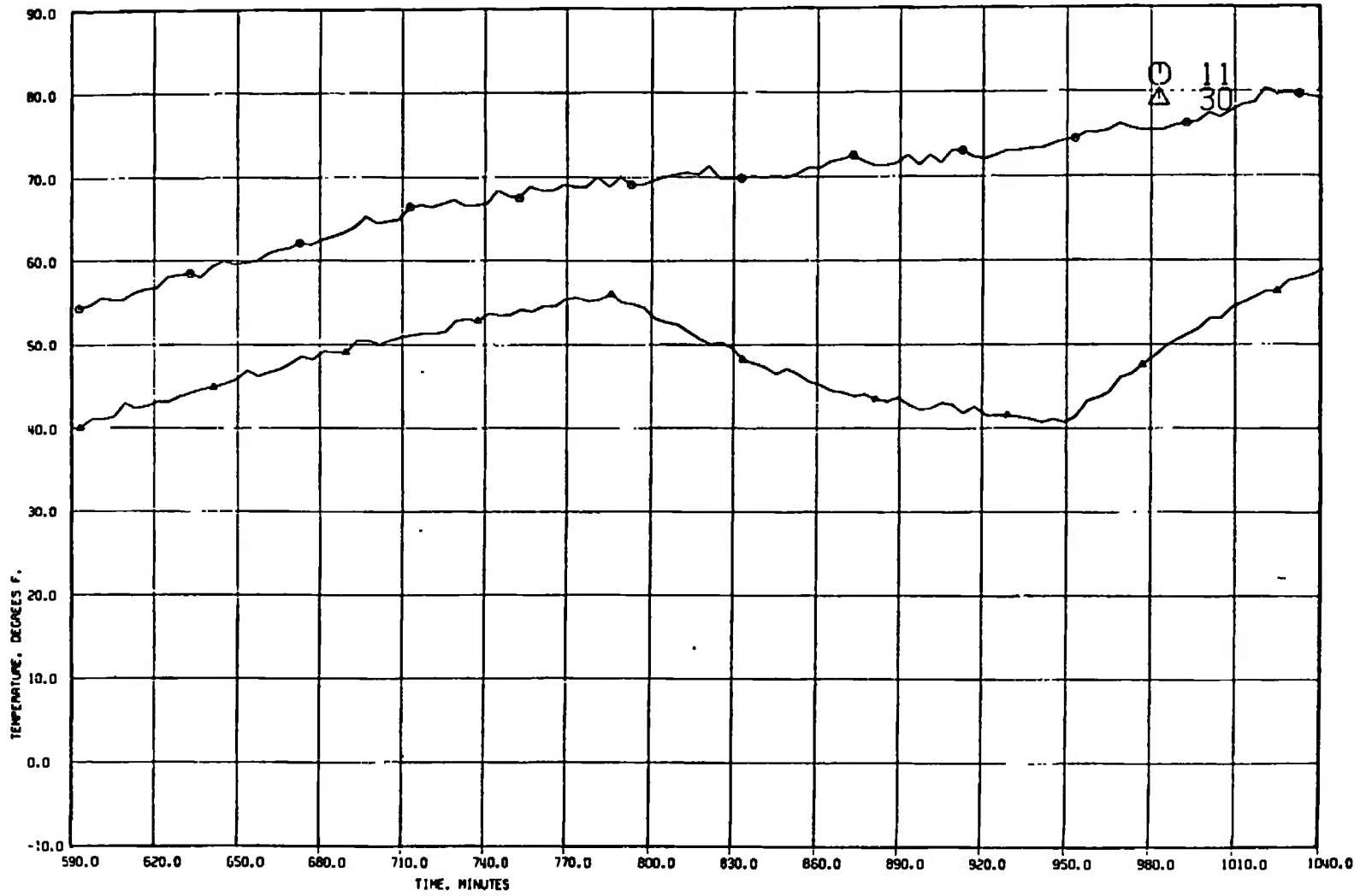
d. Continued  
Fig. 15 Continued



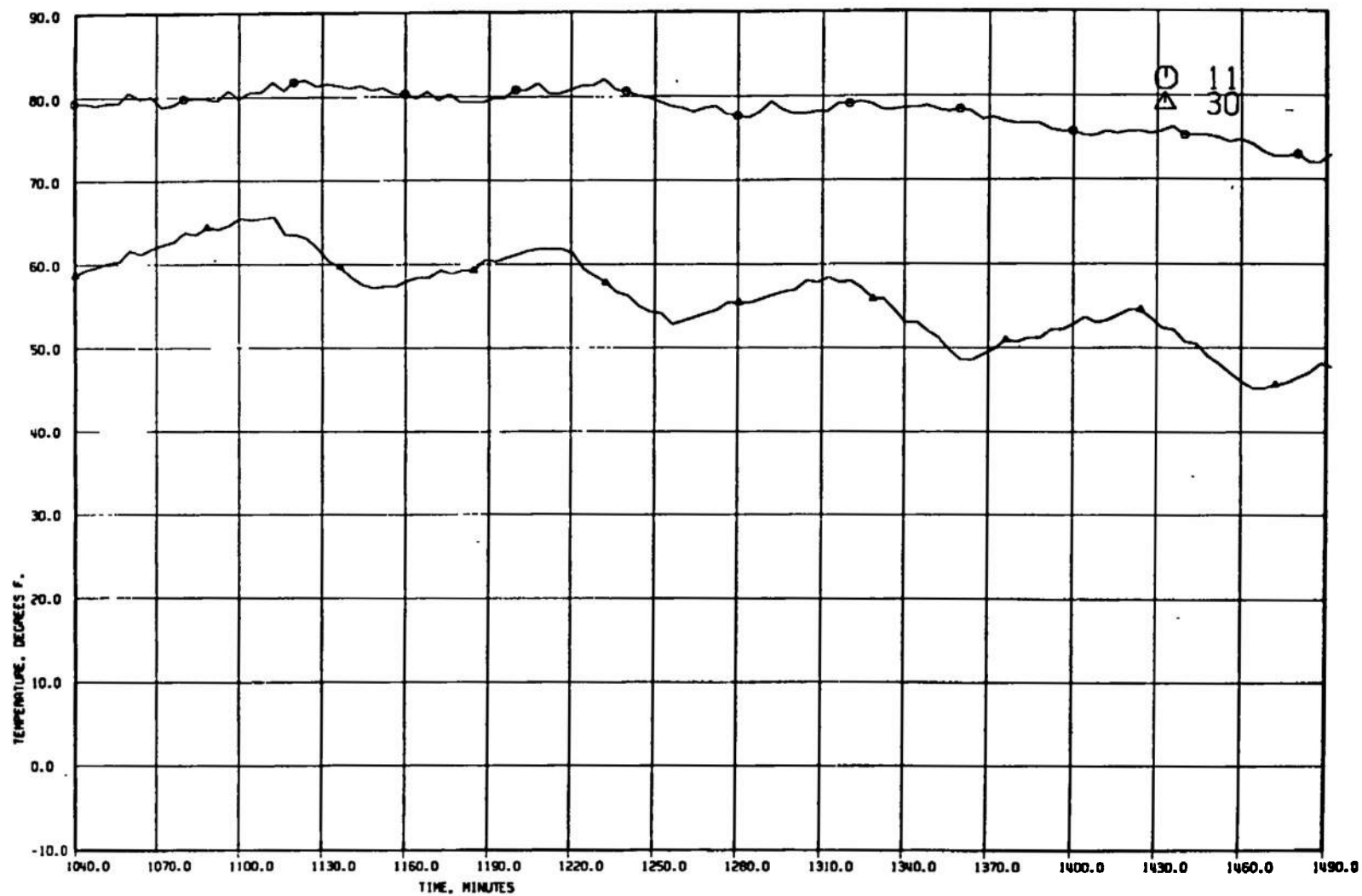
d. Concluded  
Fig. 15 Continued



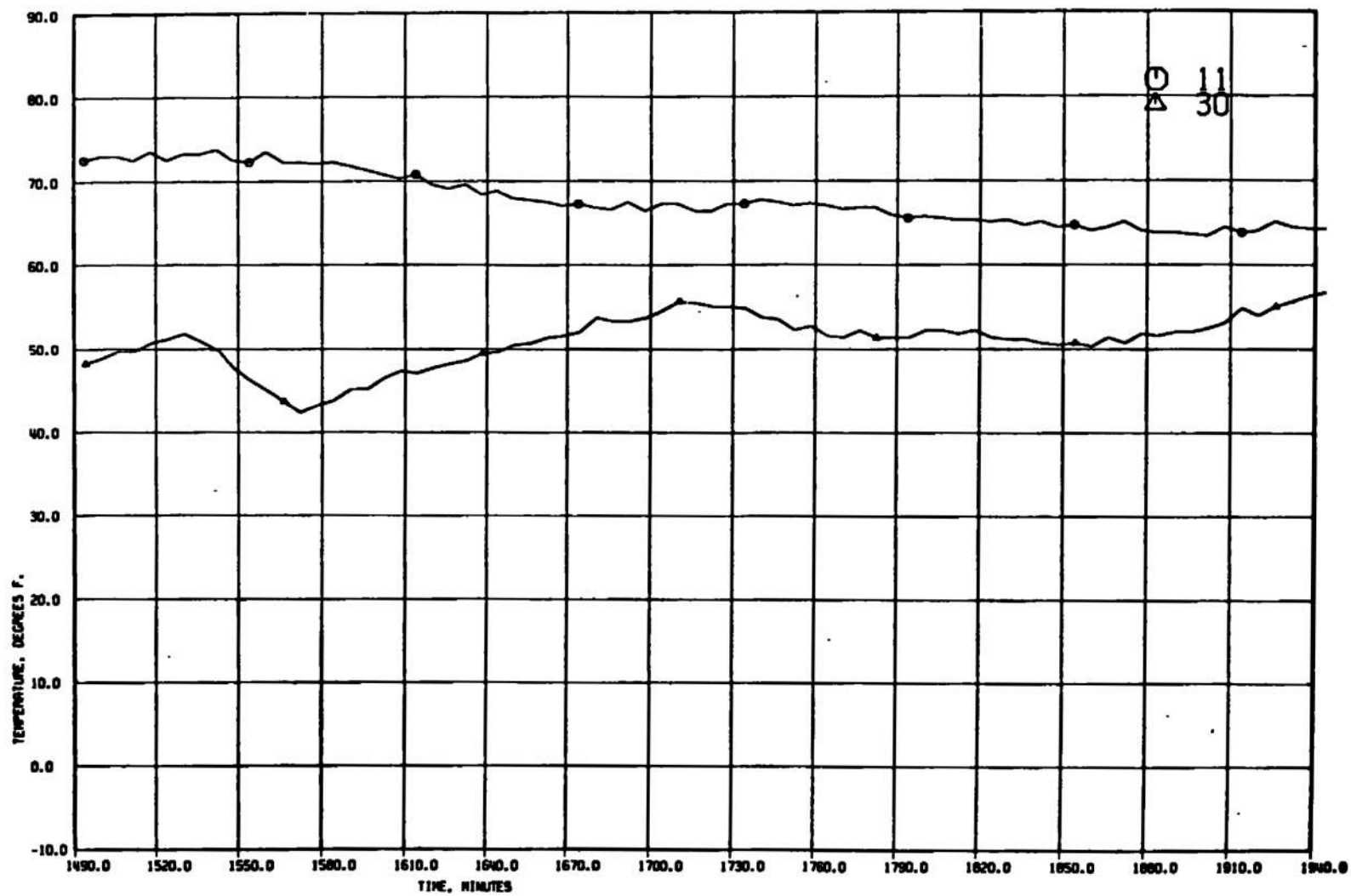
e. T/C 11 and 30  
Fig. 15 Continued



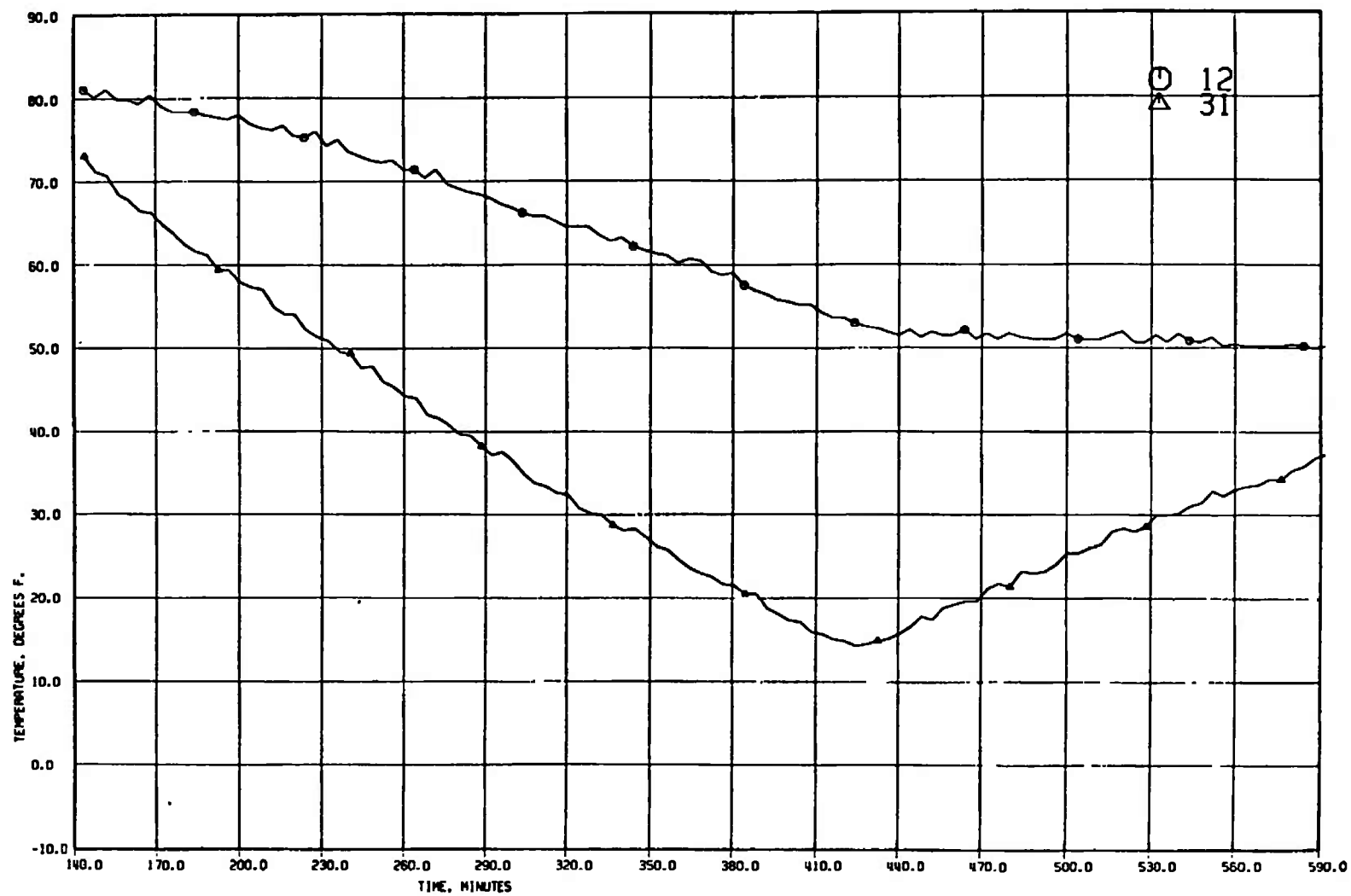
e. Continued  
Fig. 15 Continued



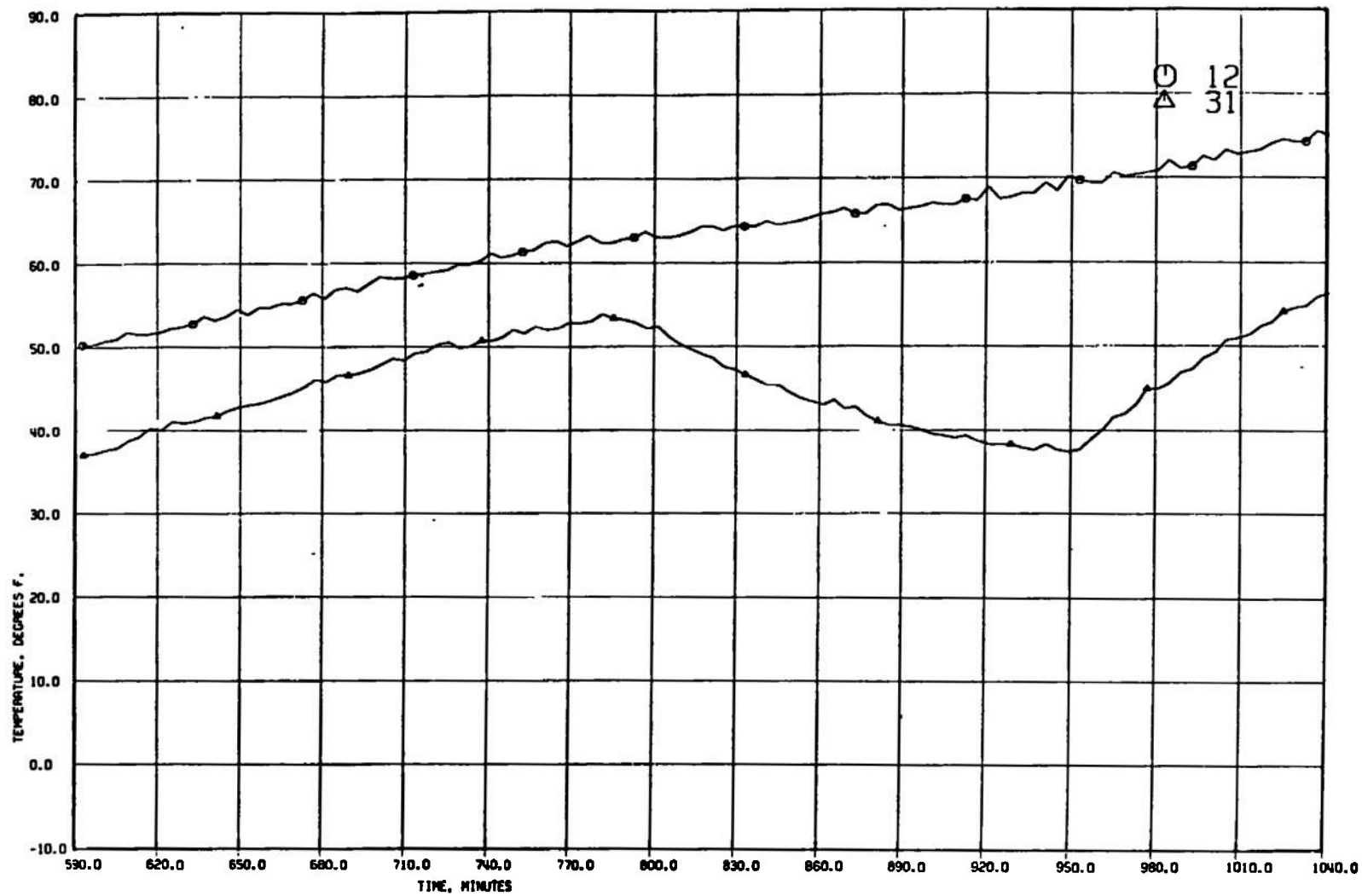
e. Continued  
Fig. 15 Continued



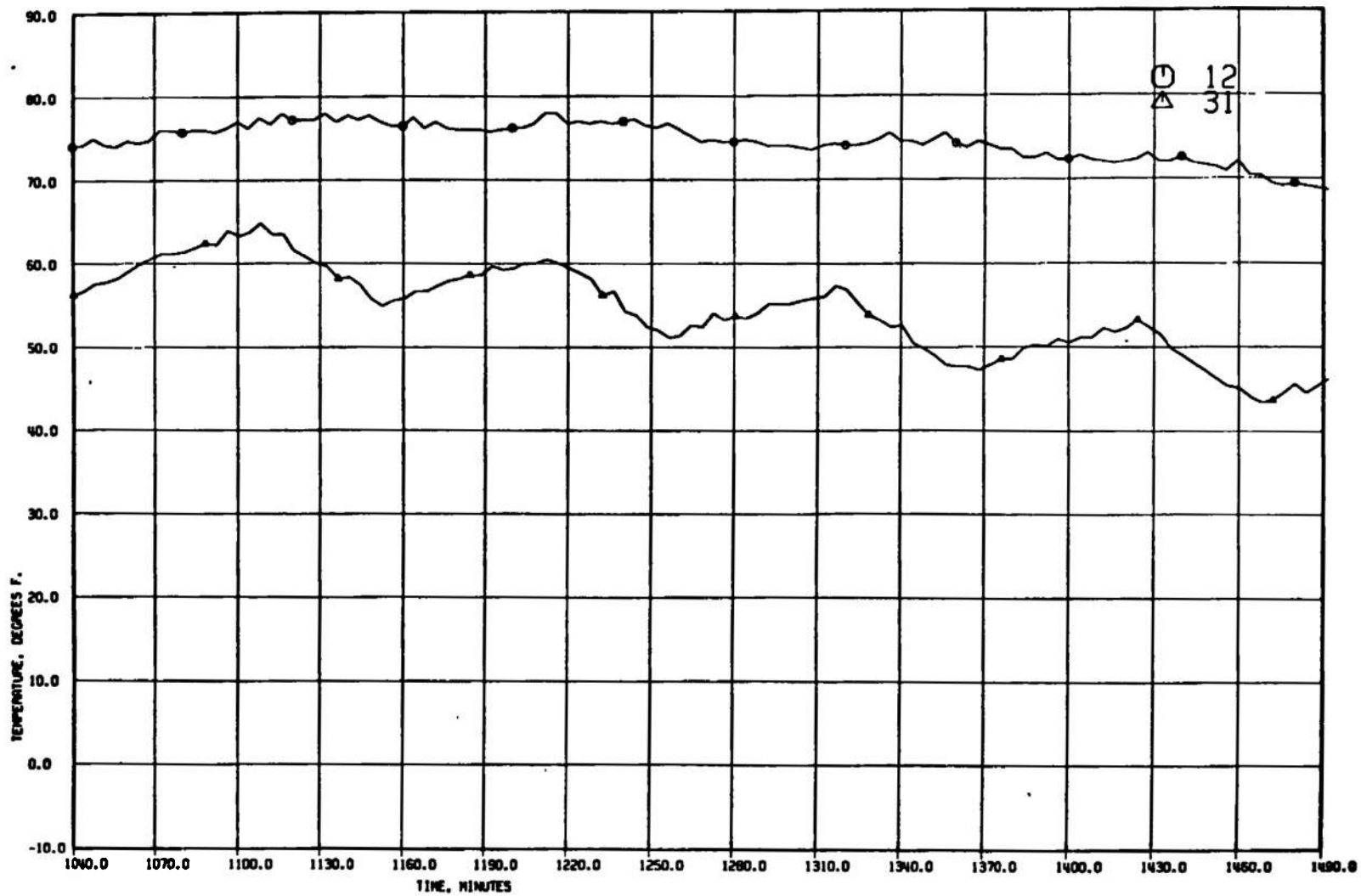
e. Concluded  
Fig. 15 Continued



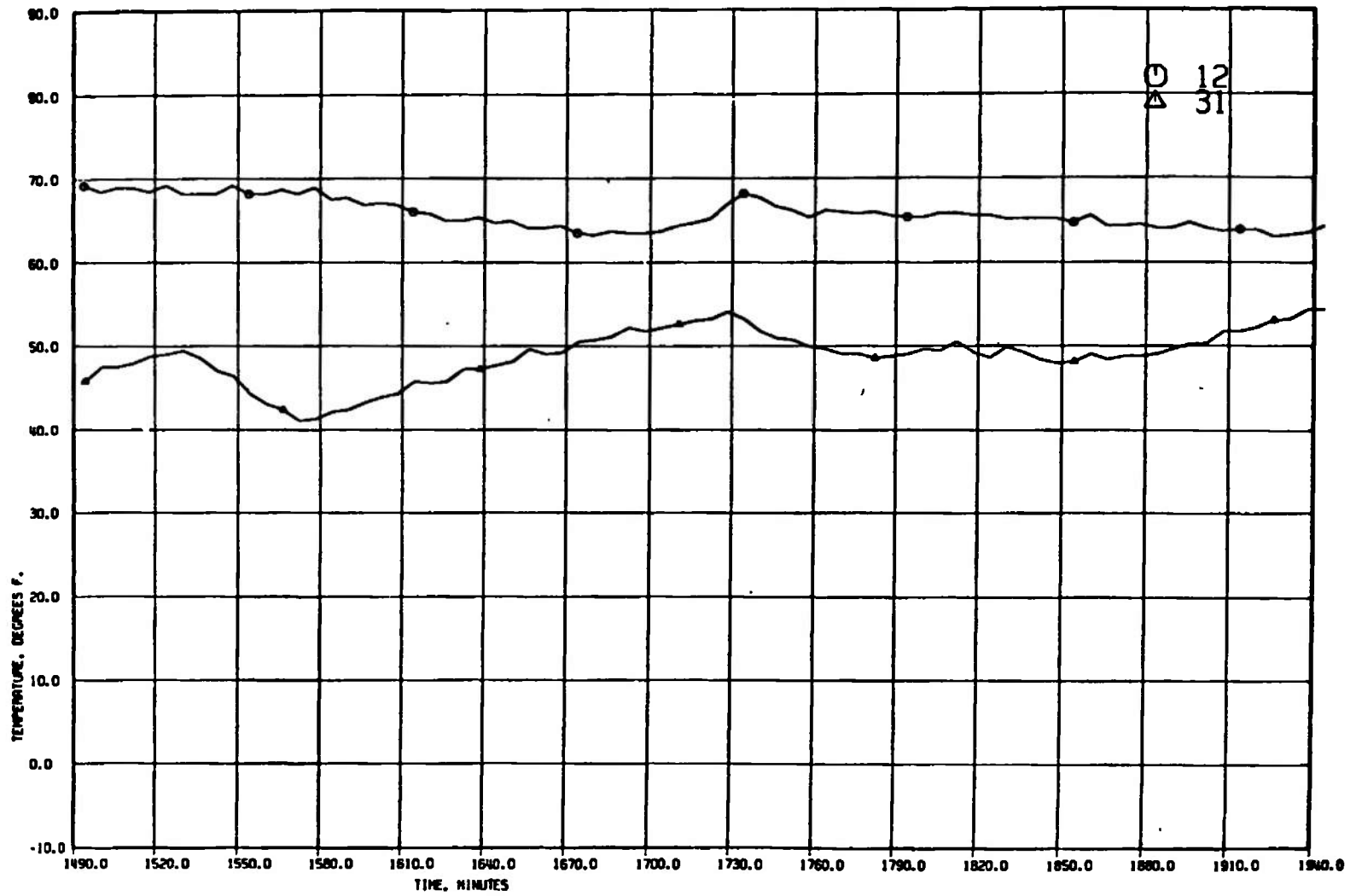
f. T/C 12 and 31  
Fig. 15 Continued



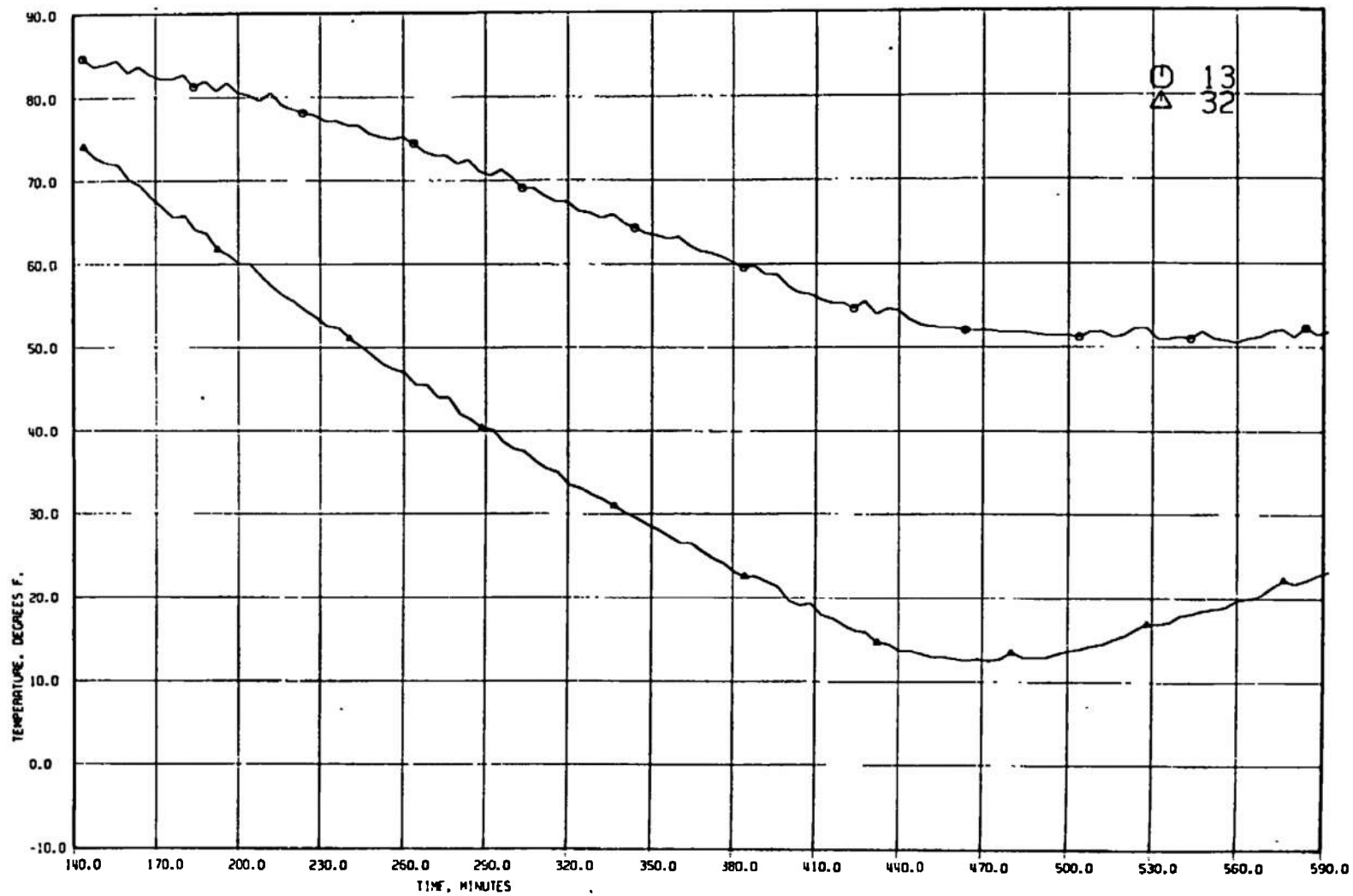
f. Continued  
Fig. 15 Continued



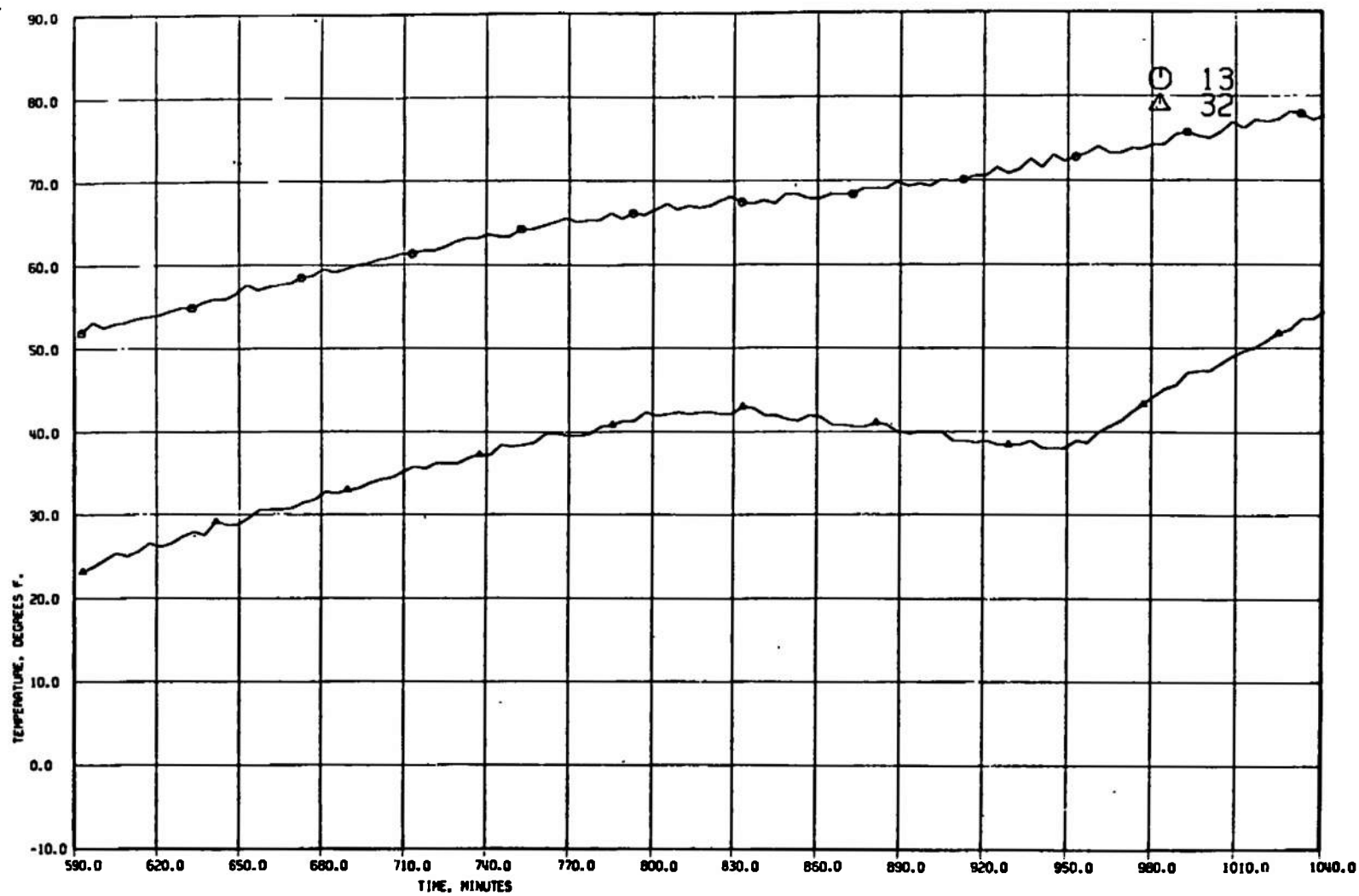
f. Continued  
Fig. 15 Continued



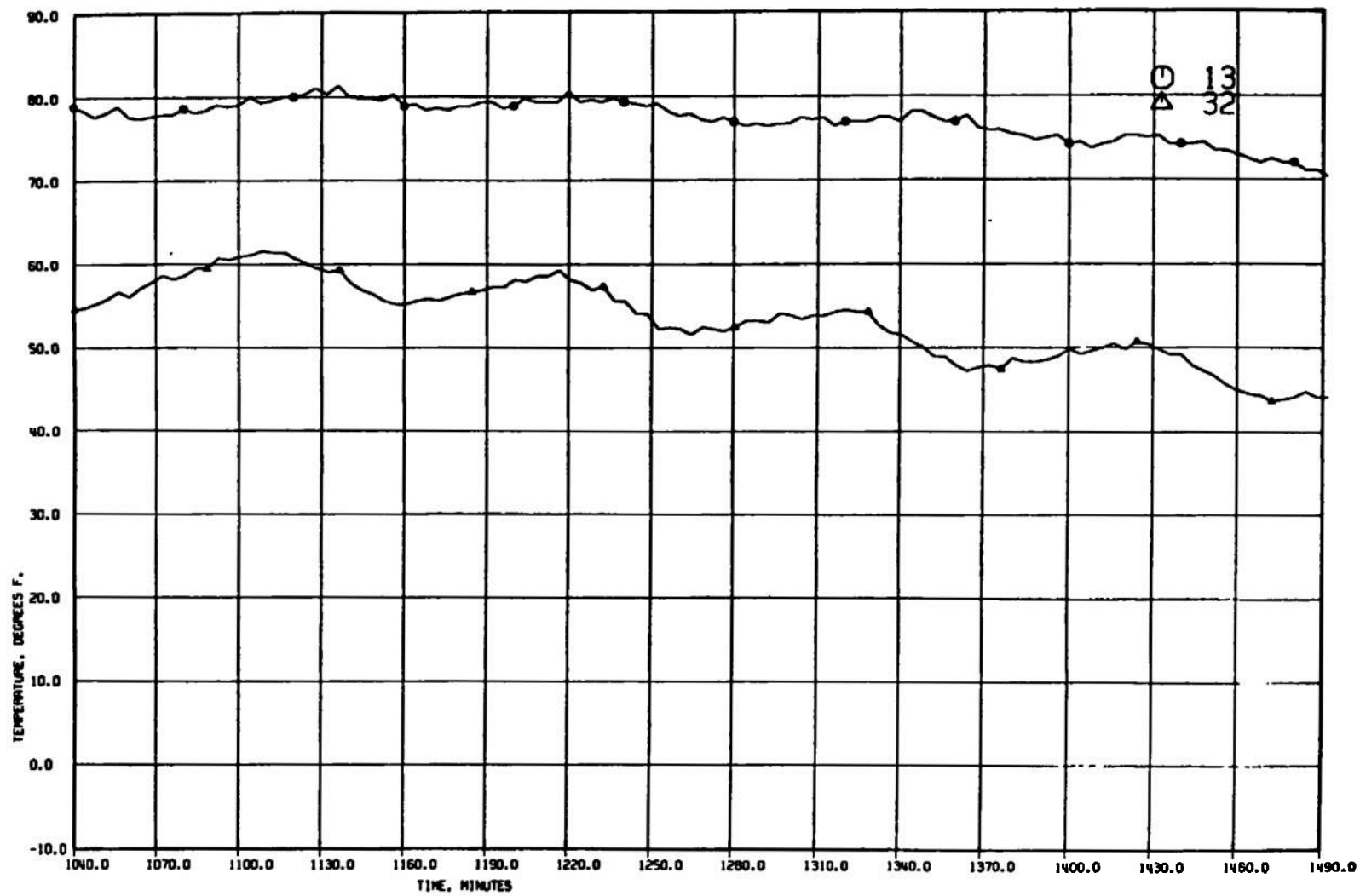
f. Concluded  
Fig. 15 Continued



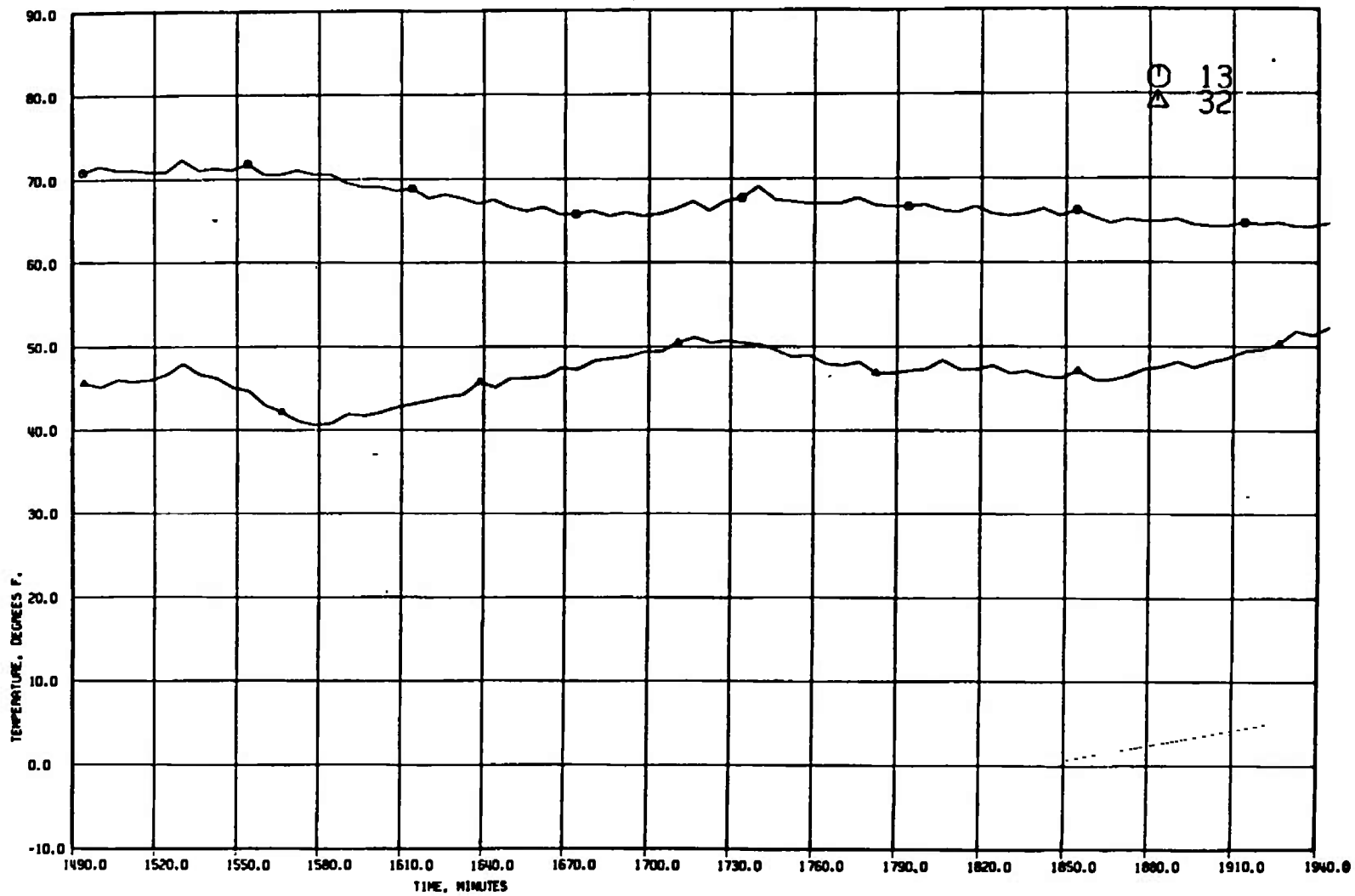
g. T/C 13 and 32  
Fig. 15 Continued



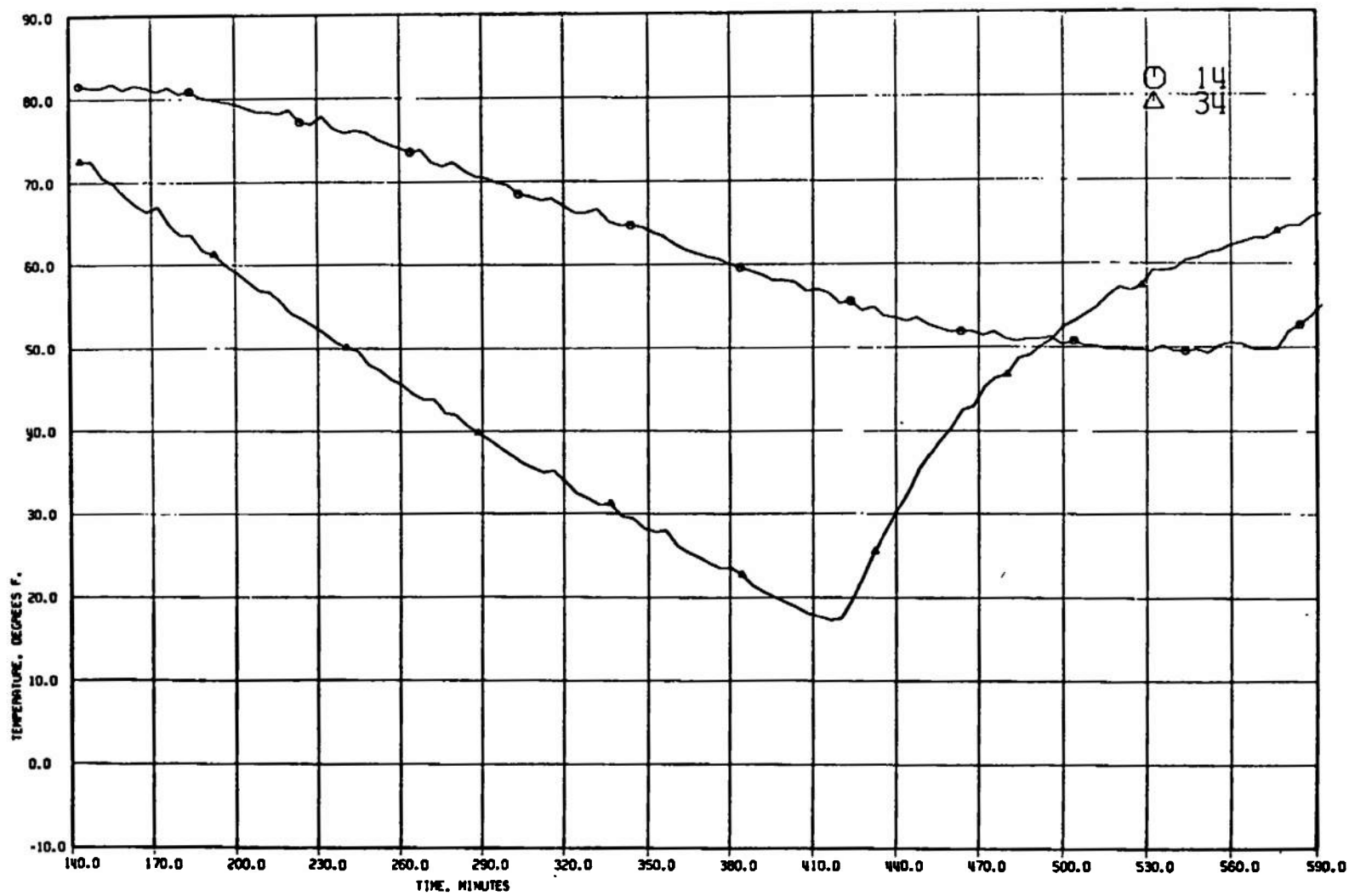
g. Continued  
Fig. 15 Continued



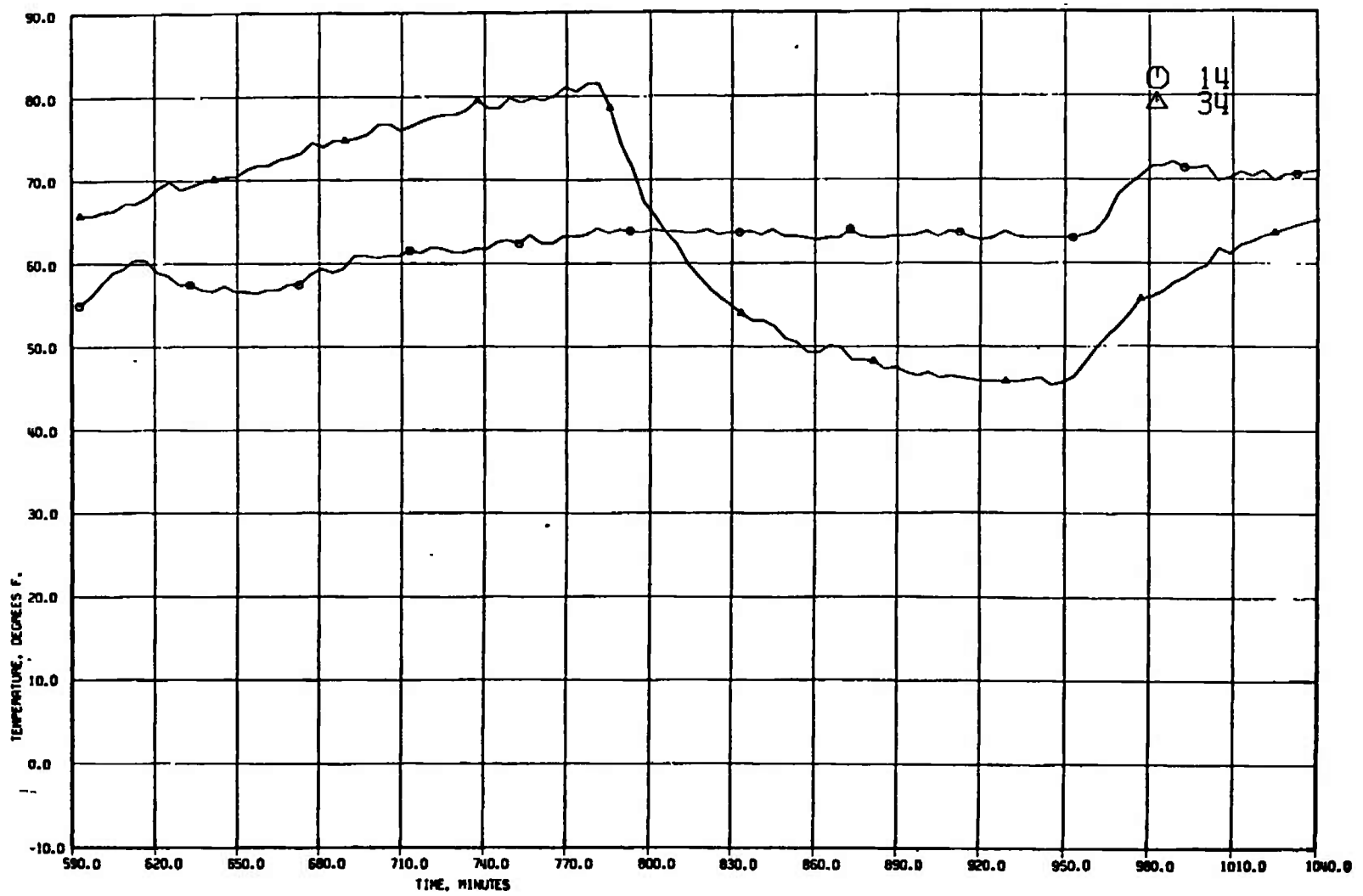
g. Continued  
Fig. 15 Continued



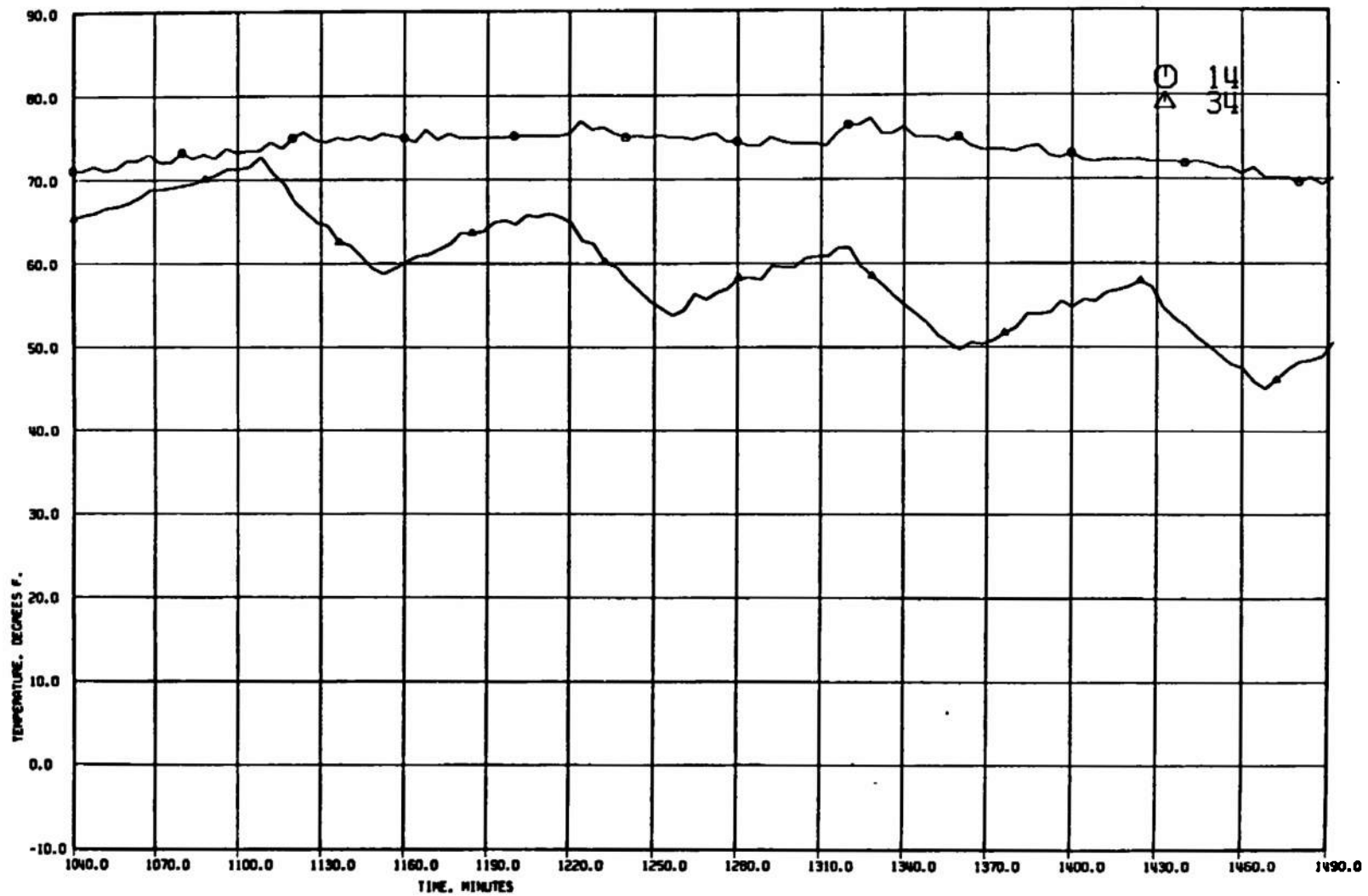
g. Concluded  
Fig. 15 Continued



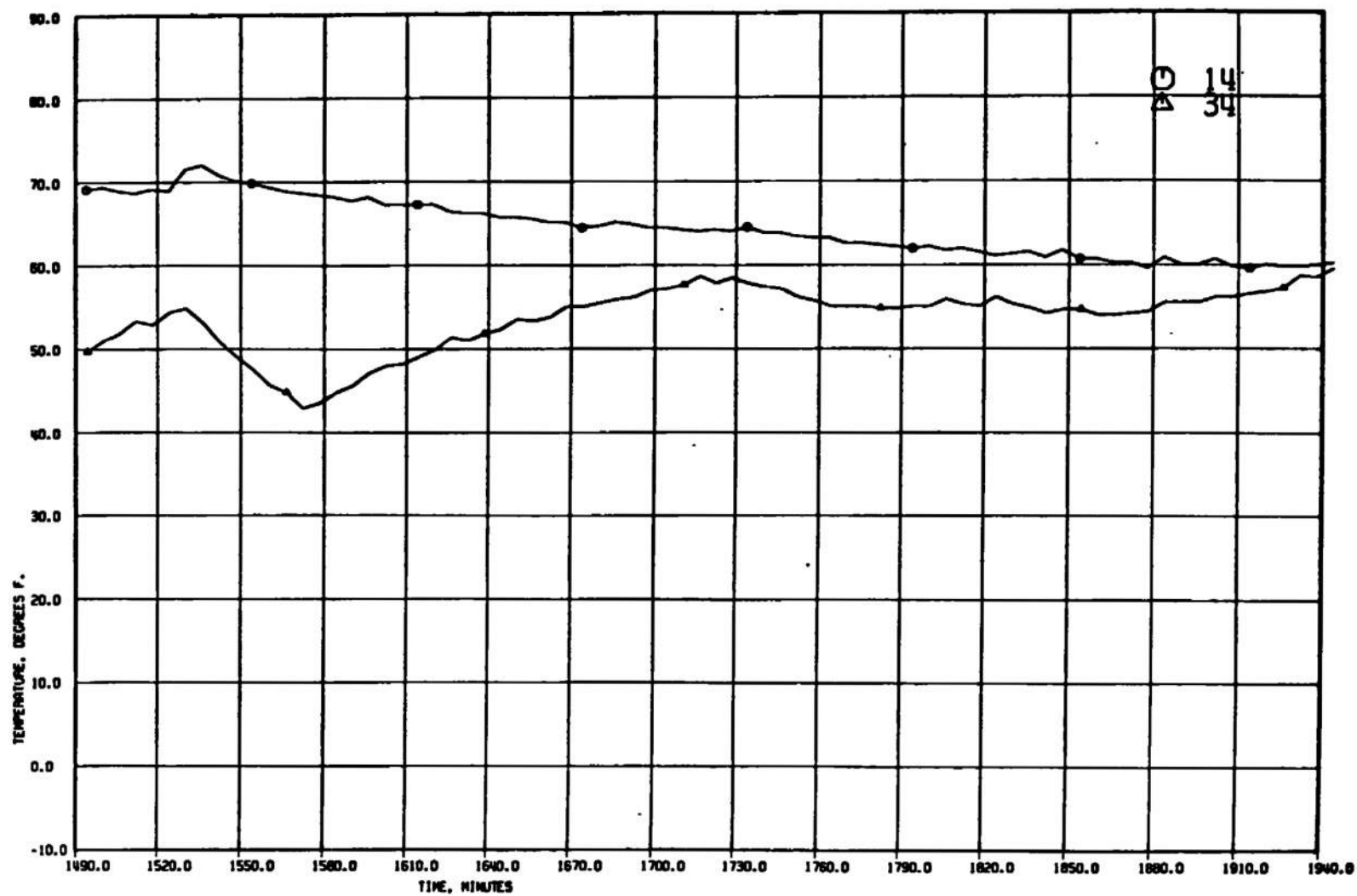
h. T/C 14 and 34  
Fig. 15 Continued



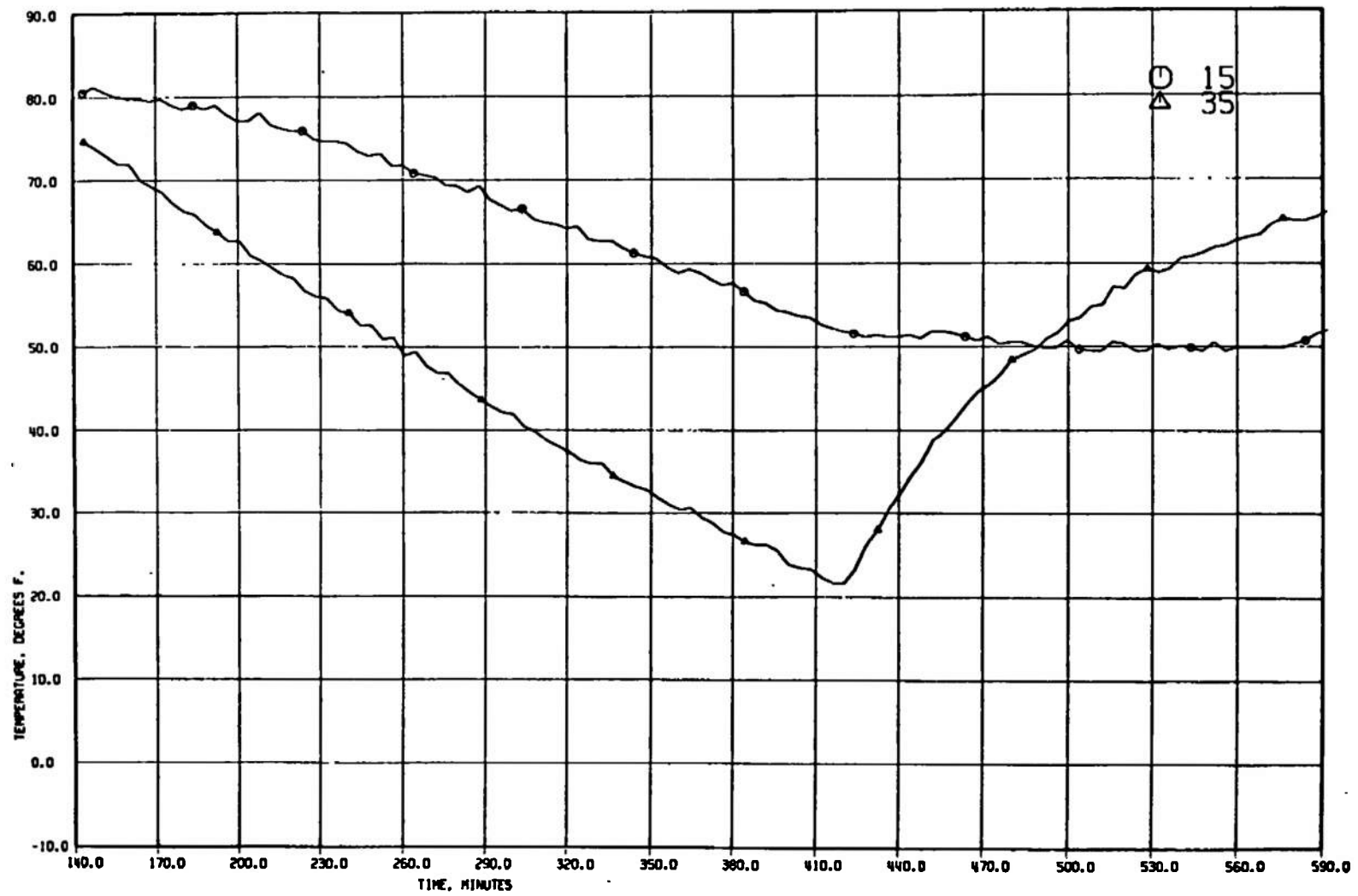
h. Continued  
Fig. 15 Continued



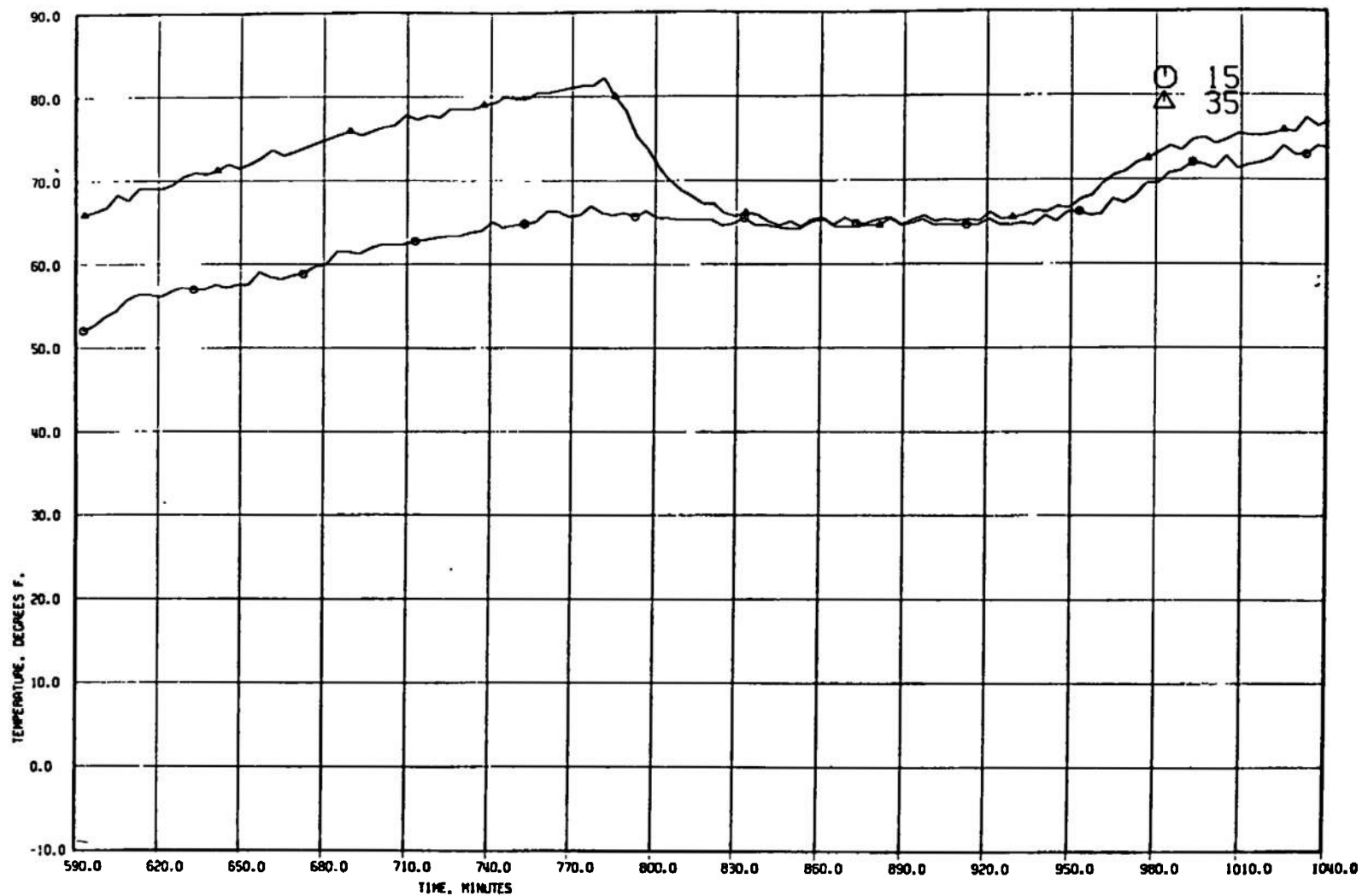
h. Continued  
Fig. 15 Continued



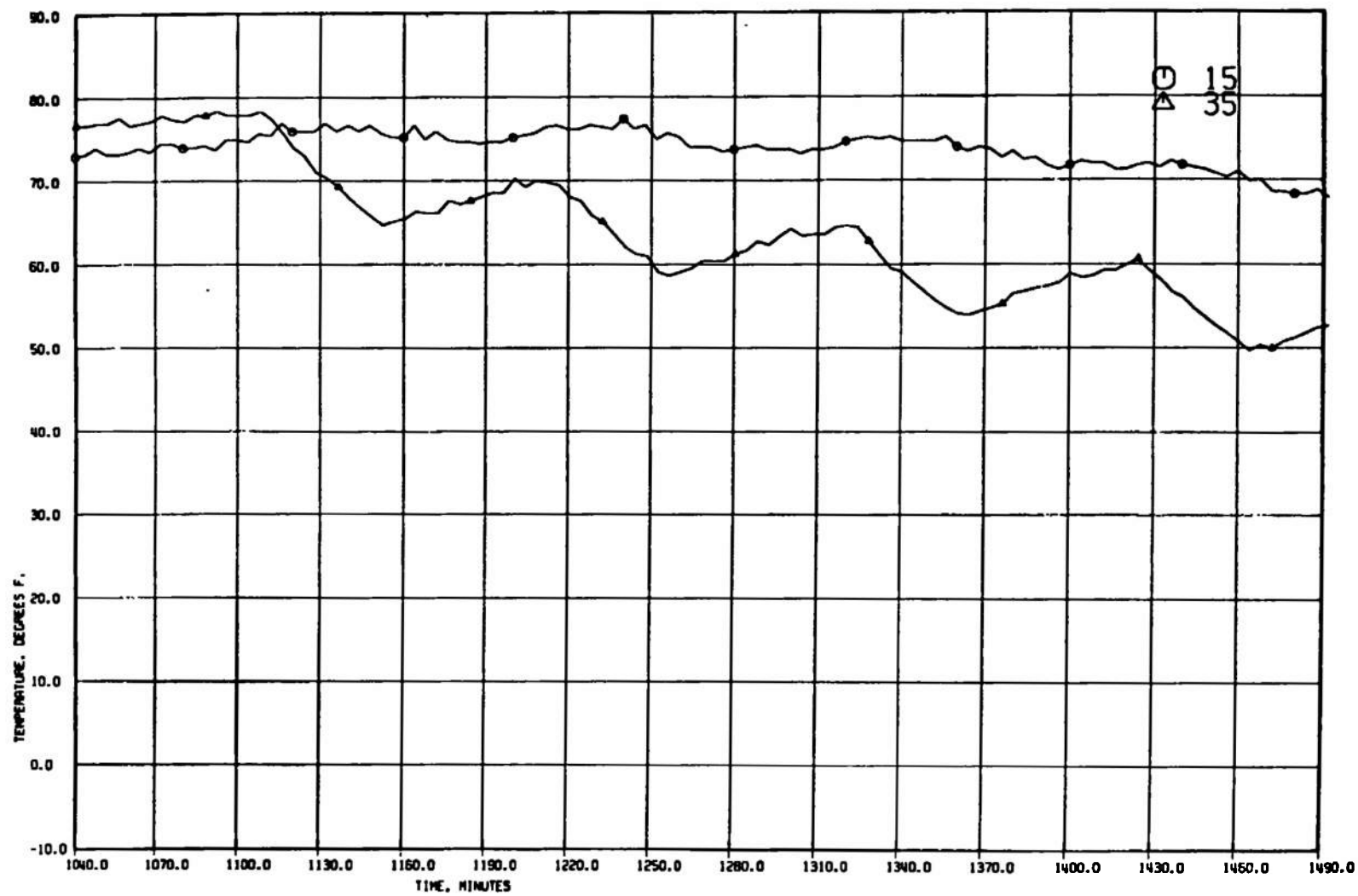
h. Concluded  
Fig. 15 Continued



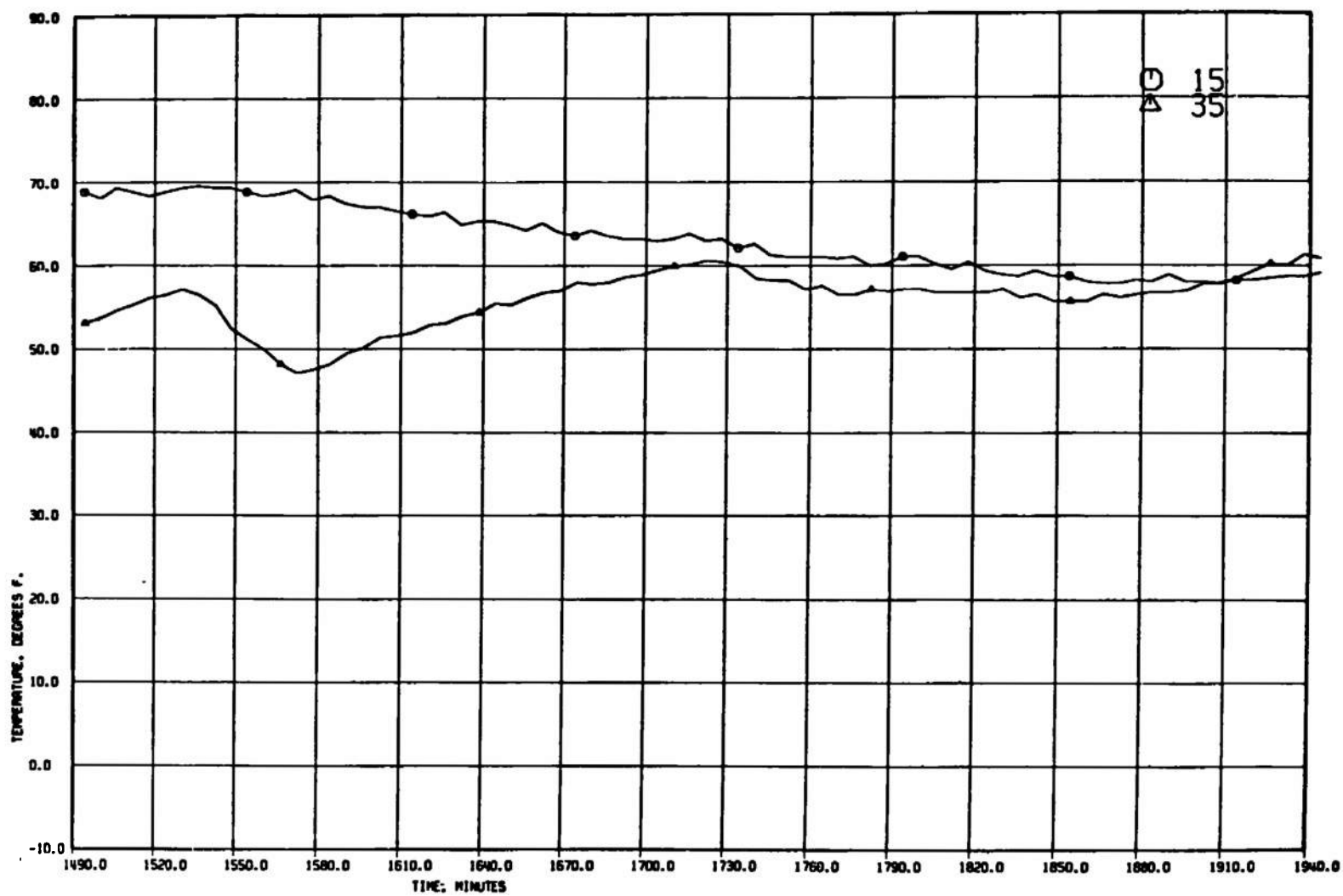
i. T/C 15 and 35  
Fig. 15 Continued



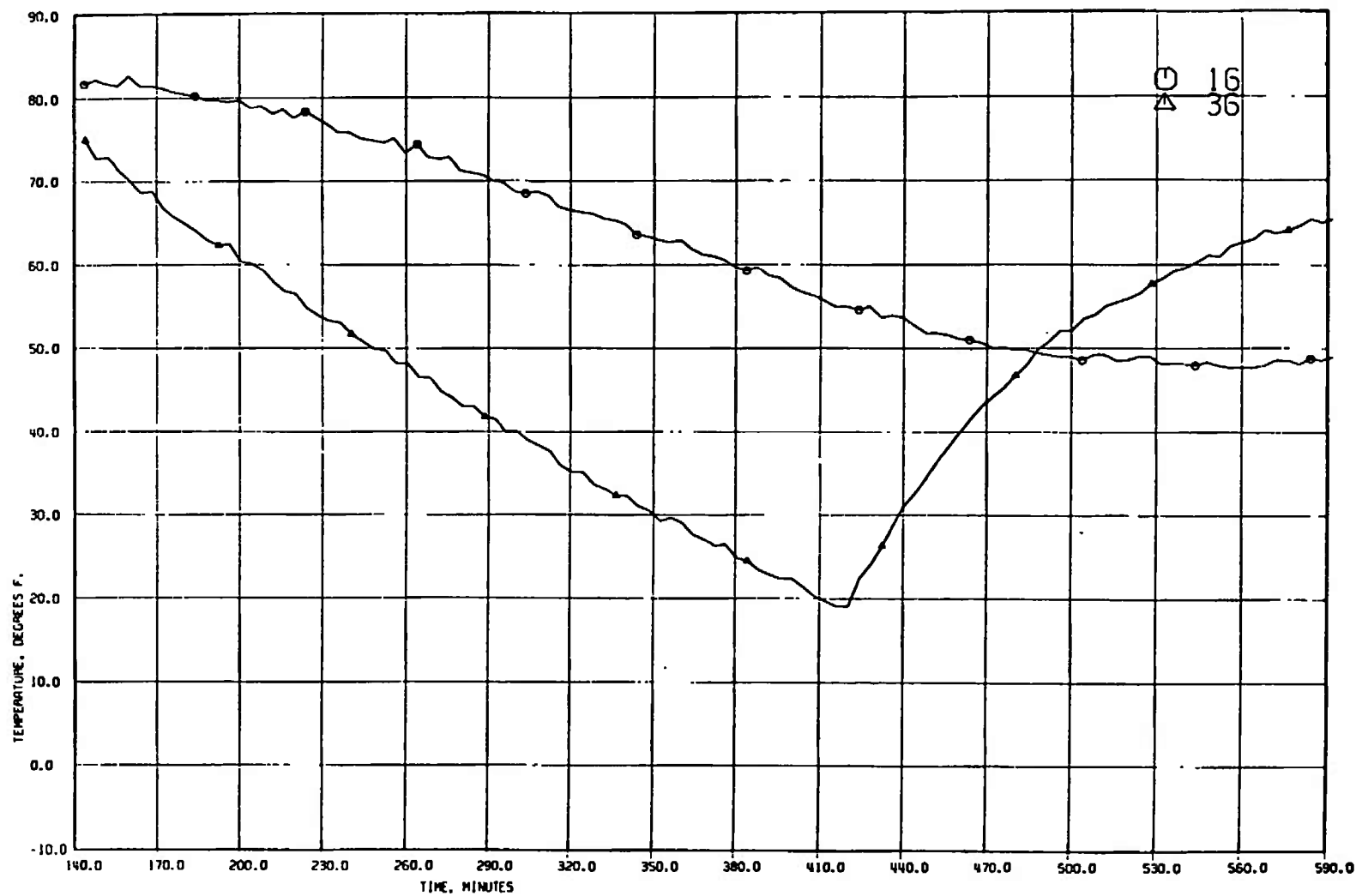
i. Continued  
Fig. 15 Continued



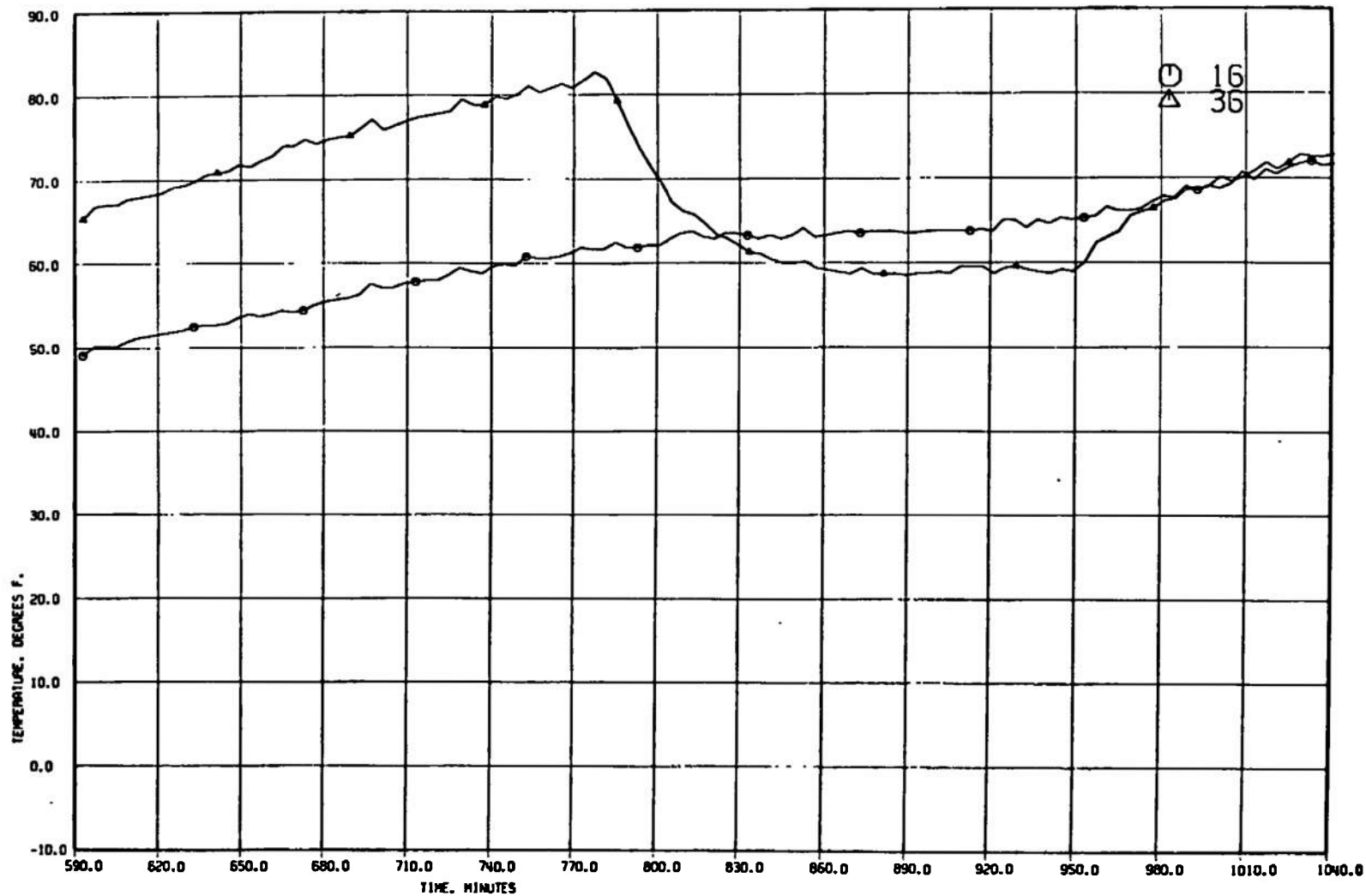
i. Continued  
Fig. 15 Continued



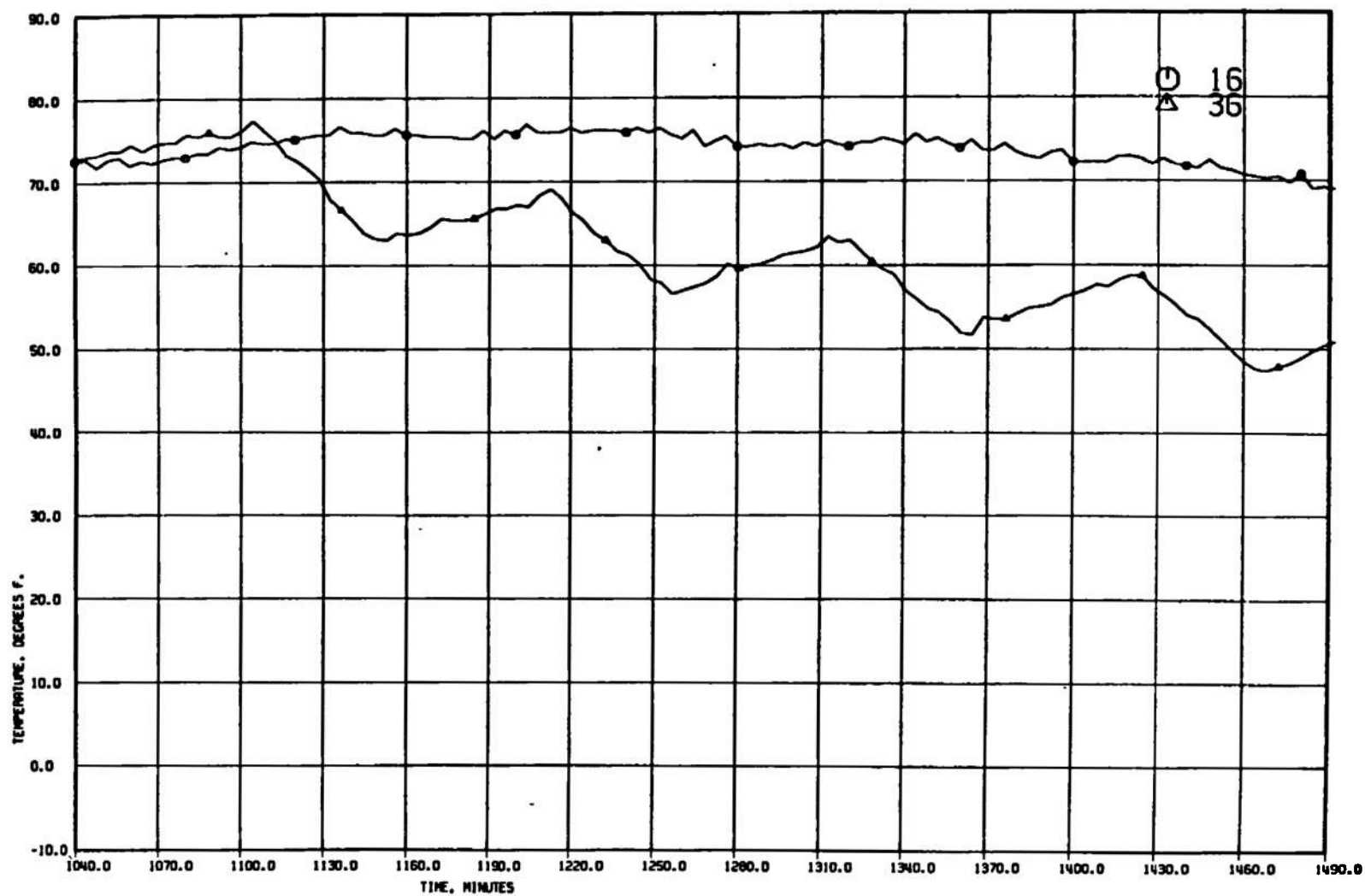
i. Concluded  
Fig. 15 Continued



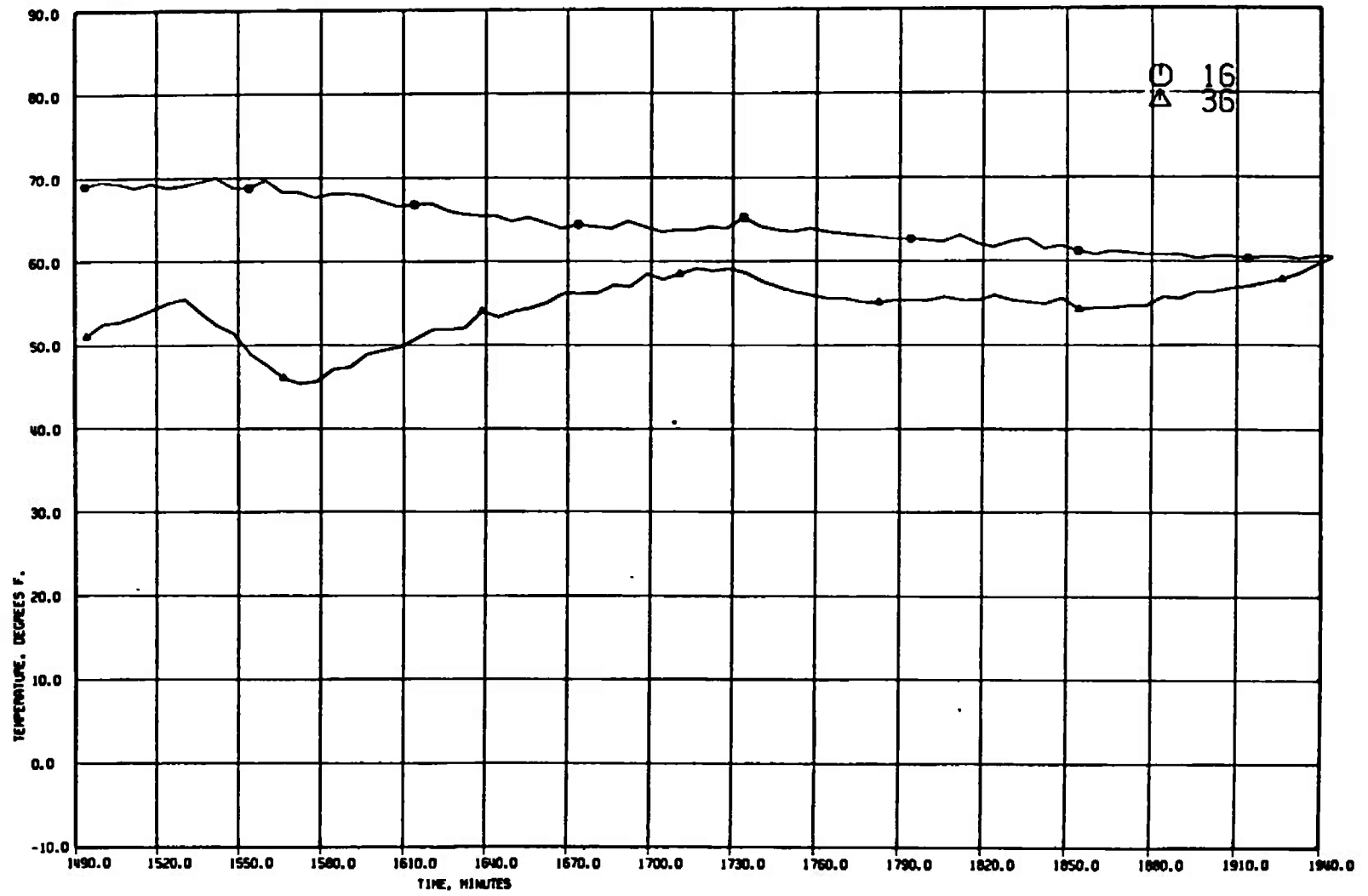
j: T/C 16 and 36  
Fig. 15 Continued



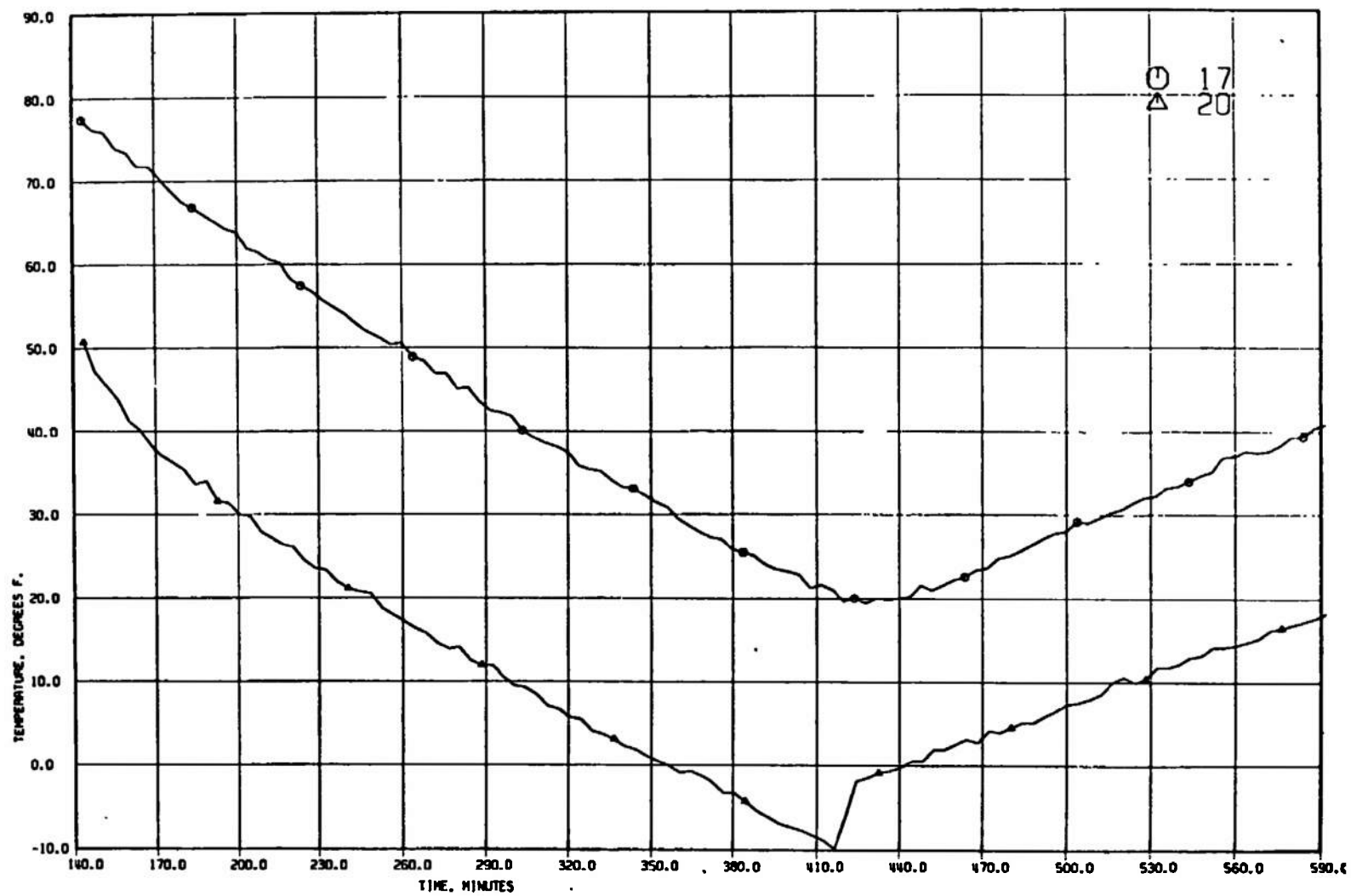
j. Continued  
Fig. 15 Continued



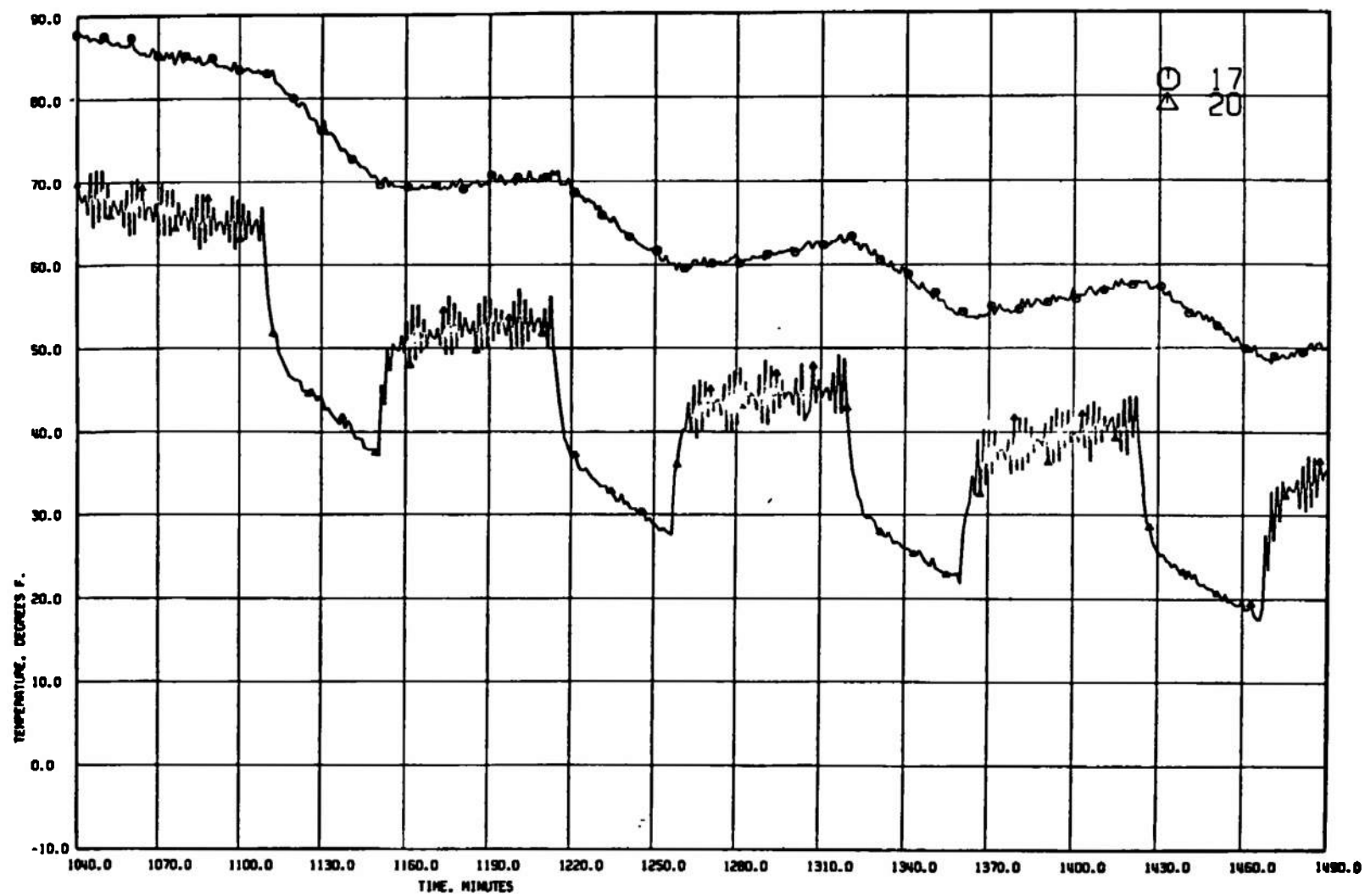
j. Continued  
Fig. 15 Continued



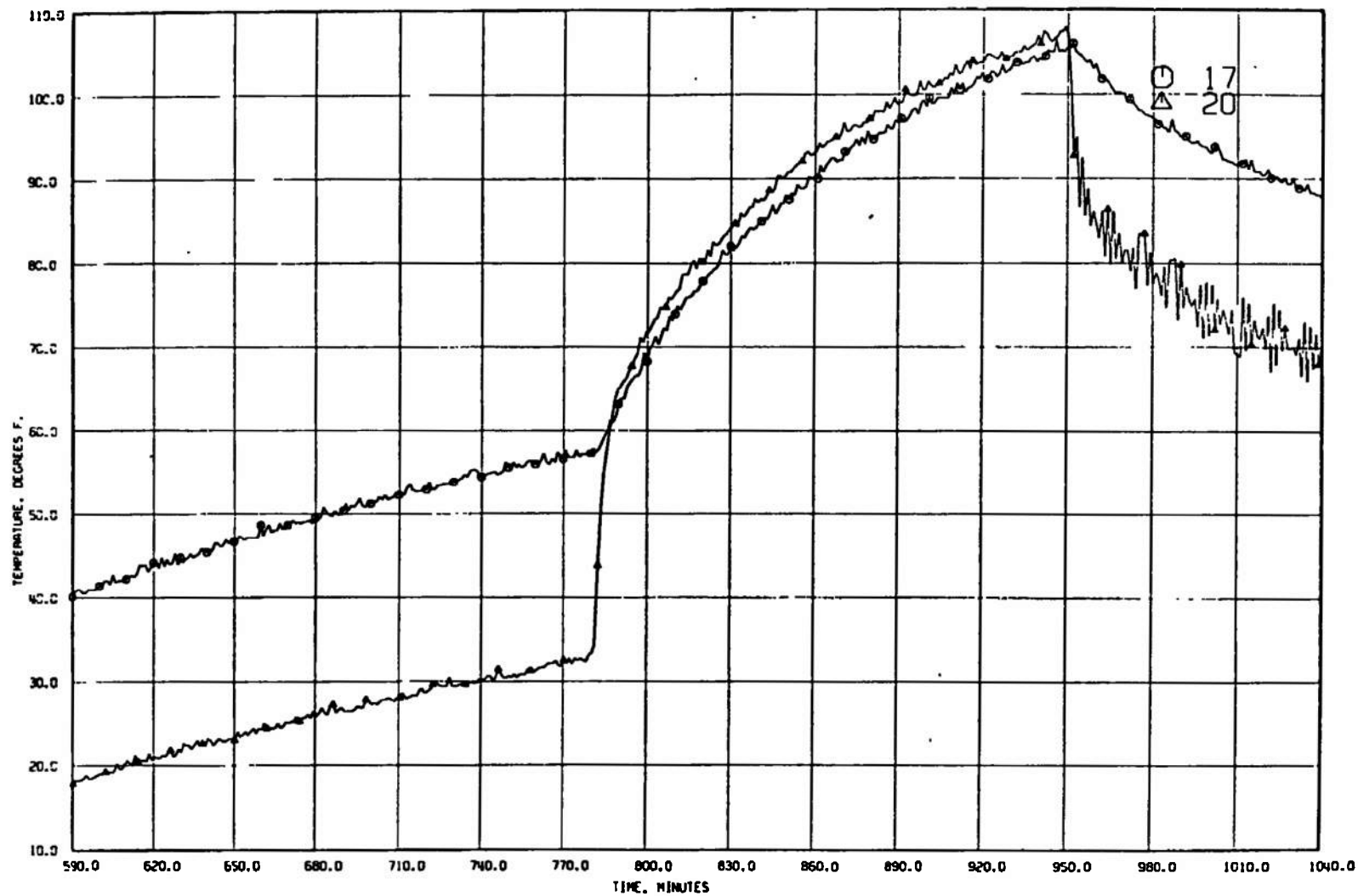
j. Concluded  
Fig. 15 Continued



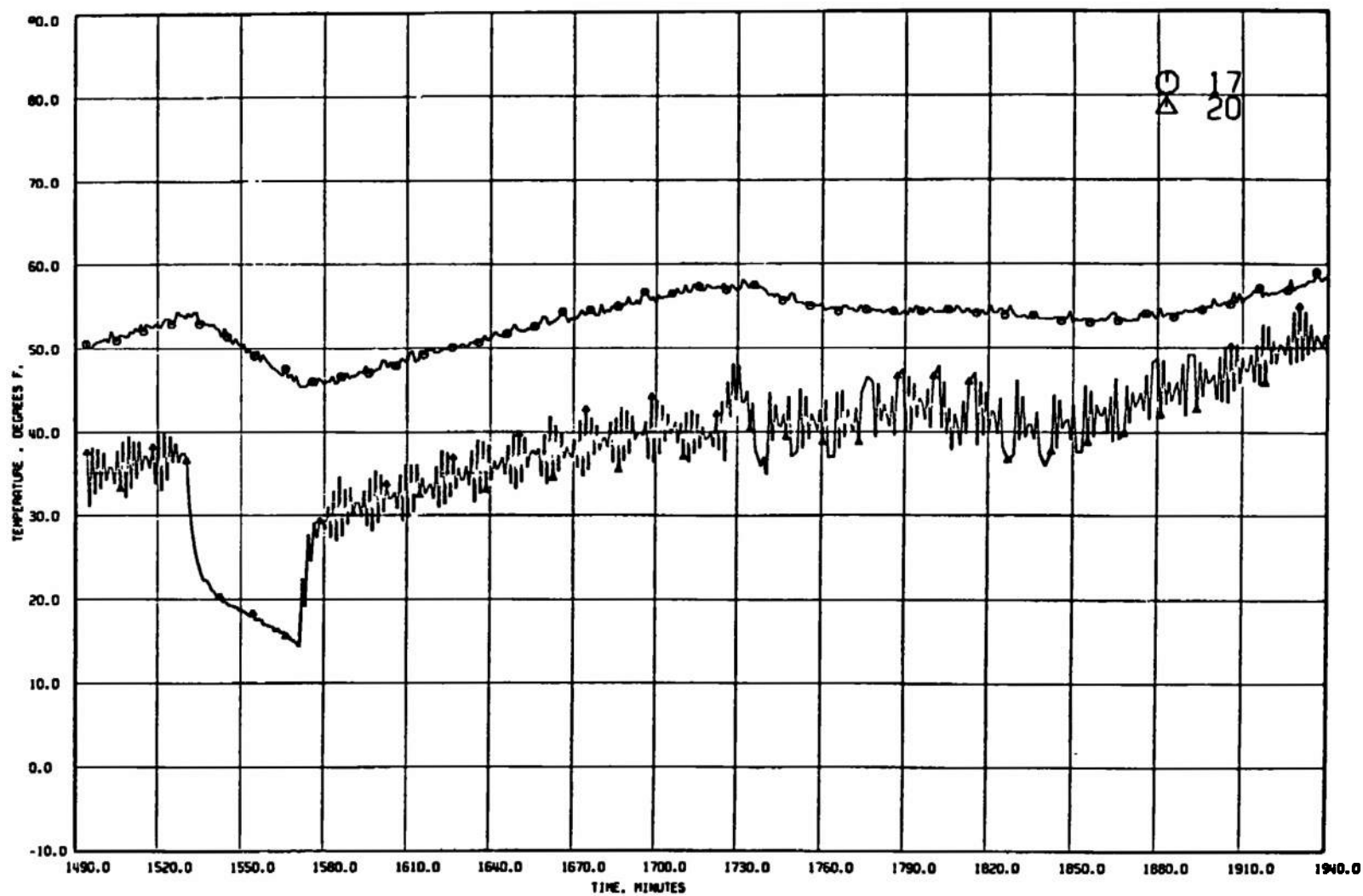
k. T/C 17 and 20  
Fig. 15 Continued



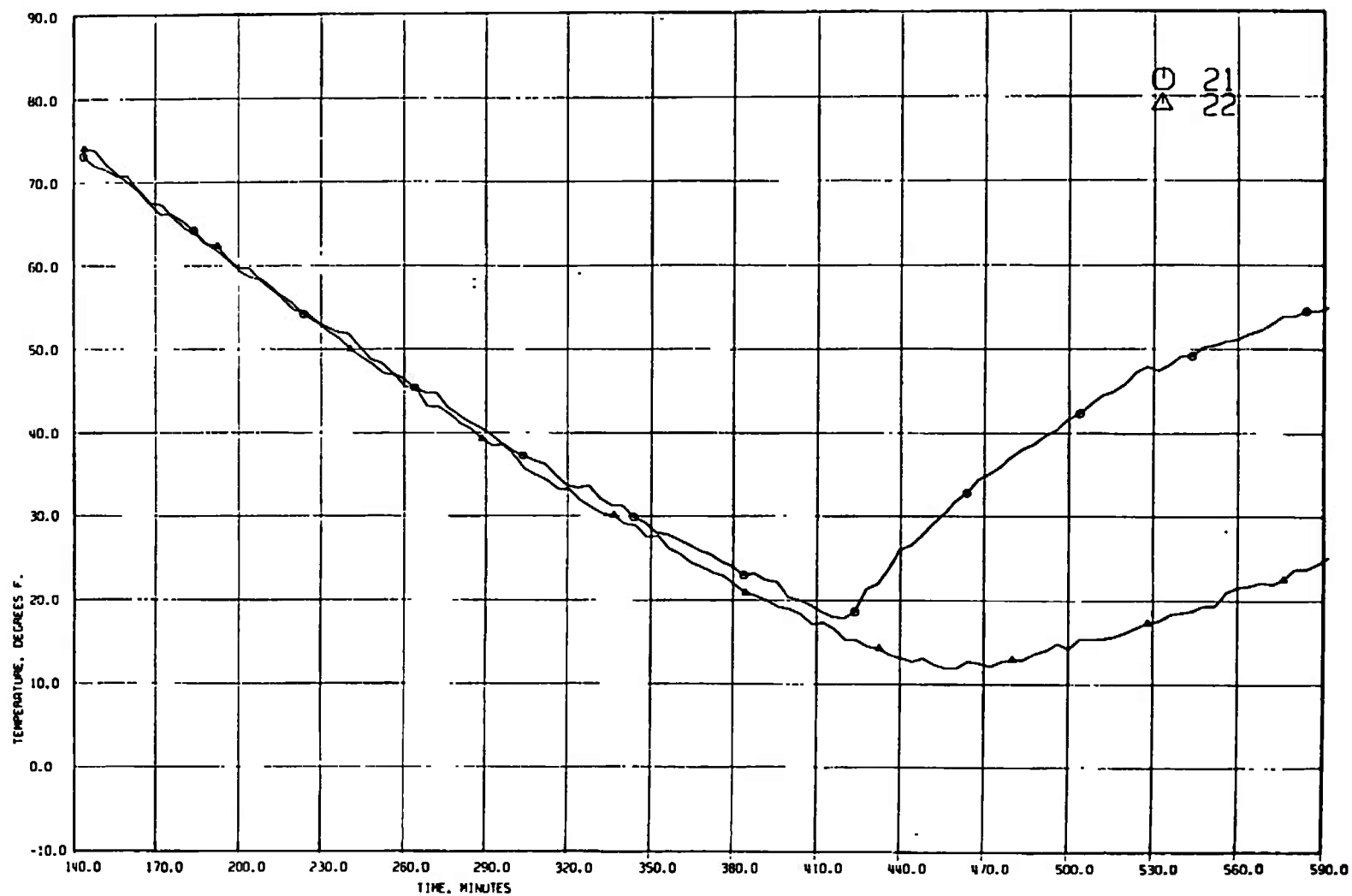
k. Continued  
Fig. 15 Continued



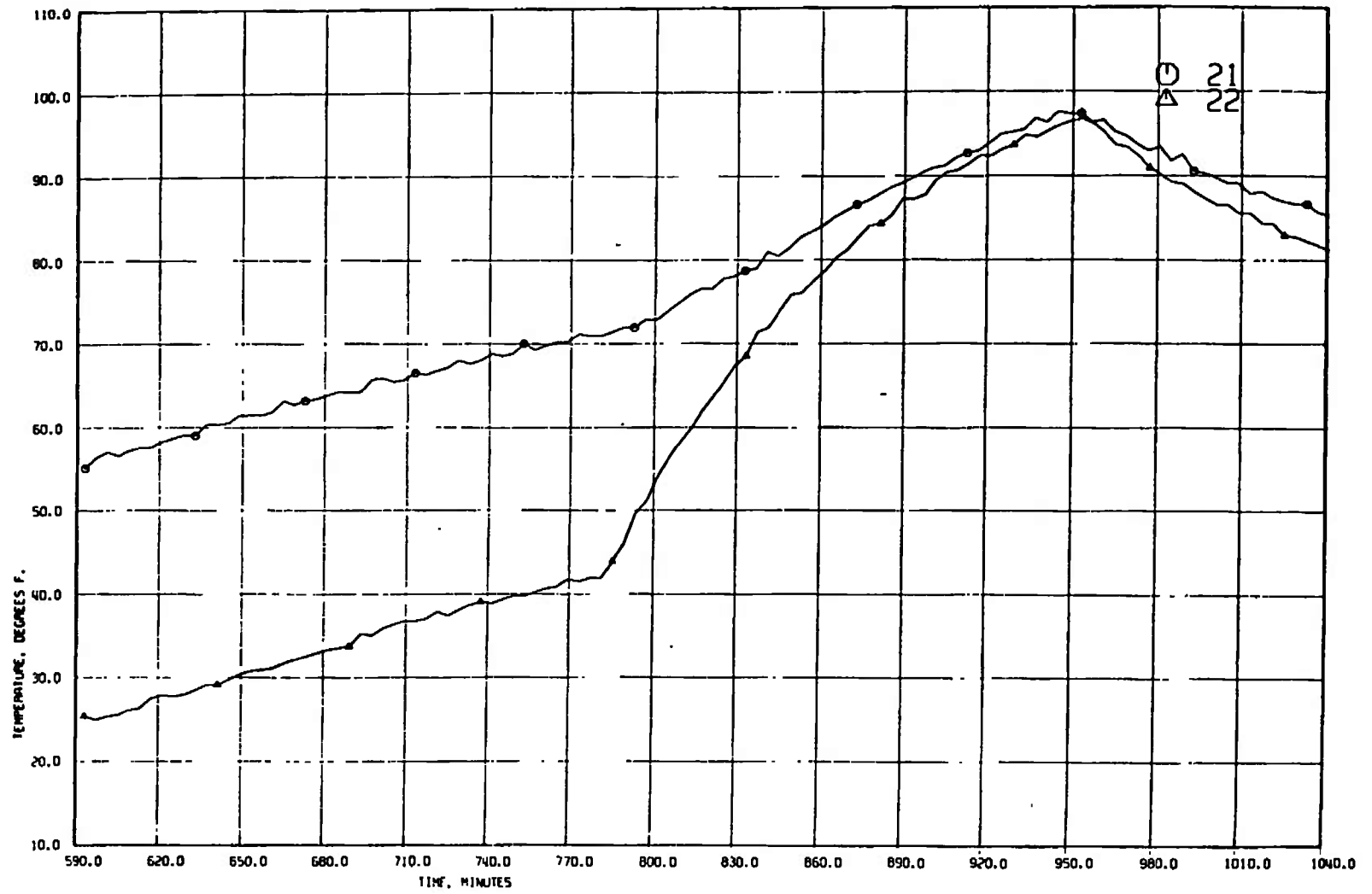
k. Continued  
Fig. 15 Continued



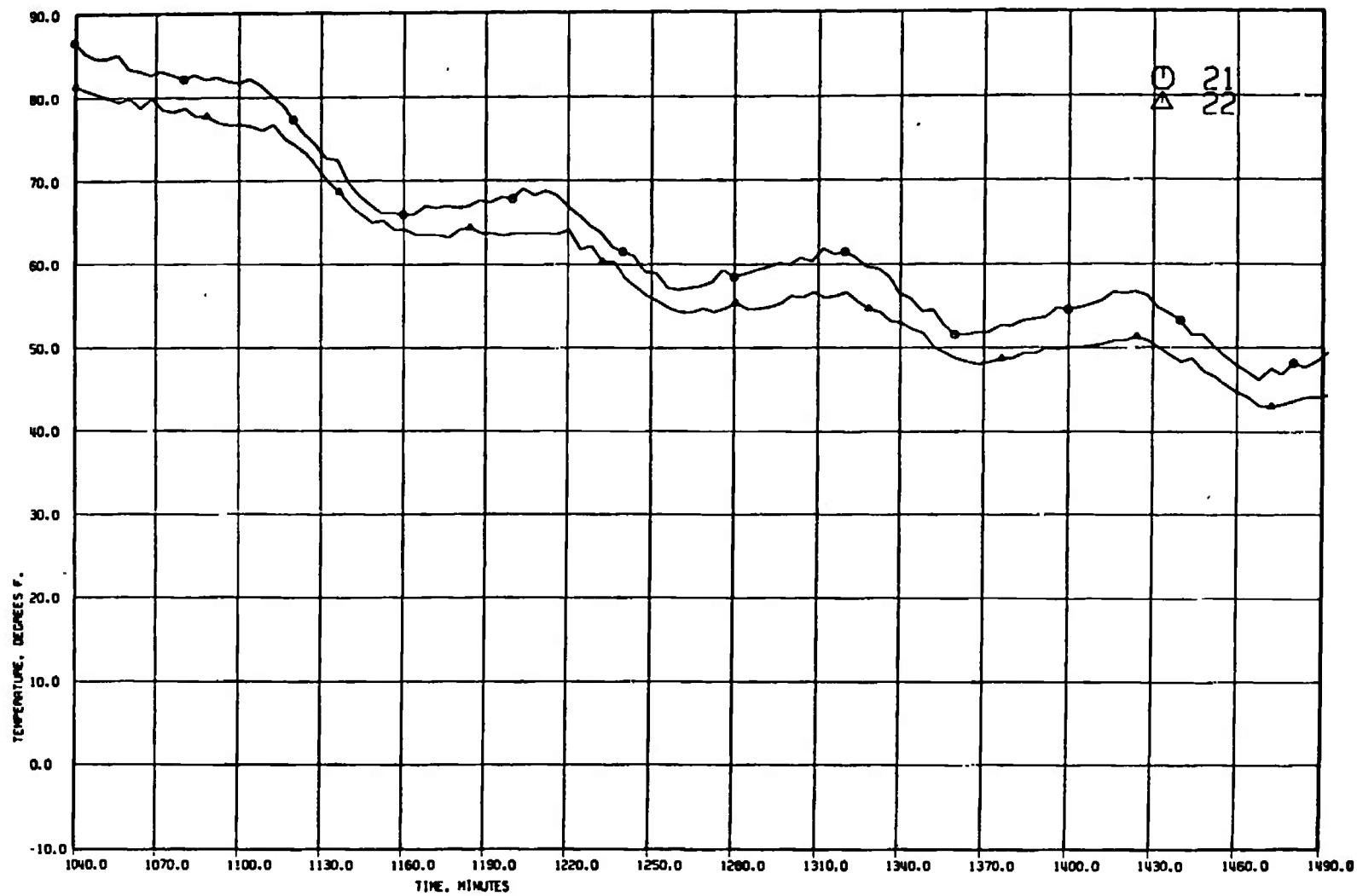
k. Concluded  
Fig. 15 Continued



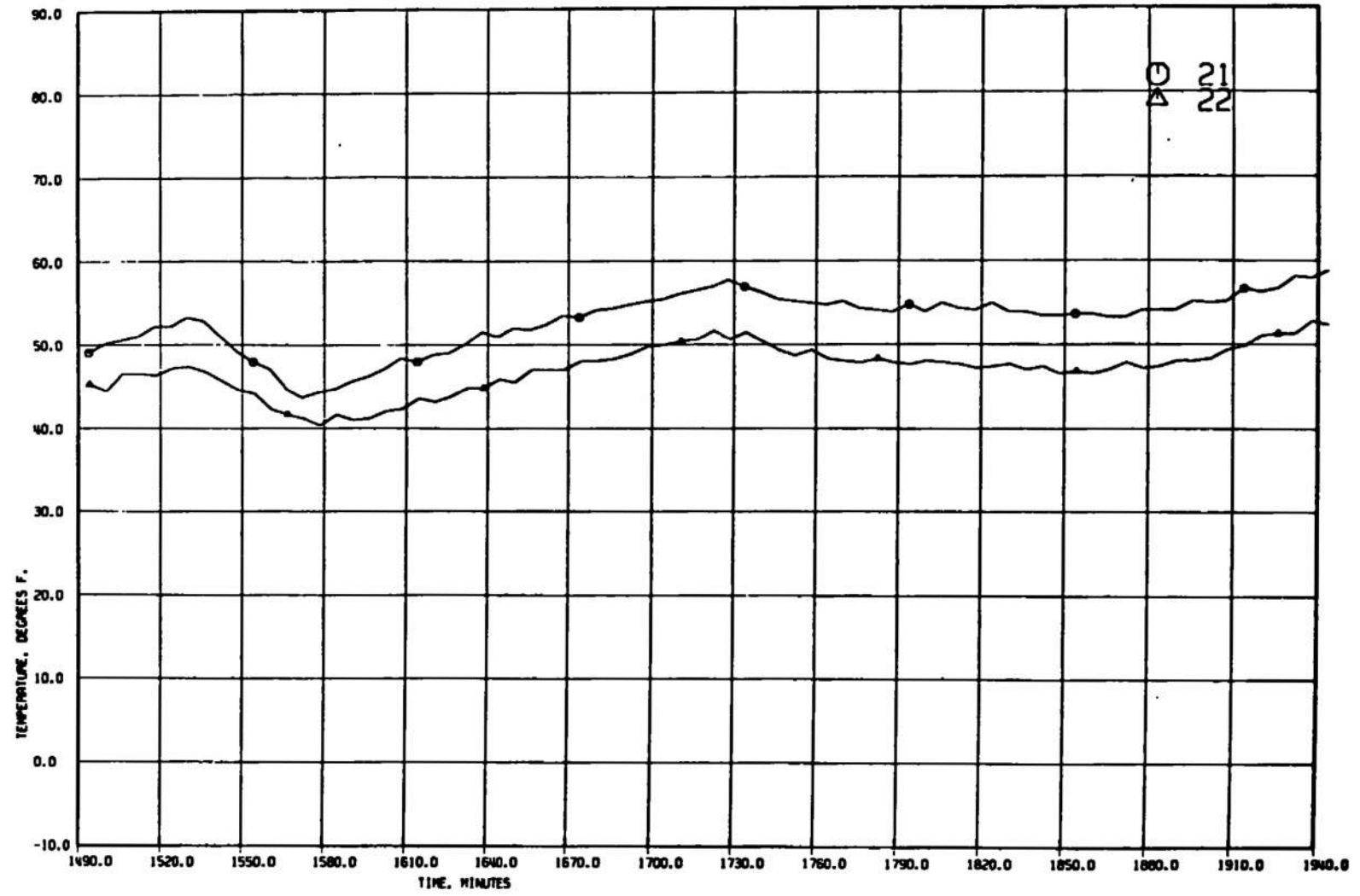
I. T/C 21 and 22  
Fig. 15 Continued



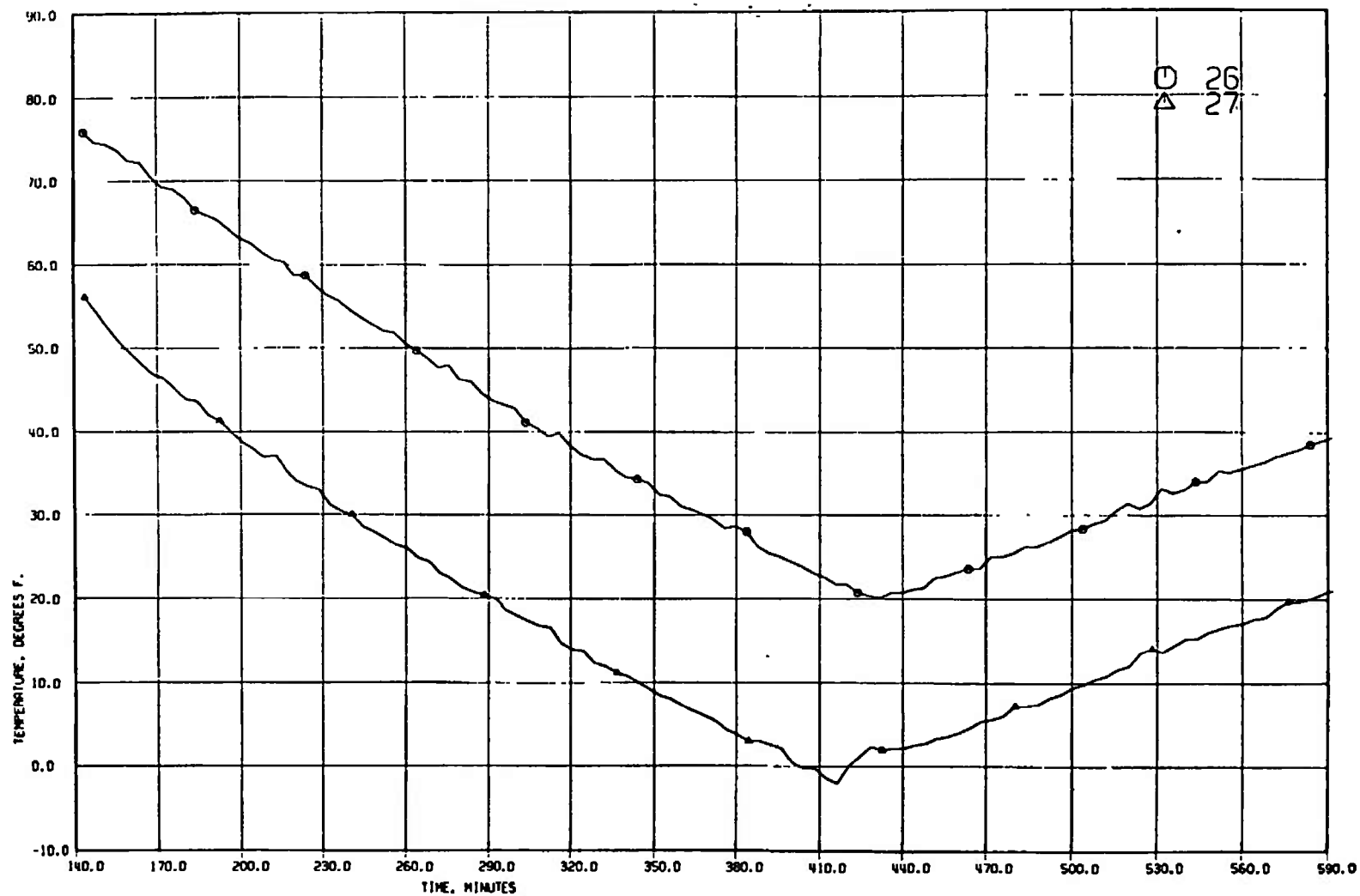
I. Continued  
Fig. 15 Continued



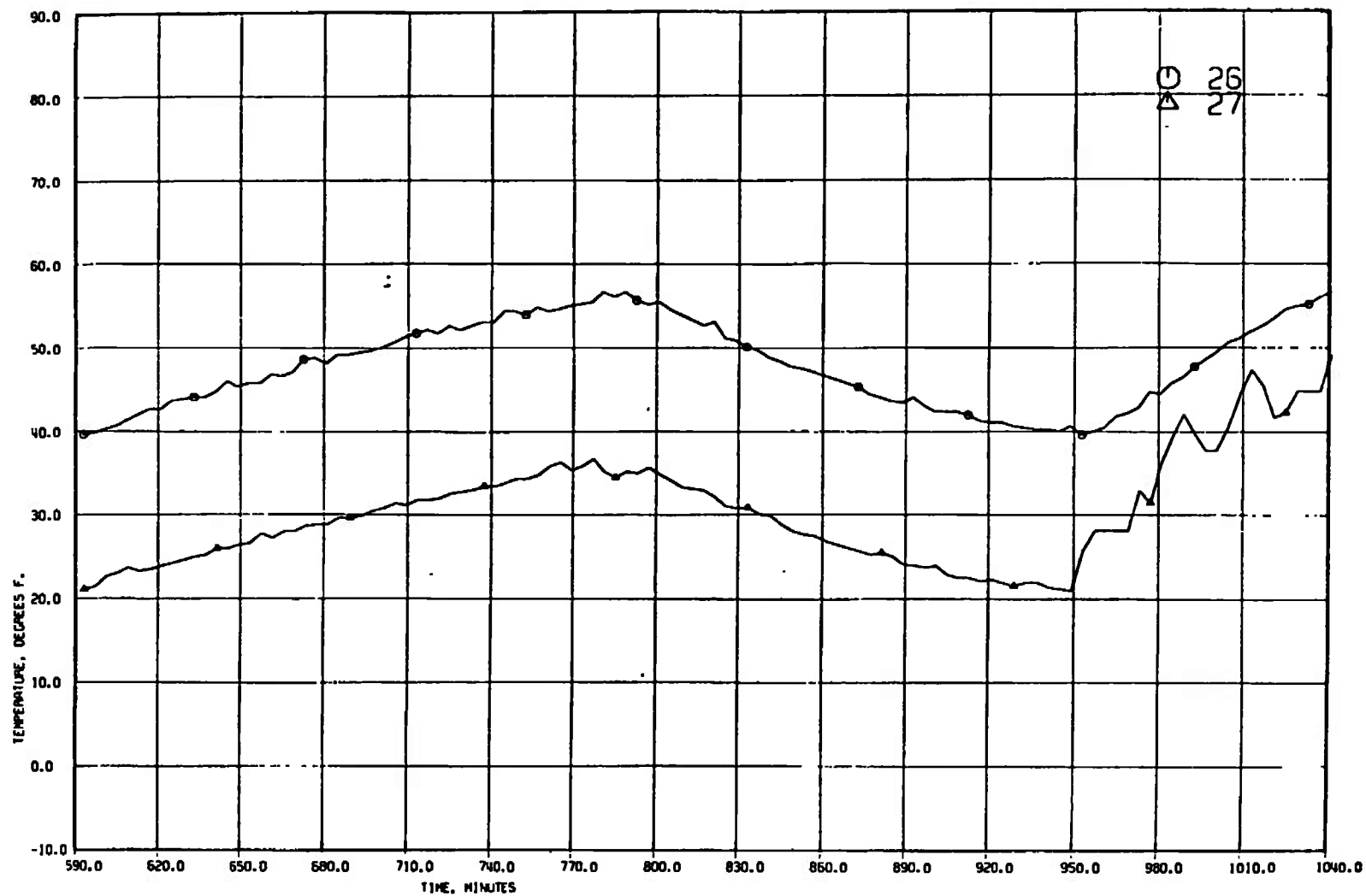
I. Continued  
Fig. 15 Continued



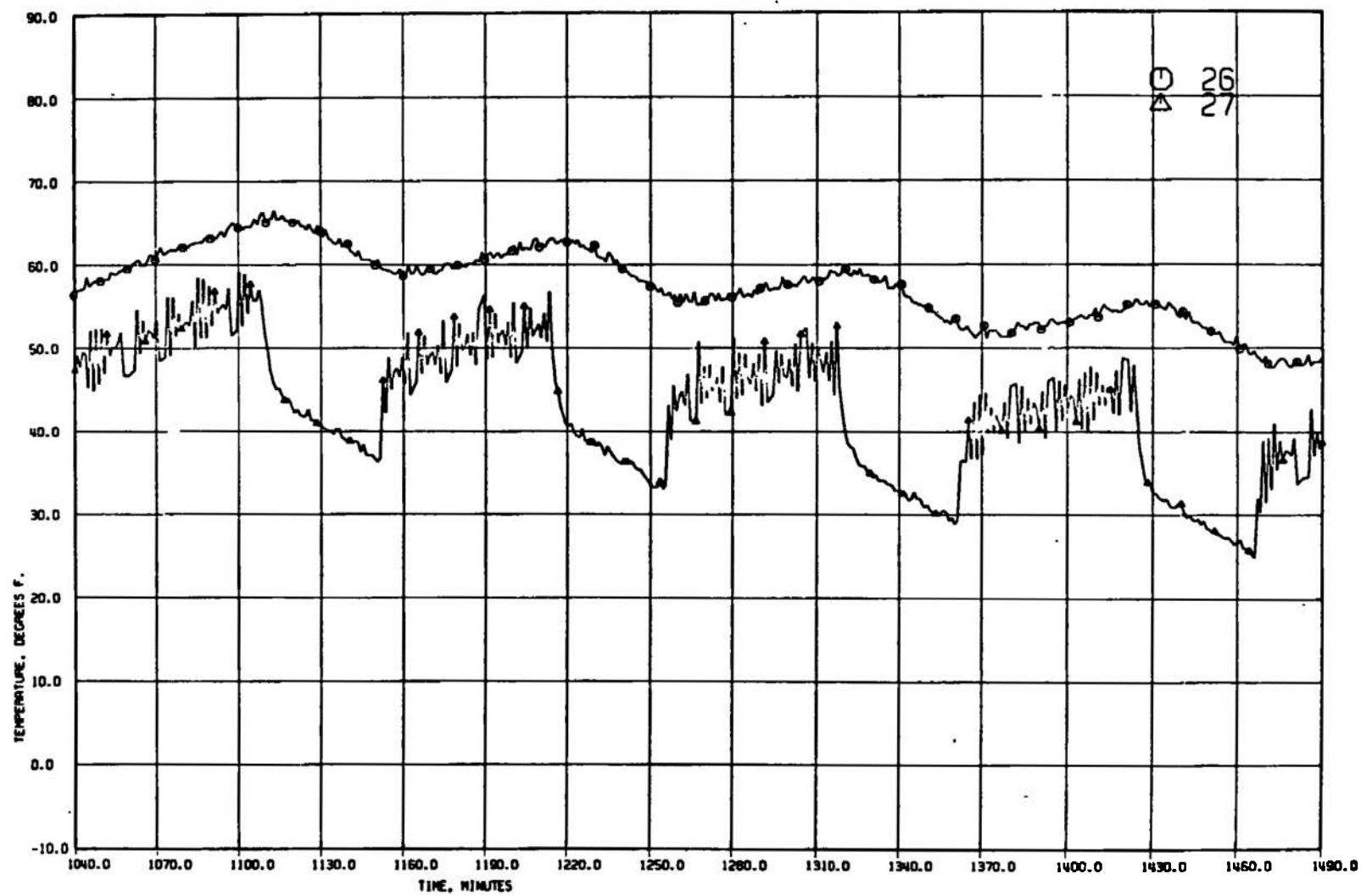
I. Concluded  
Fig. 15 Continued



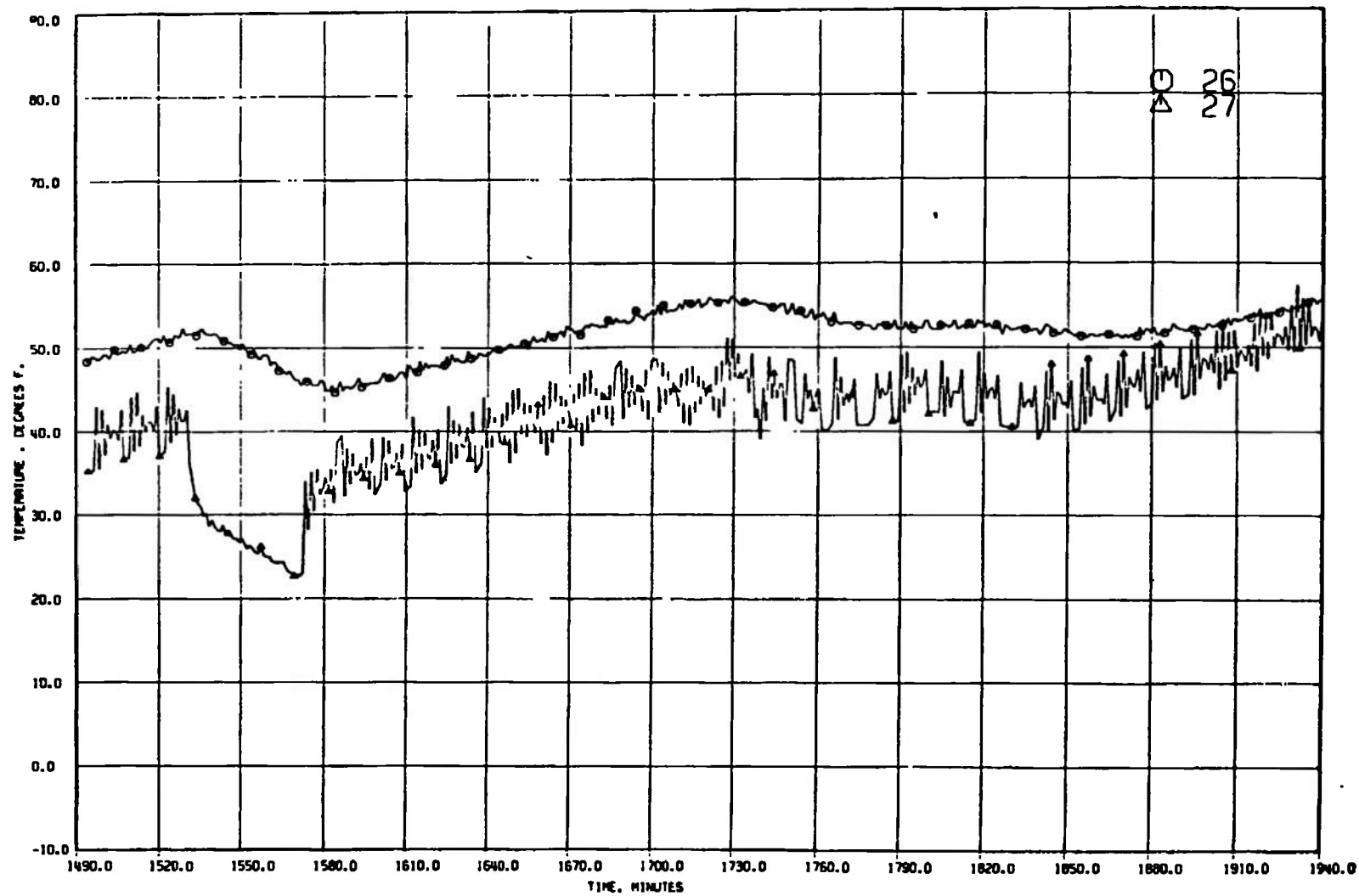
m. T/C 26 and 27  
Fig. 15 Continued



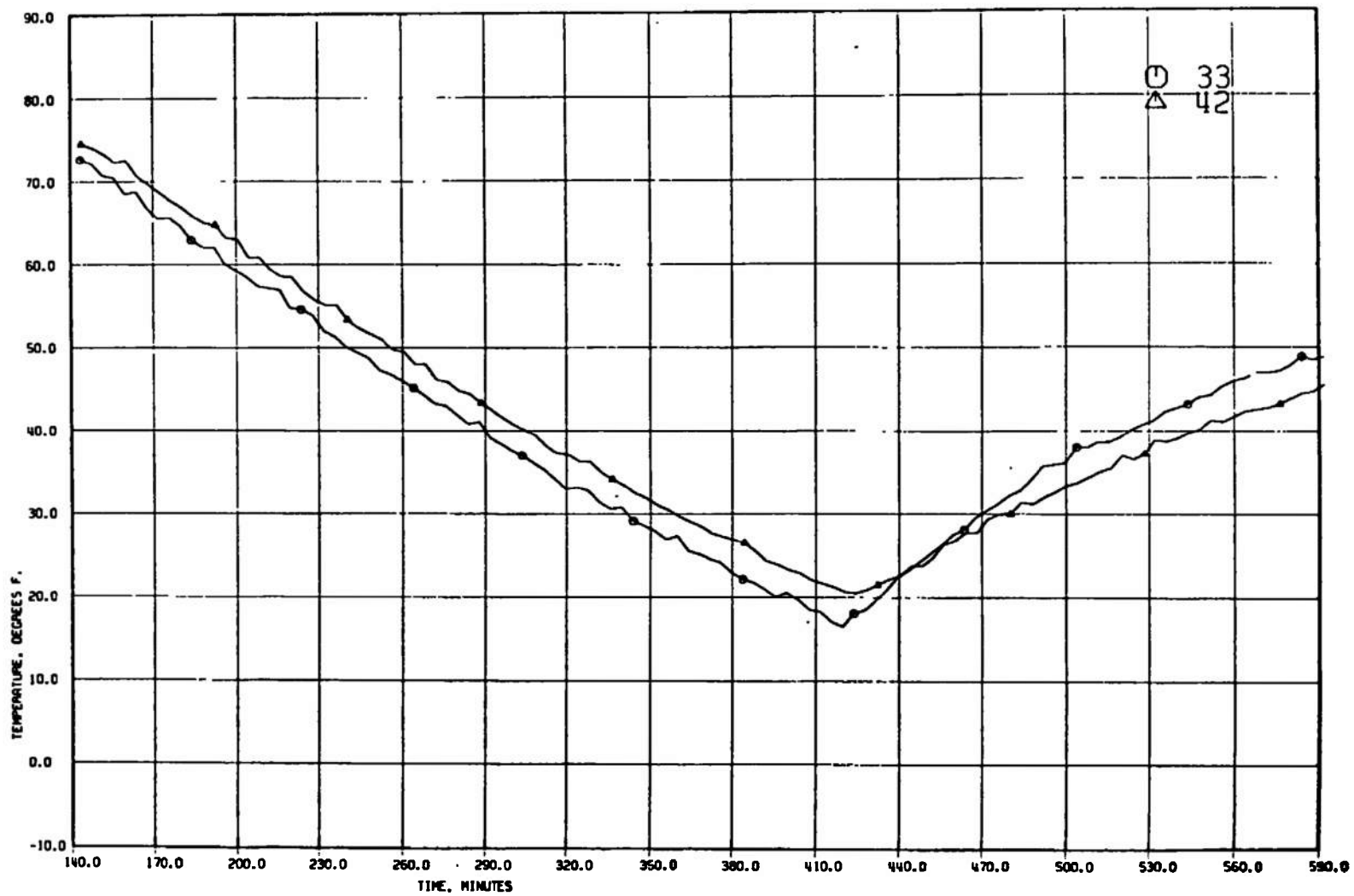
m. Continued  
Fig. 15 Continued



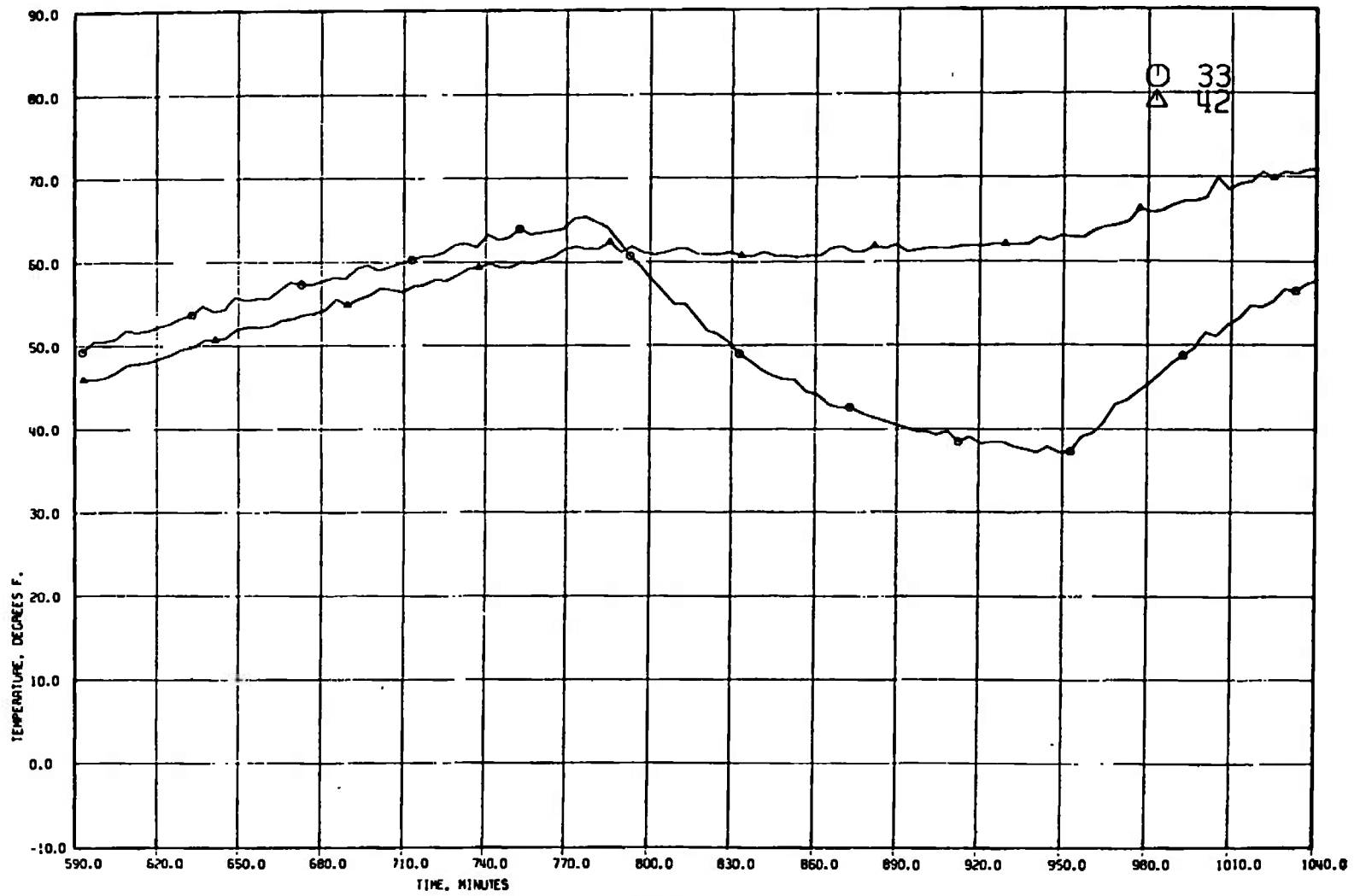
m. Continued  
Fig. 15 Continued



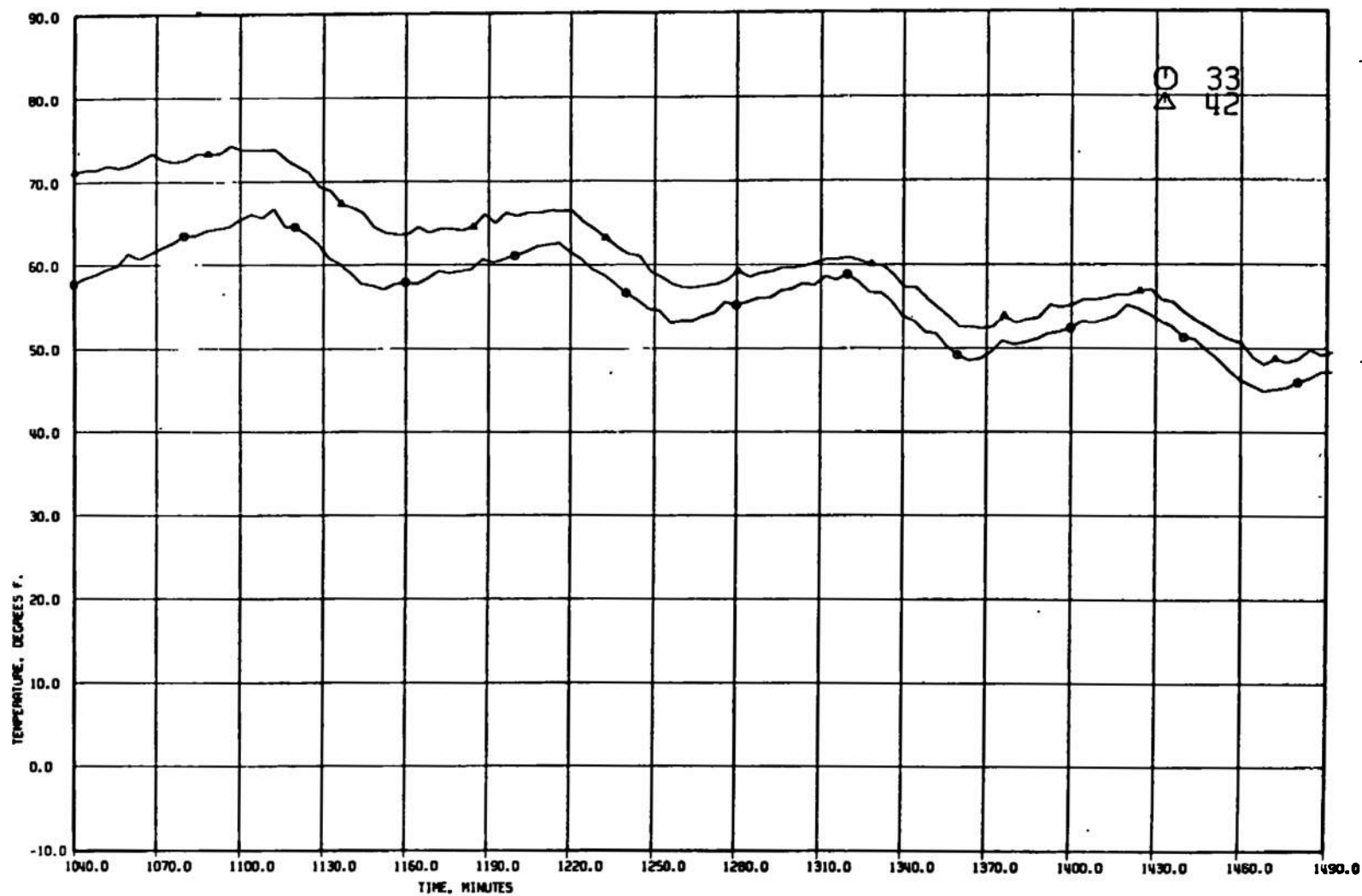
m. Concluded  
Fig. 15 Continued



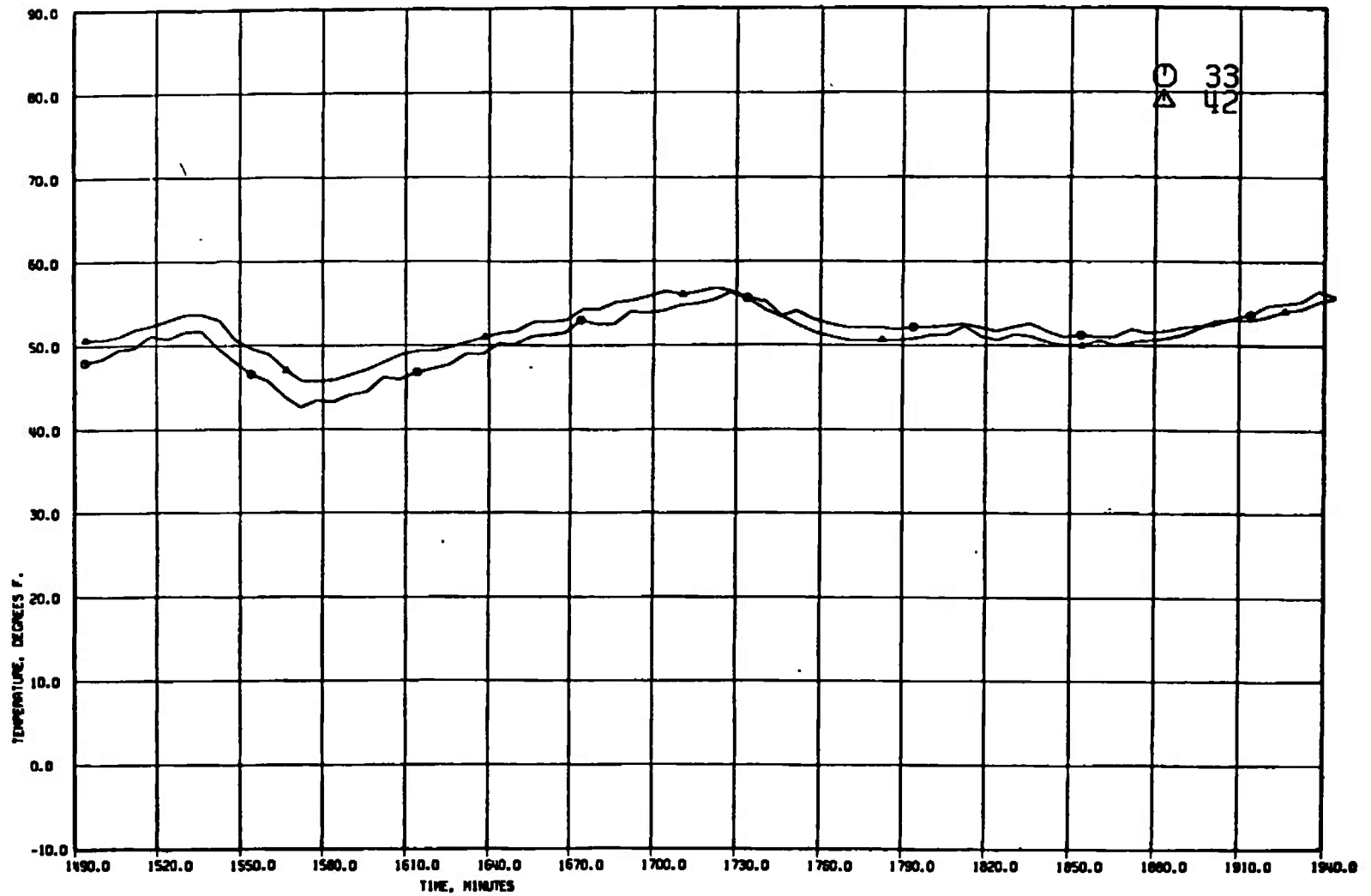
n. T/C 33 and 42  
Fig. 15 Continued



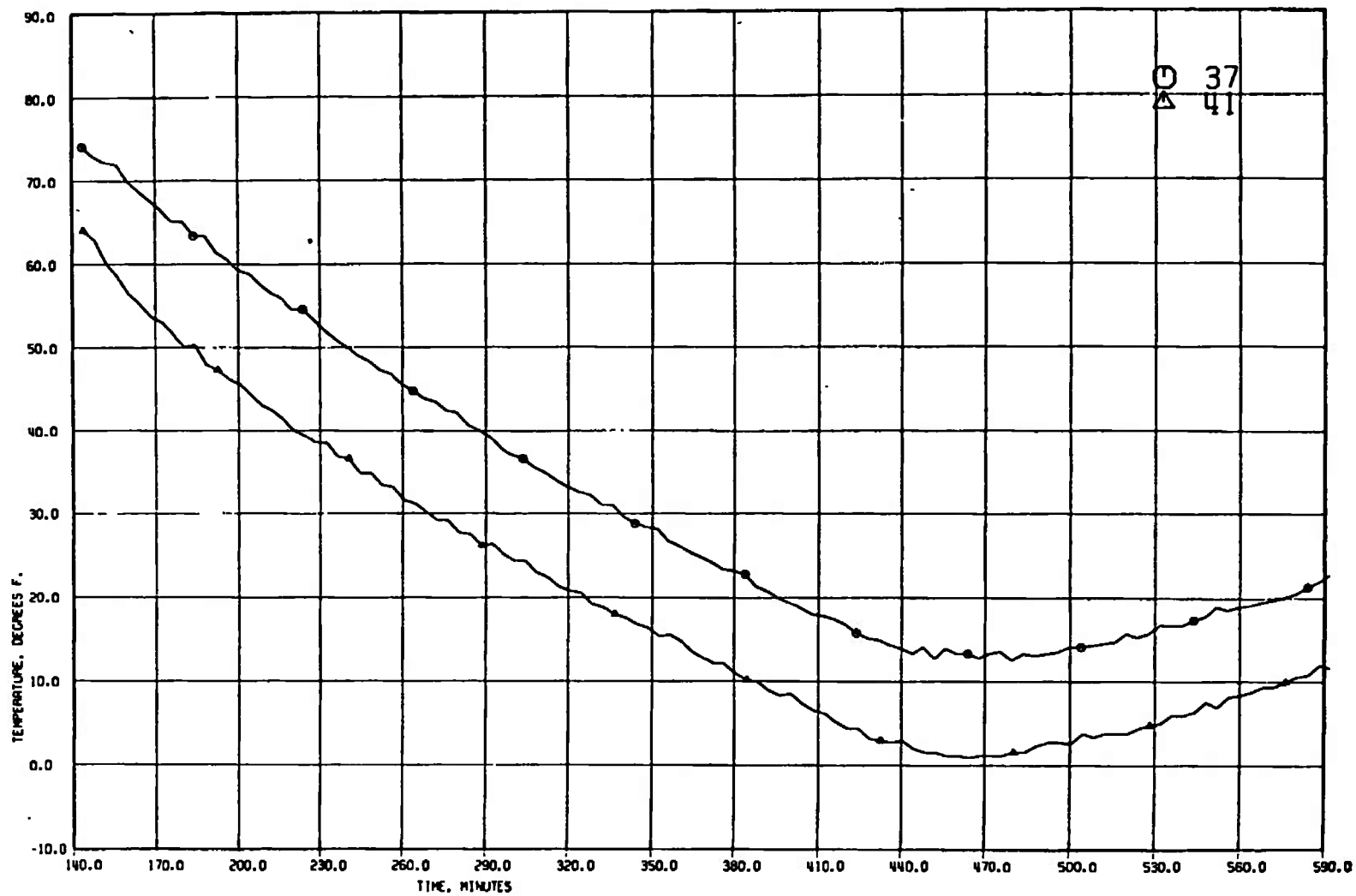
n. Continued  
Fig. 15 Continued



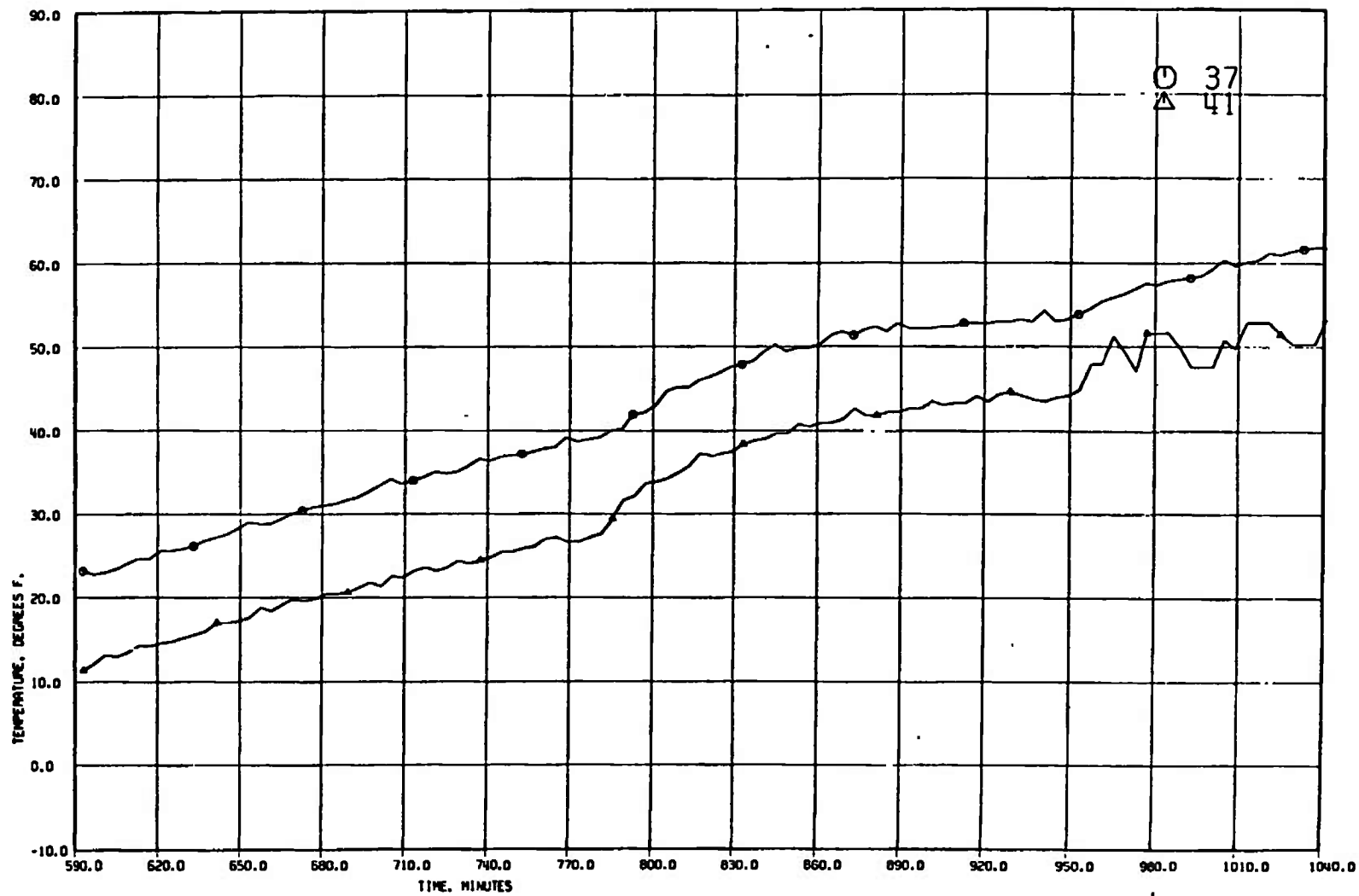
n. Continued  
Fig. 15 Continued



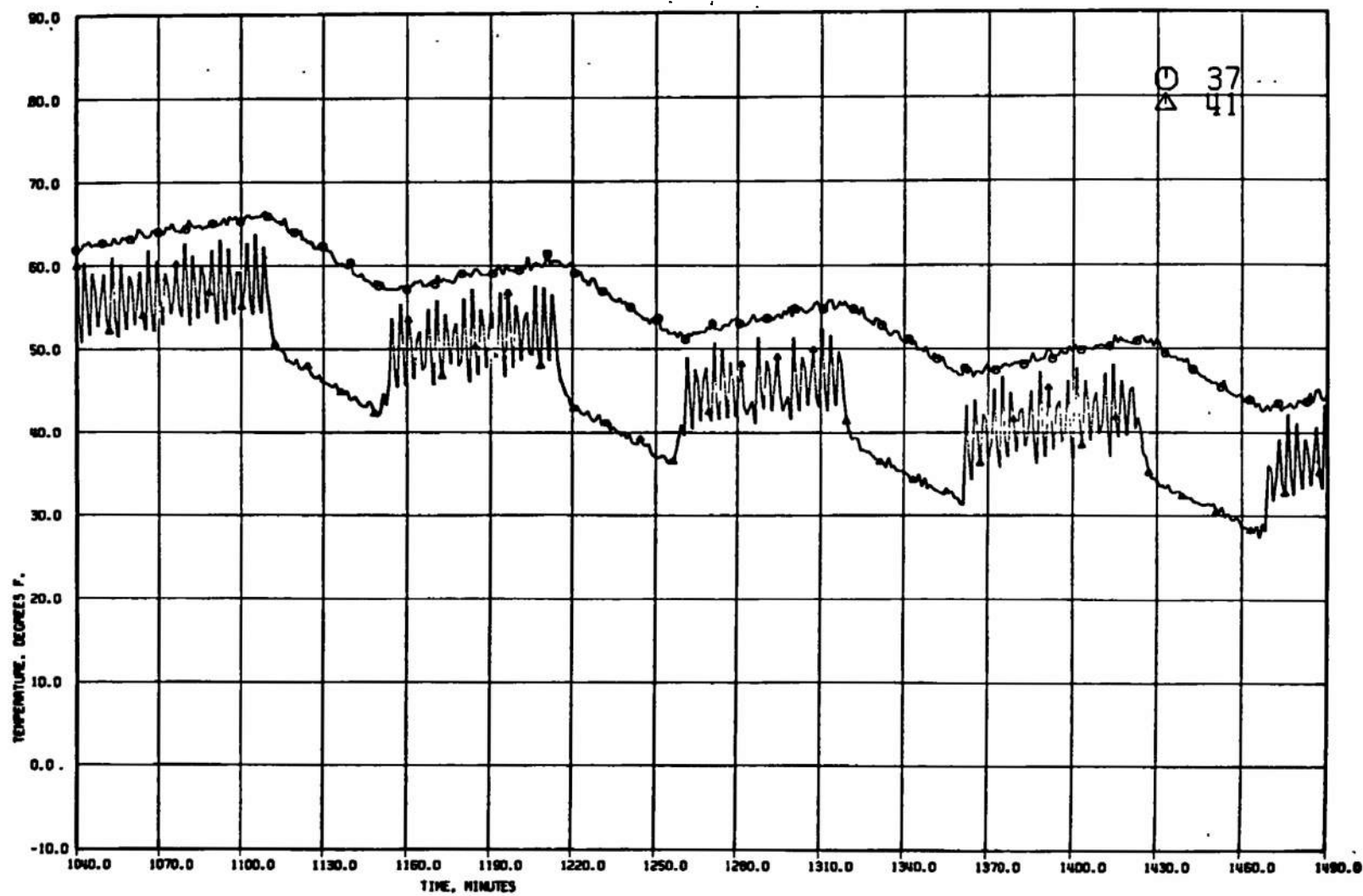
n. Concluded  
Fig. 15 Continued



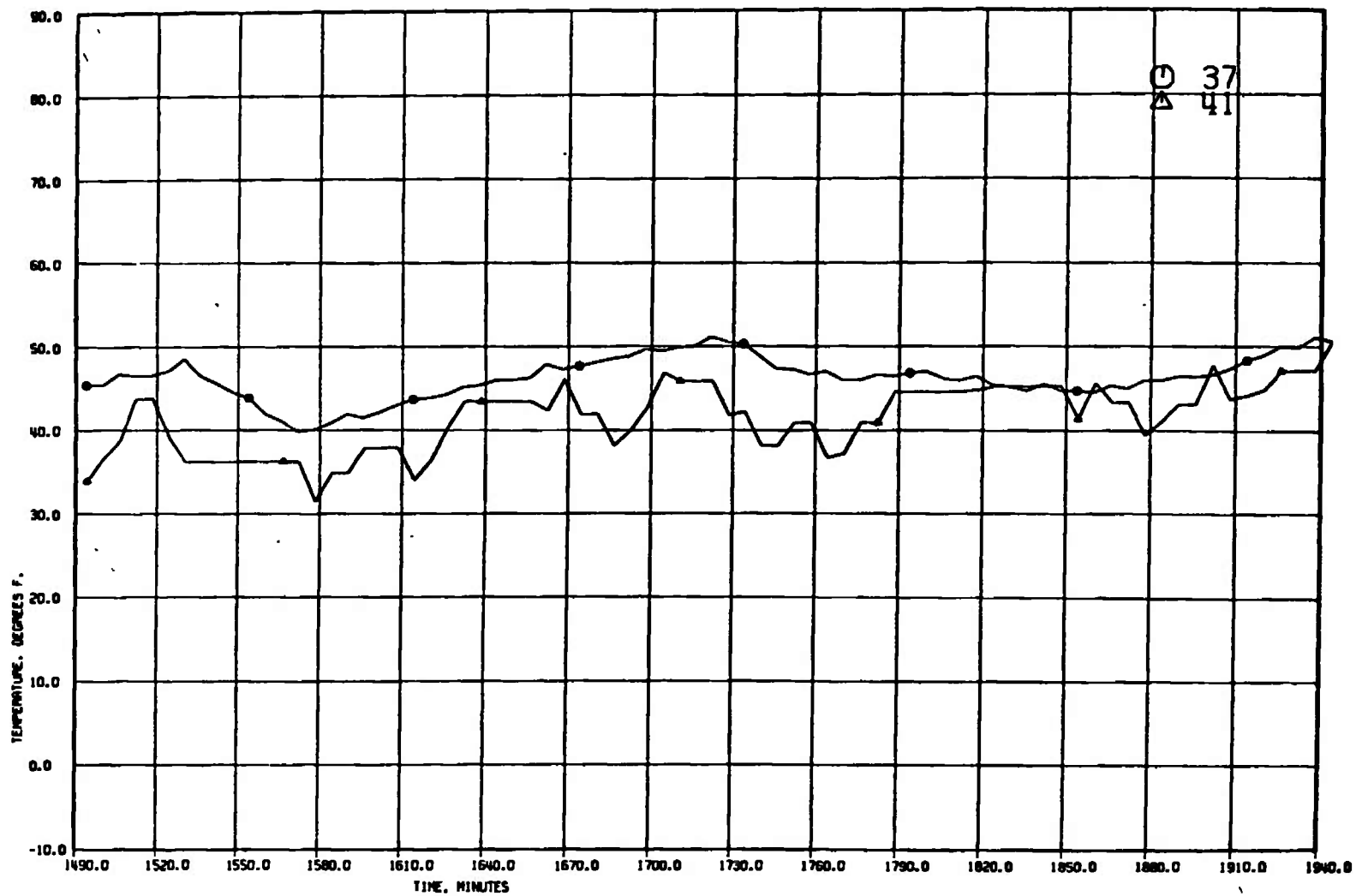
o. T/C 37 and 41  
Fig. 15 Continued



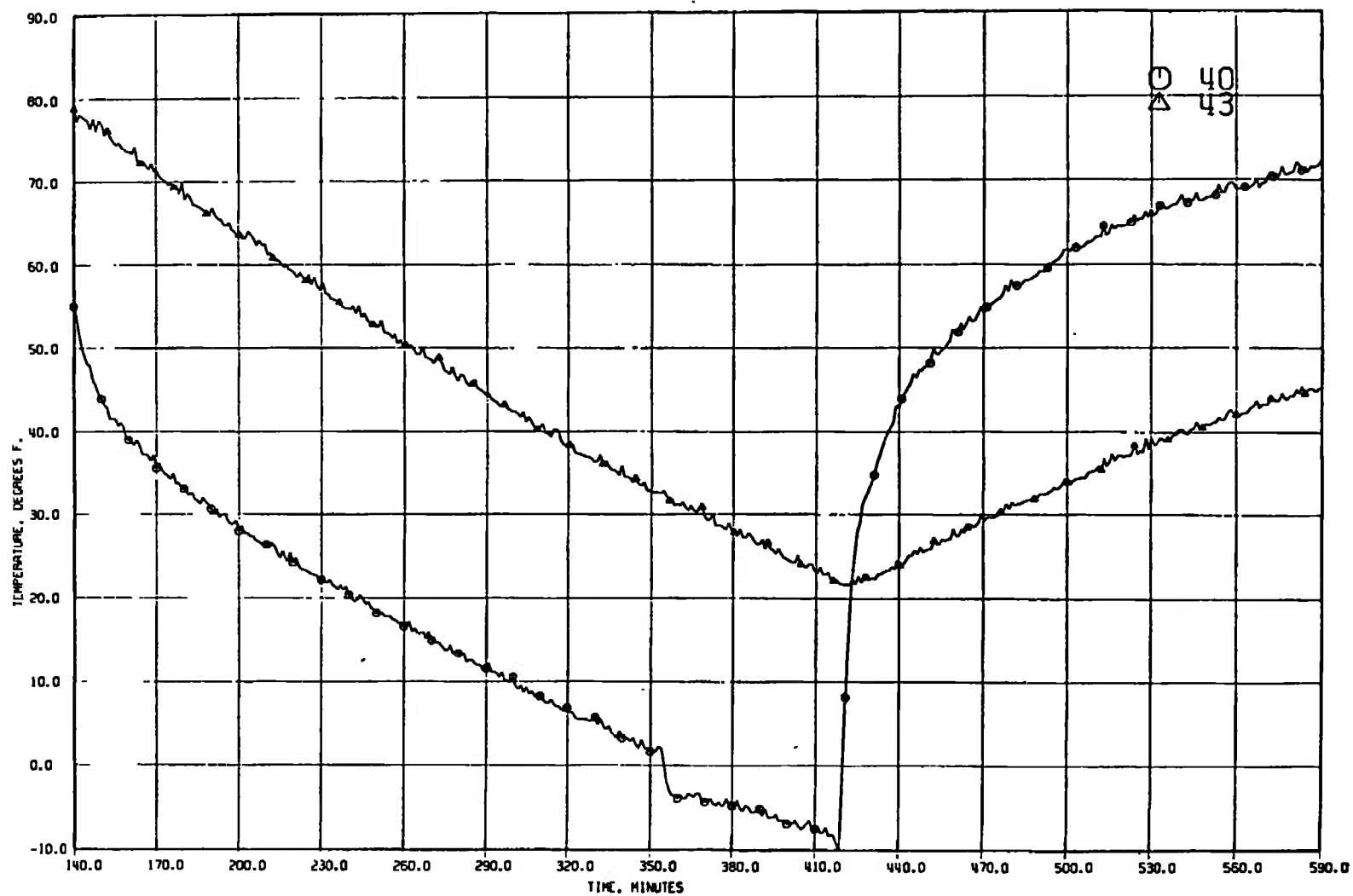
o. Continued  
Fig. 15 Continued



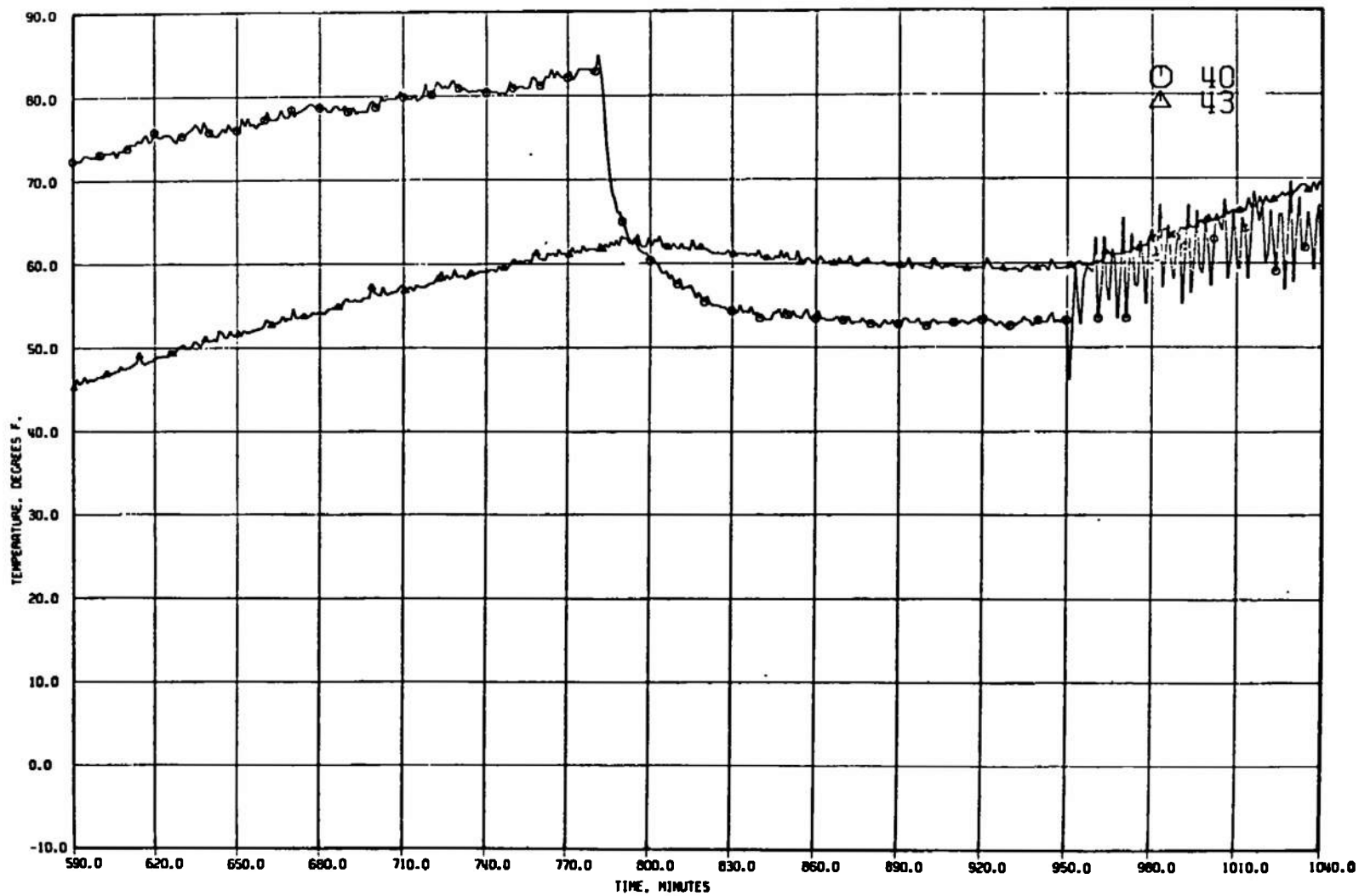
o. Continued  
Fig. 15 Continued



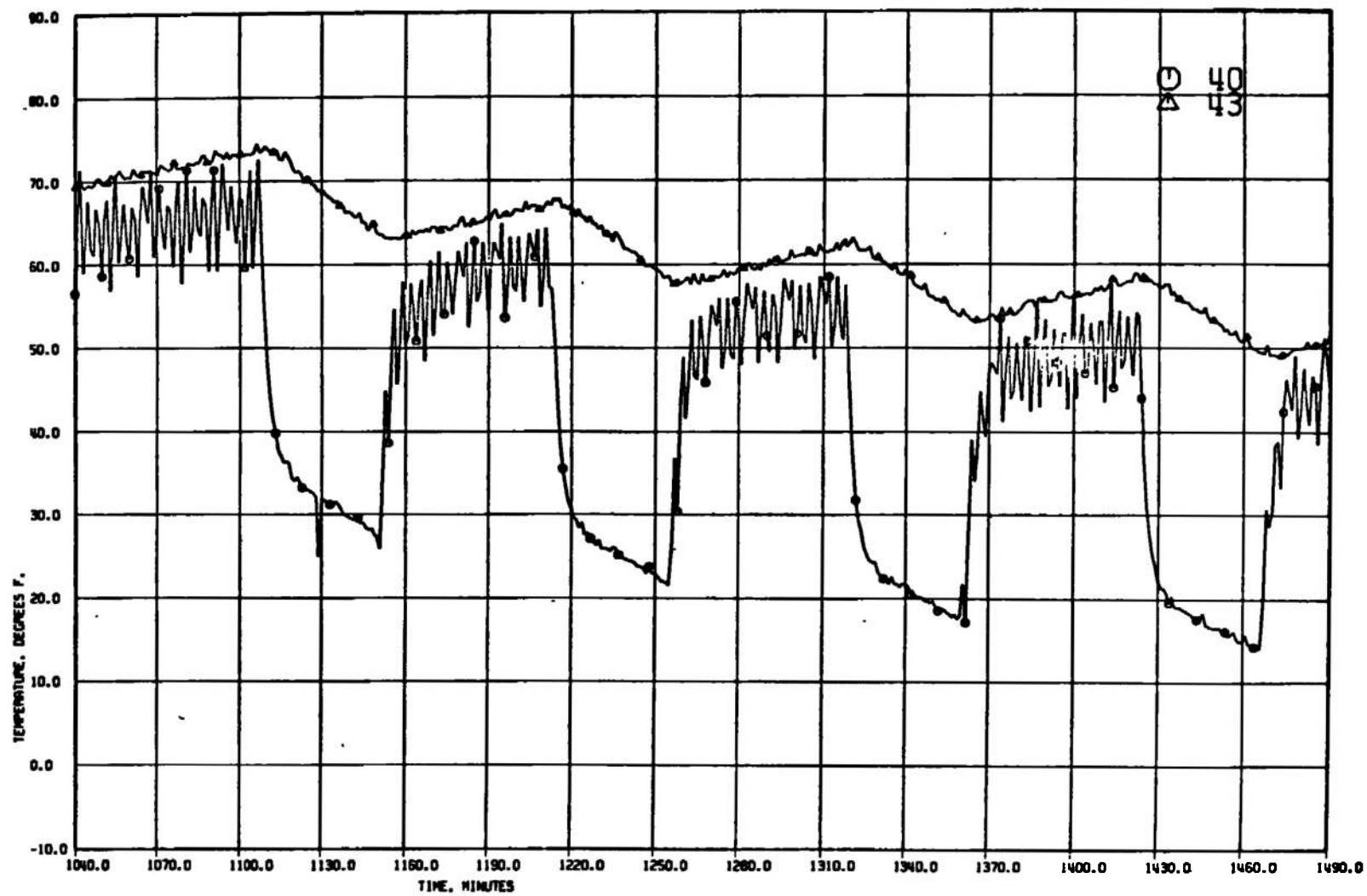
o. Concluded  
Fig. 15 Continued



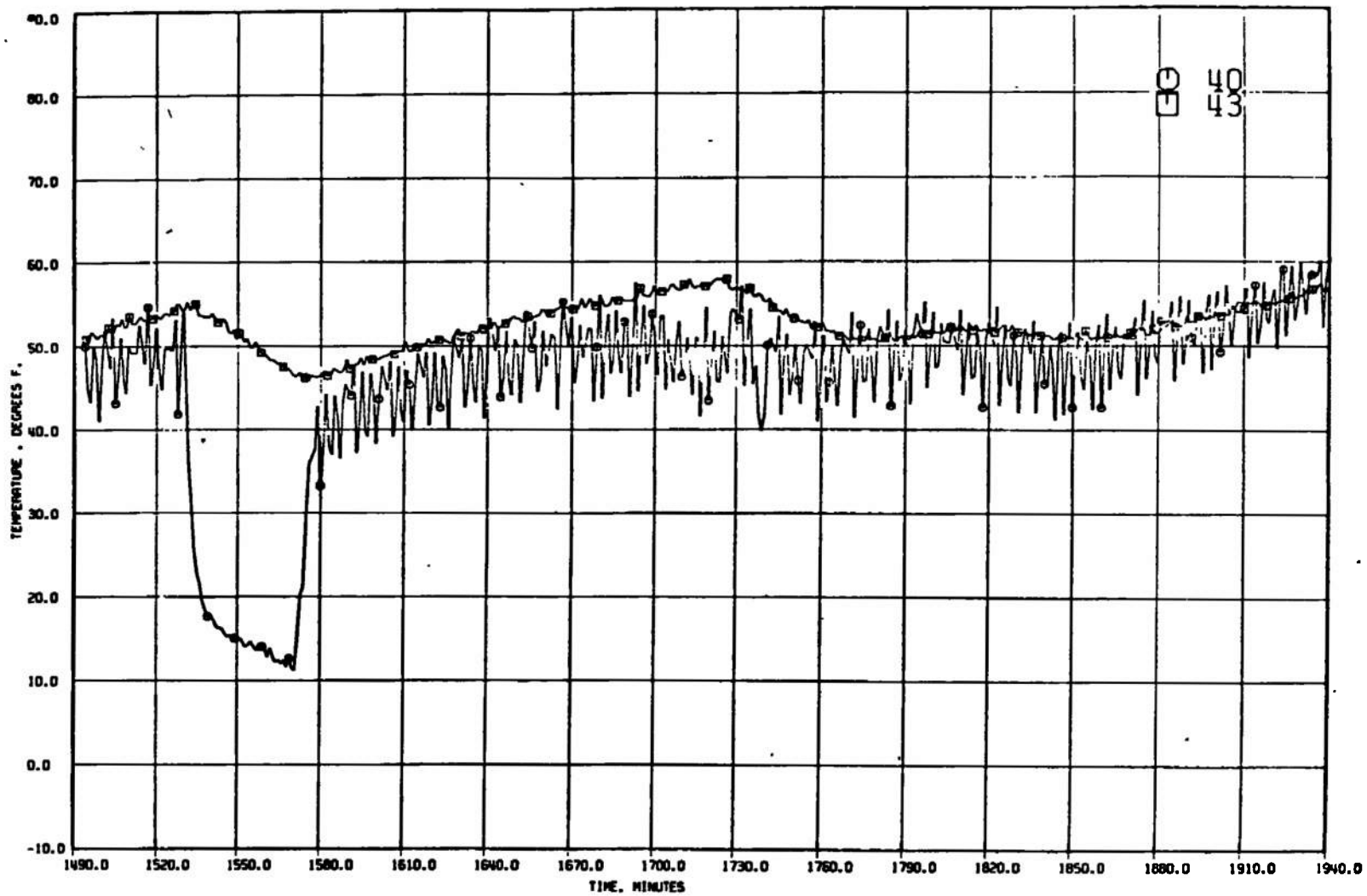
p. T/C 40 and 43  
Fig. 15 Continued



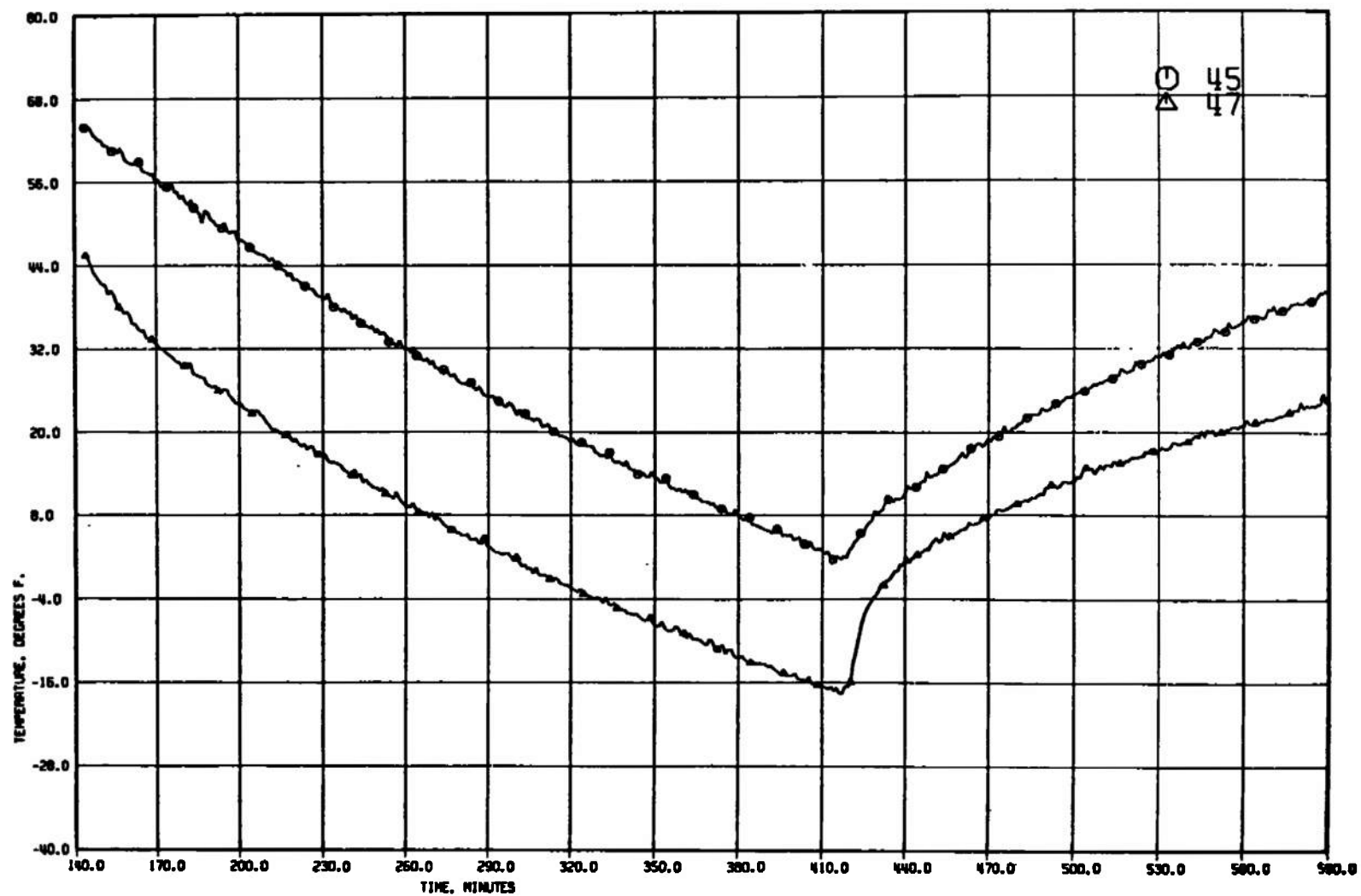
p. Continued  
Fig. 15 Continued



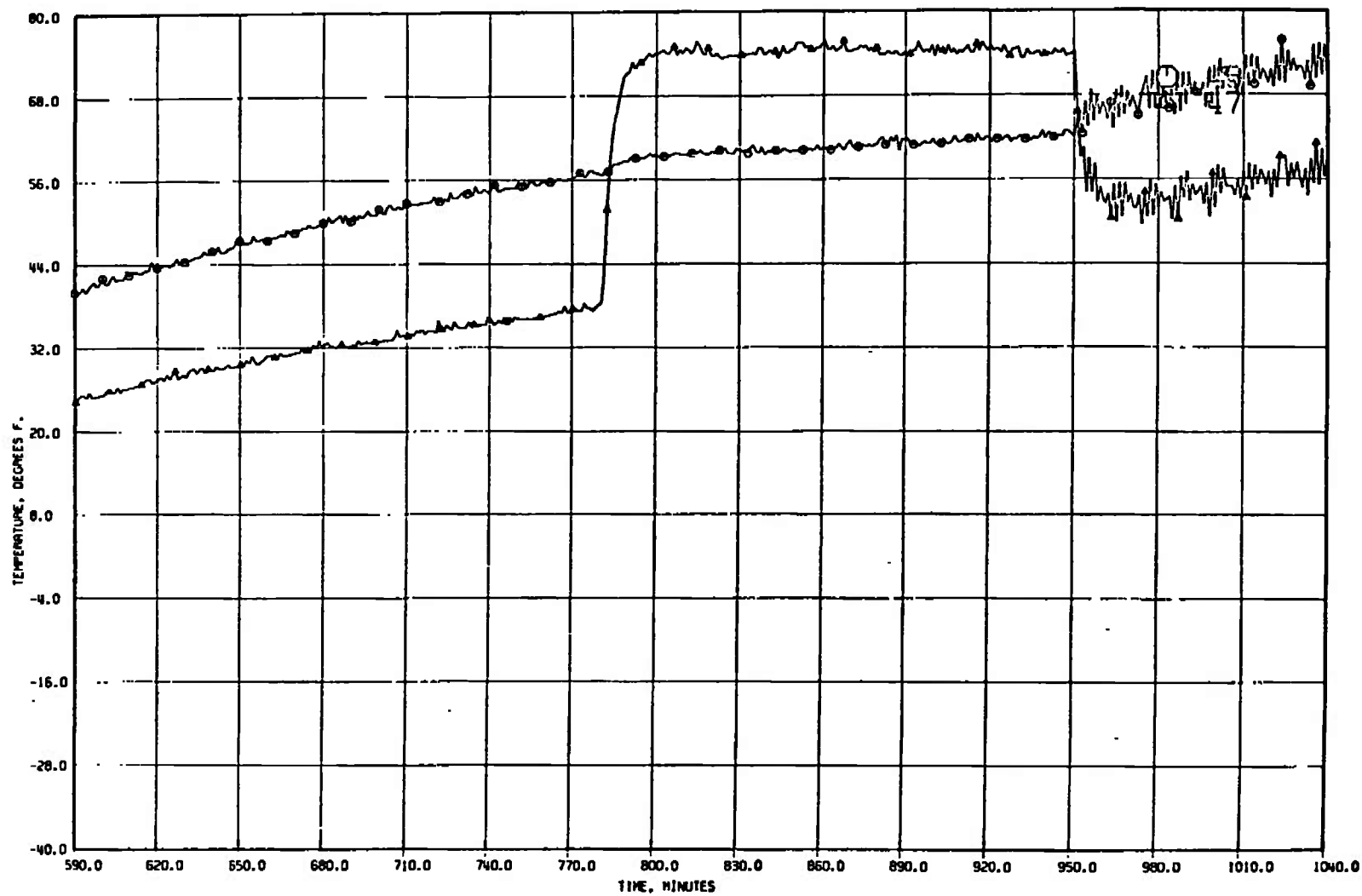
p. Continued  
Fig. 15 Continued



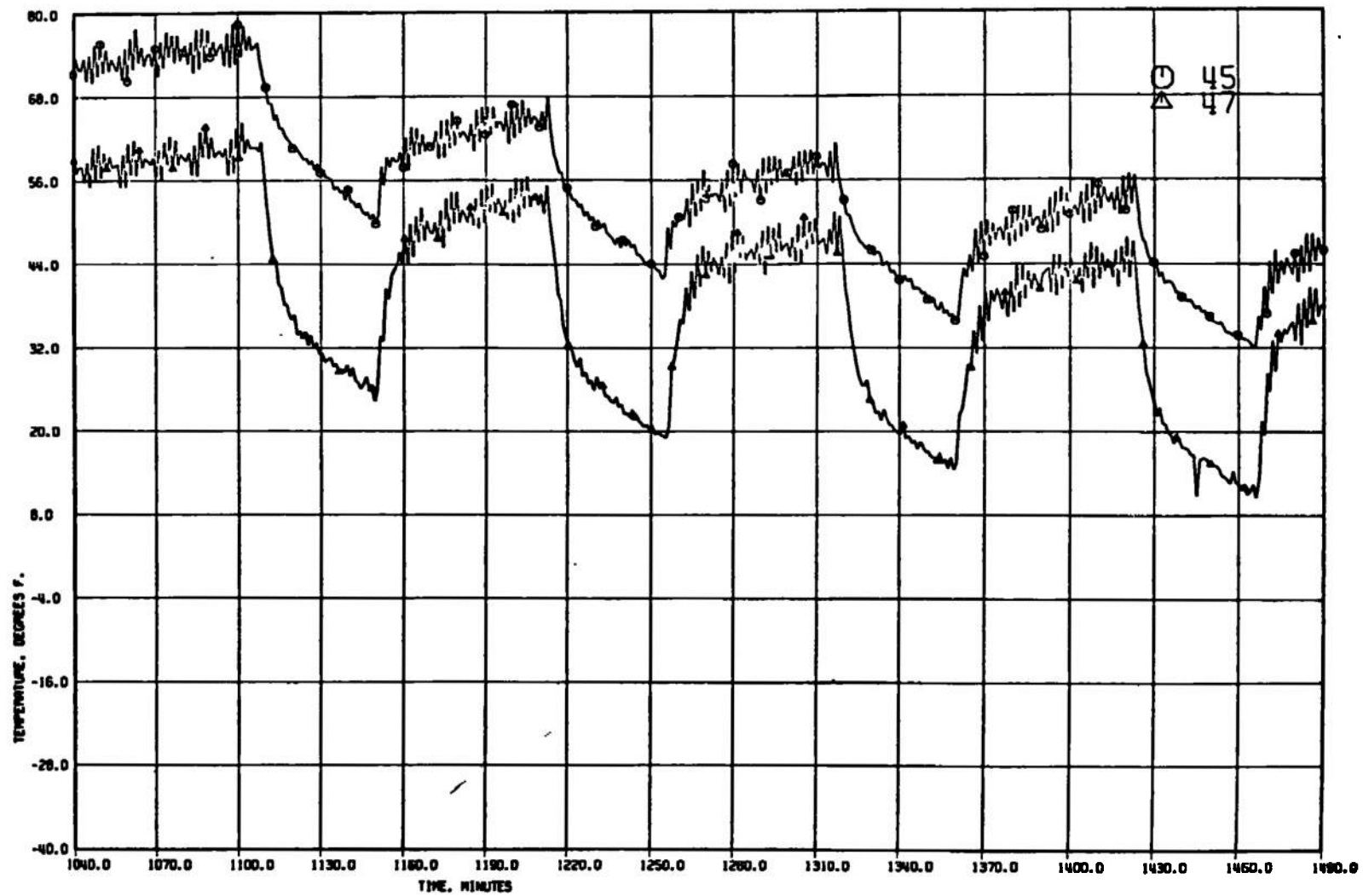
p. Concluded  
Fig. 15 Continued



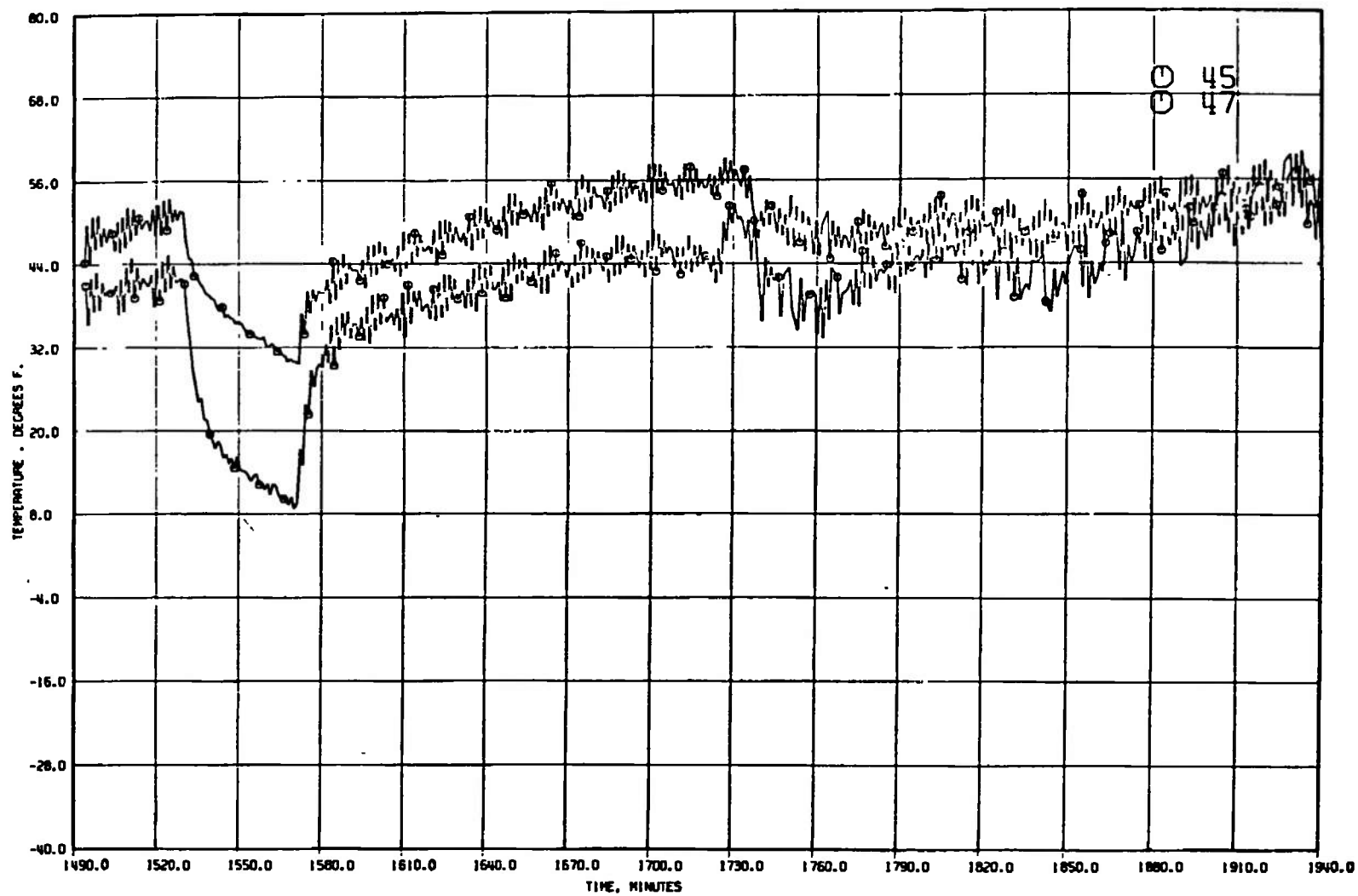
q. T/C 45 and 47  
Fig. 15 Continued



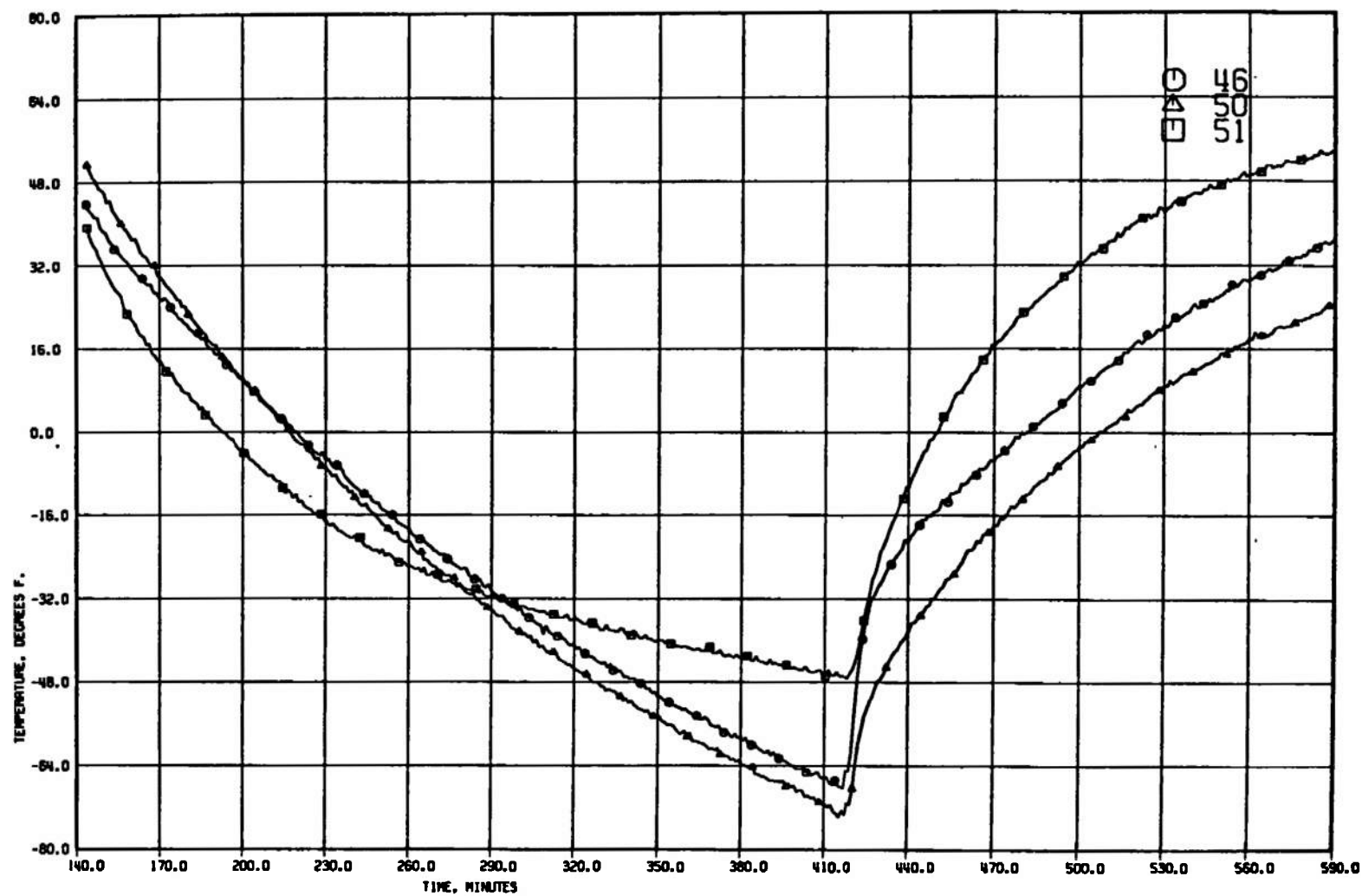
q. Continued  
Fig. 15 Continued



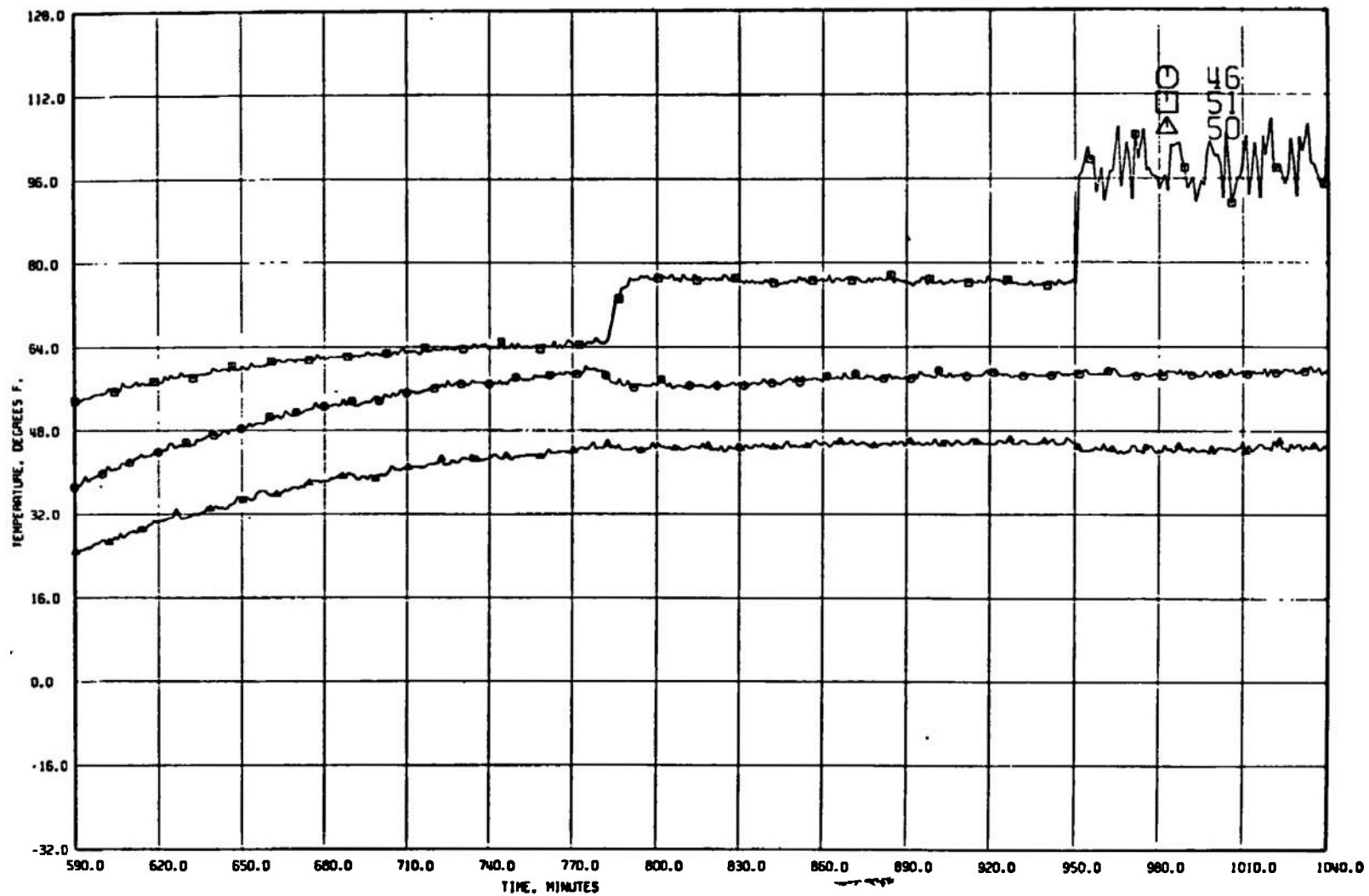
q. Continued  
Fig. 15 Continued



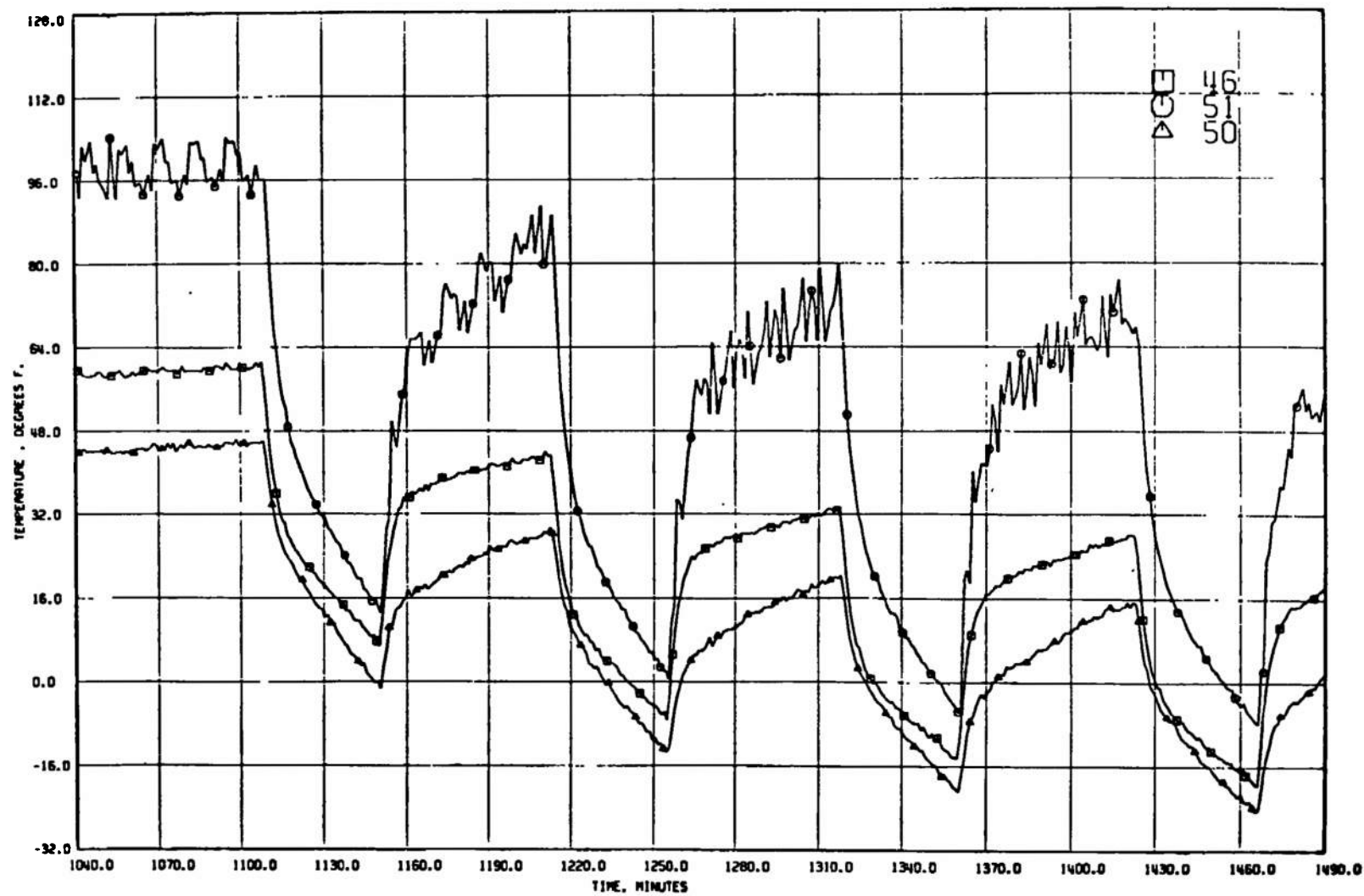
q. Concluded  
Fig. 15 Continued



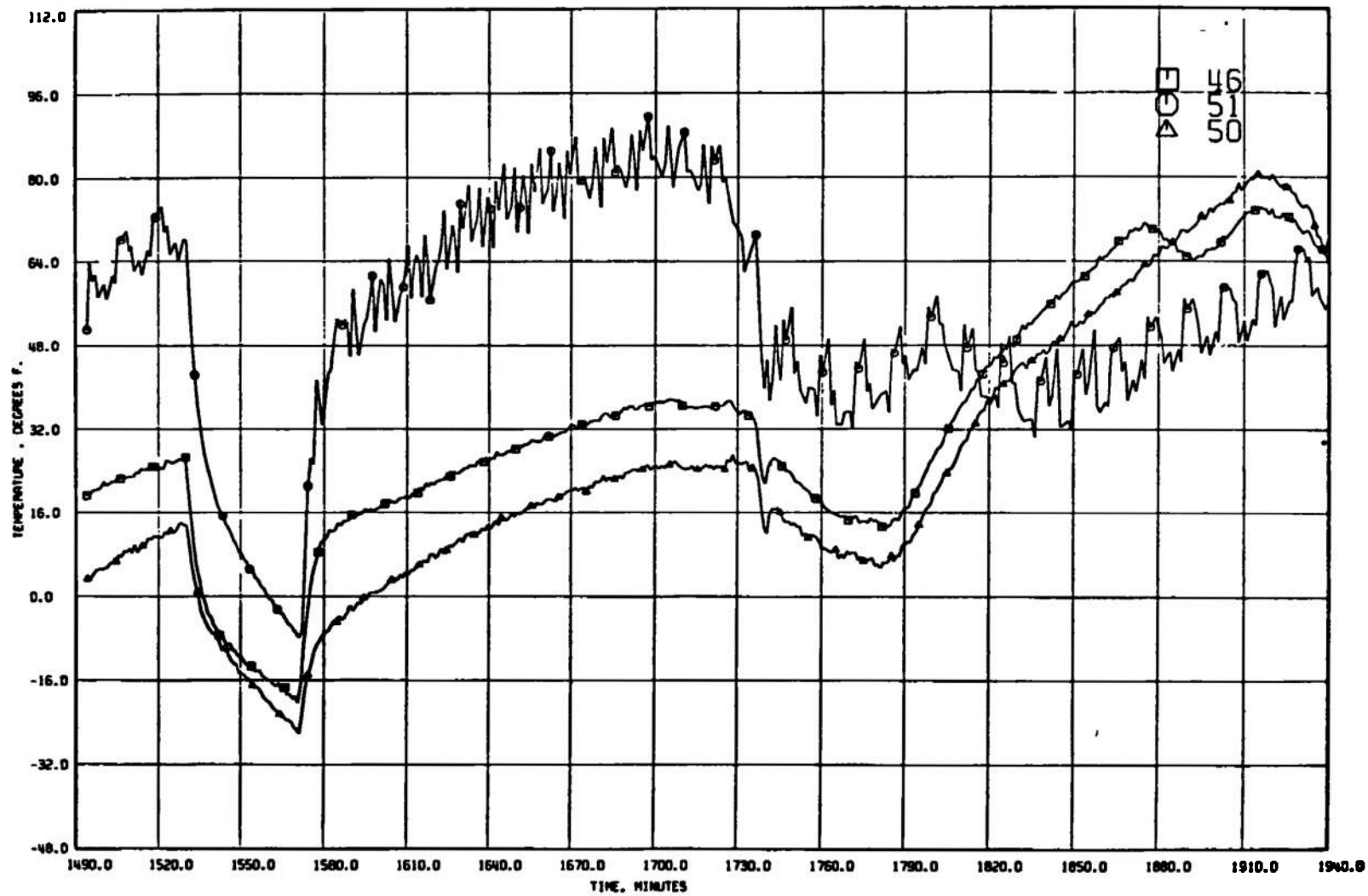
r. T/C 46, 50, and 51  
Fig. 15 Continued



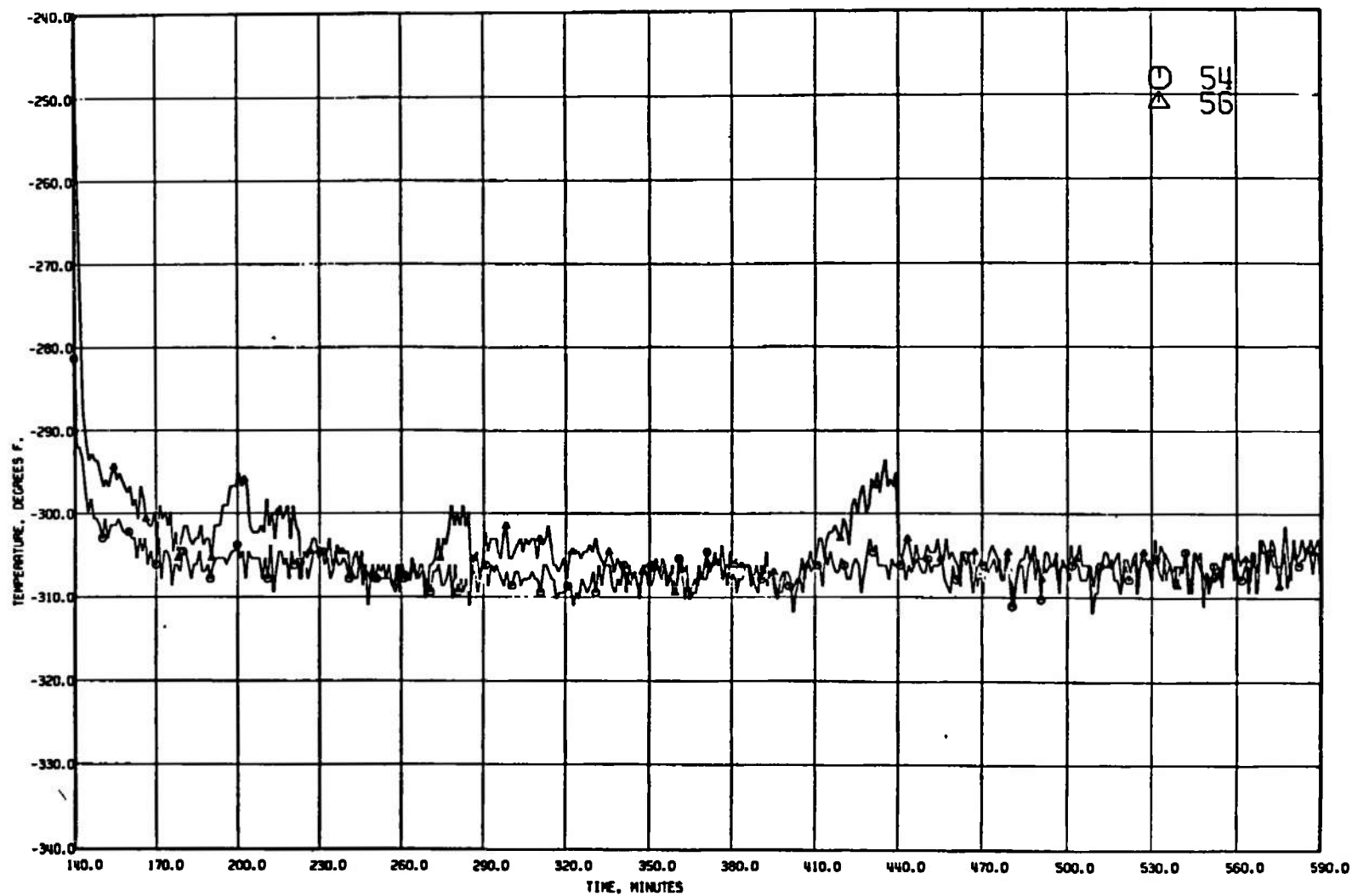
r. Continued  
Fig. 15 Continued



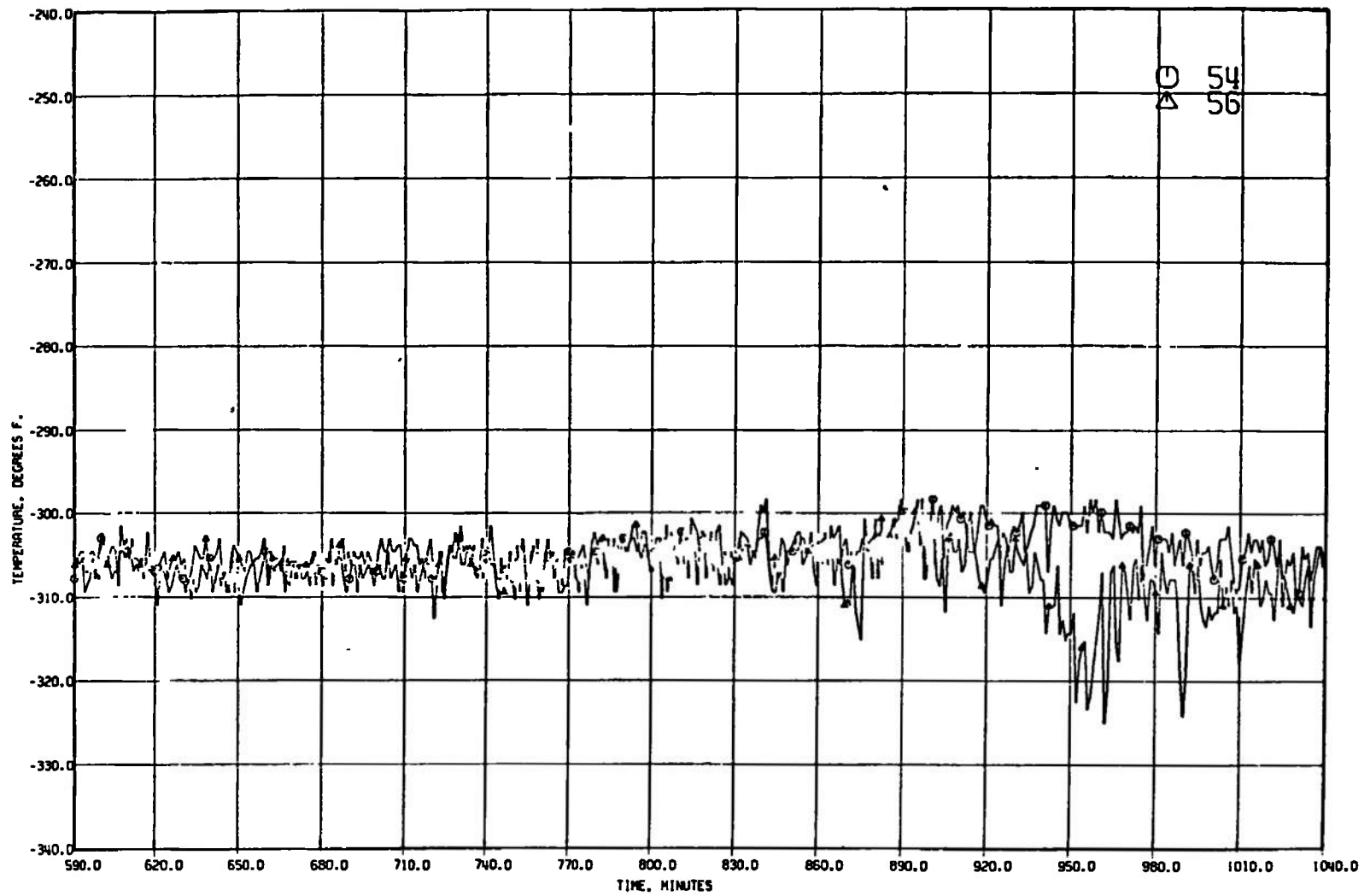
r. Continued  
Fig. 15 Continued



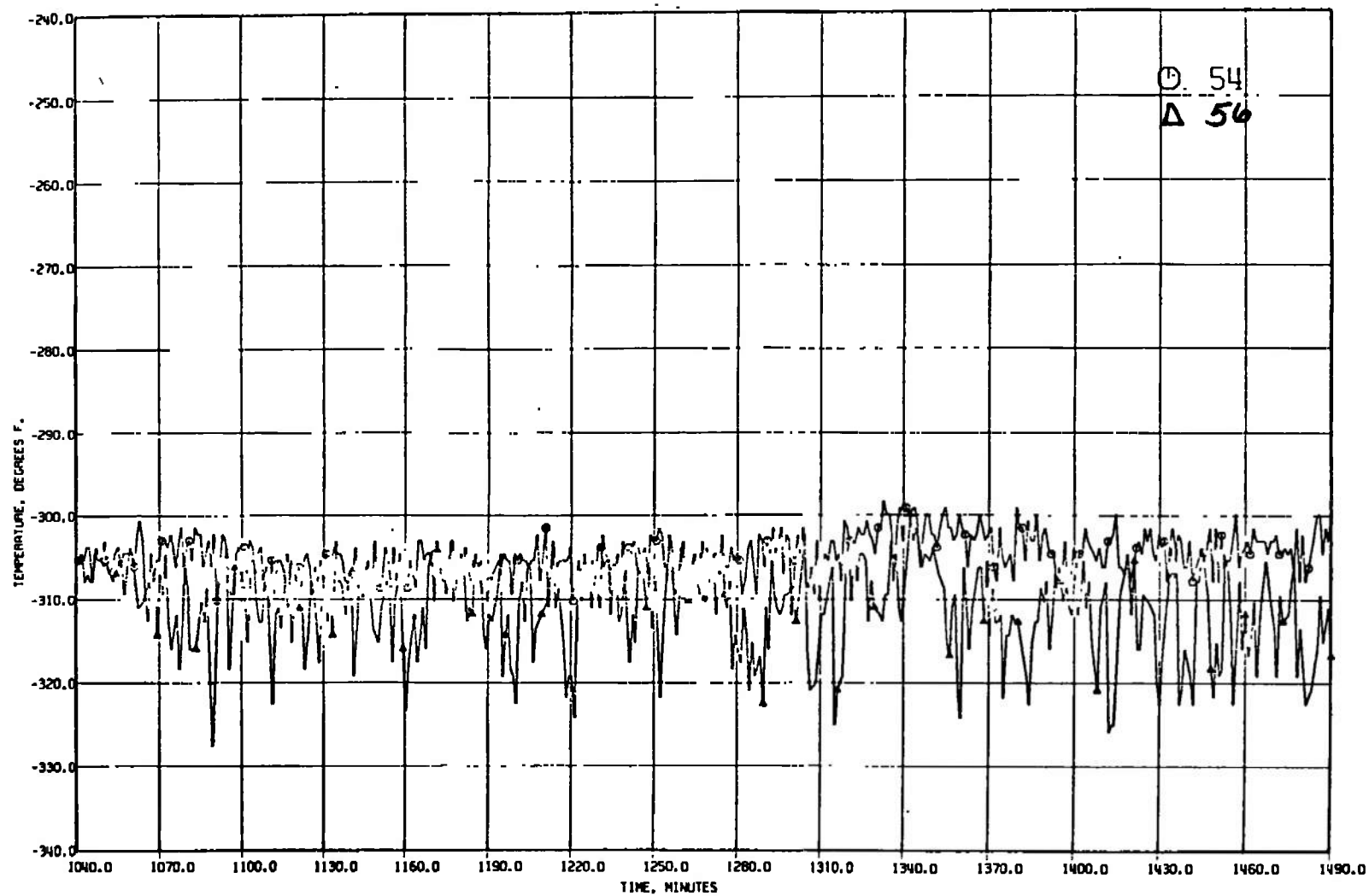
r. Concluded  
Fig. 15 Continued



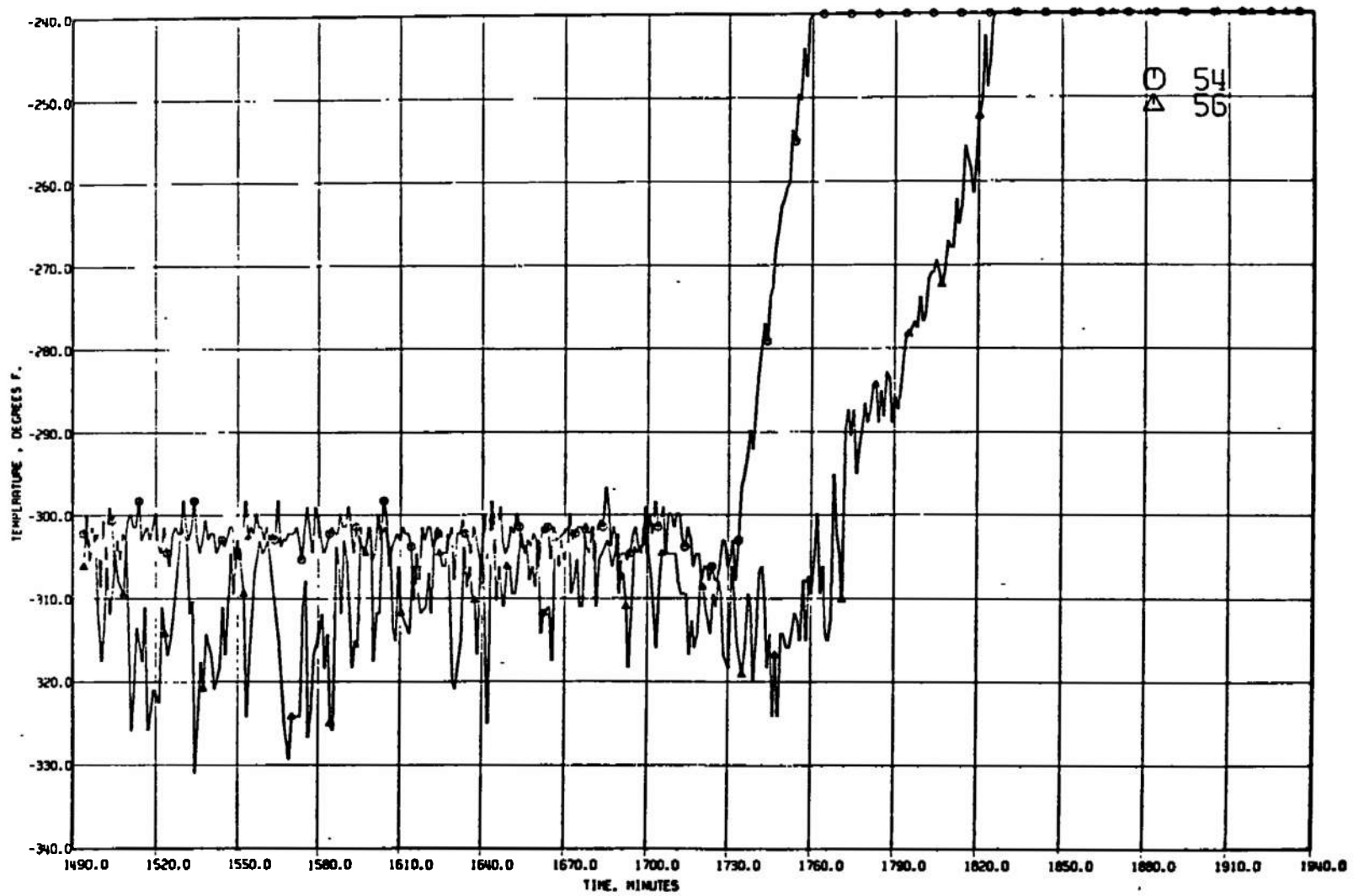
s. T/C 54 and 56  
Fig. 15 Continued



s. Continued  
Fig. 15 Continued

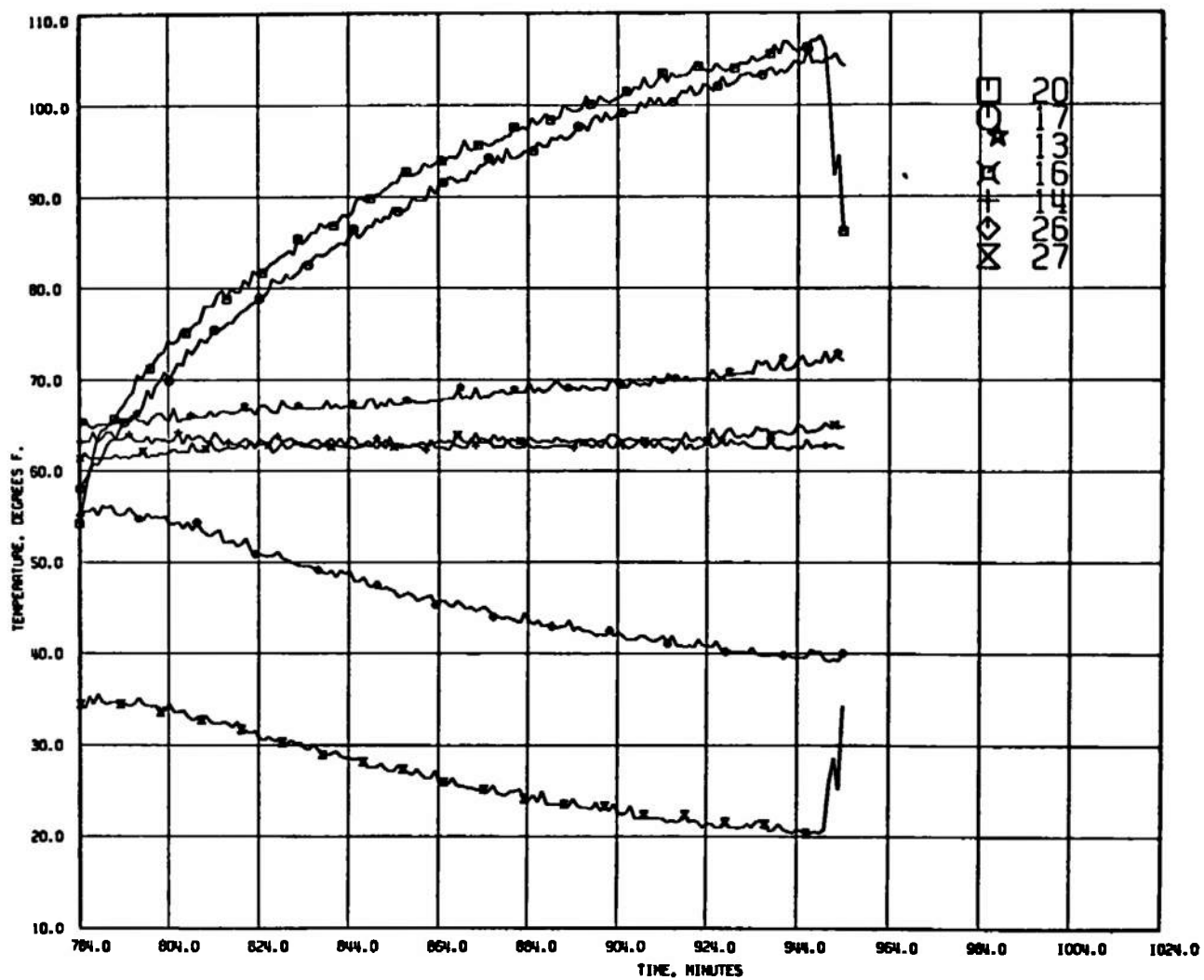


s. Continued  
Fig. 15 Continued

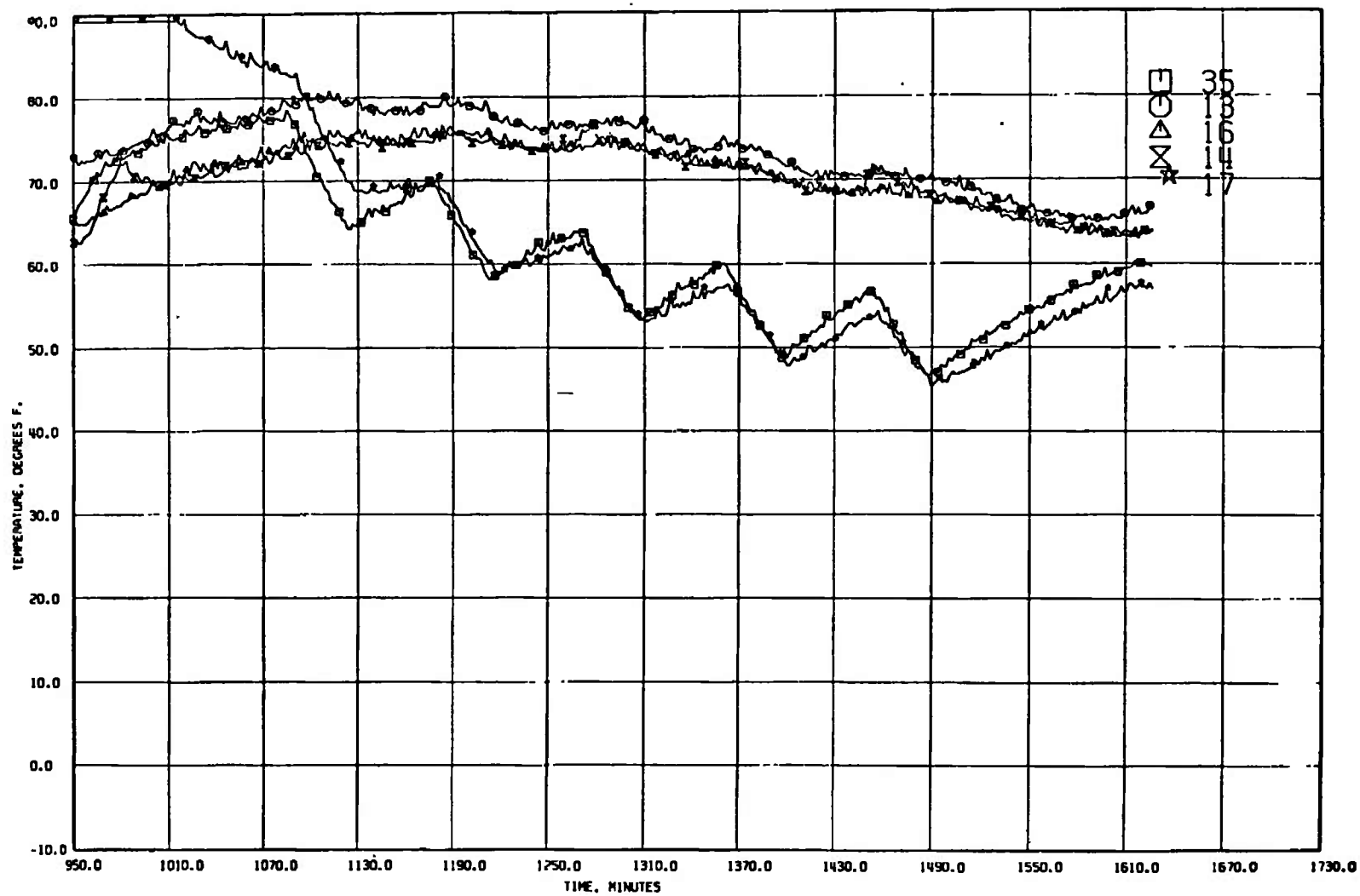


s. Concluded  
Fig. 15 Concluded

**a. Test 1, +X Axis Facing Solar Source**  
**Fig. 16 Primary Temperatures of Interest**



b. Test 2, +Z Axis Facing Solar Source  
Fig. 16 Continued



c. Test 3, Satellite Rotating about Y Axis  
Fig. 16 Concluded

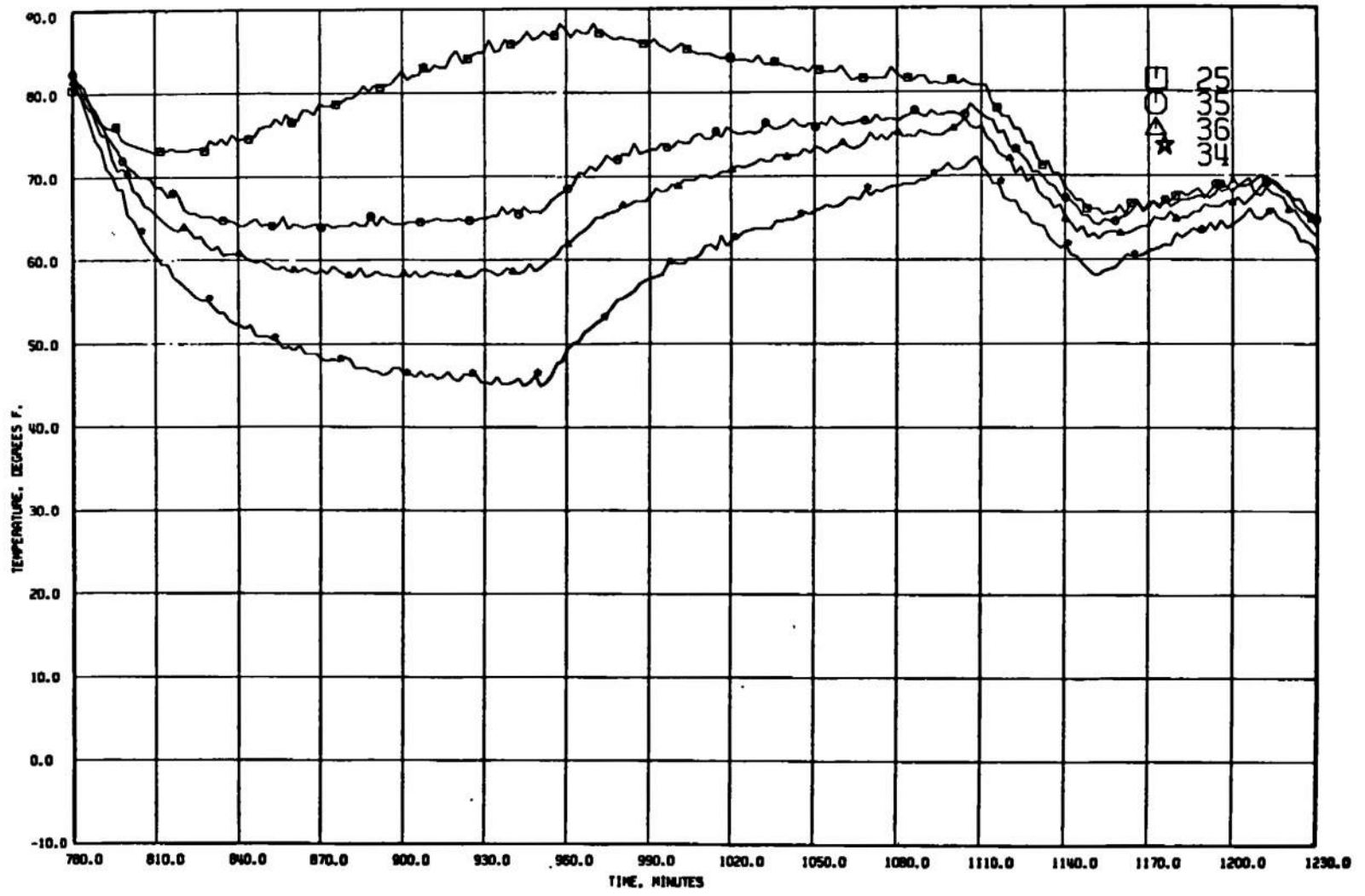


Fig. 17 Temperatures Related to Conduction through the Belly Band

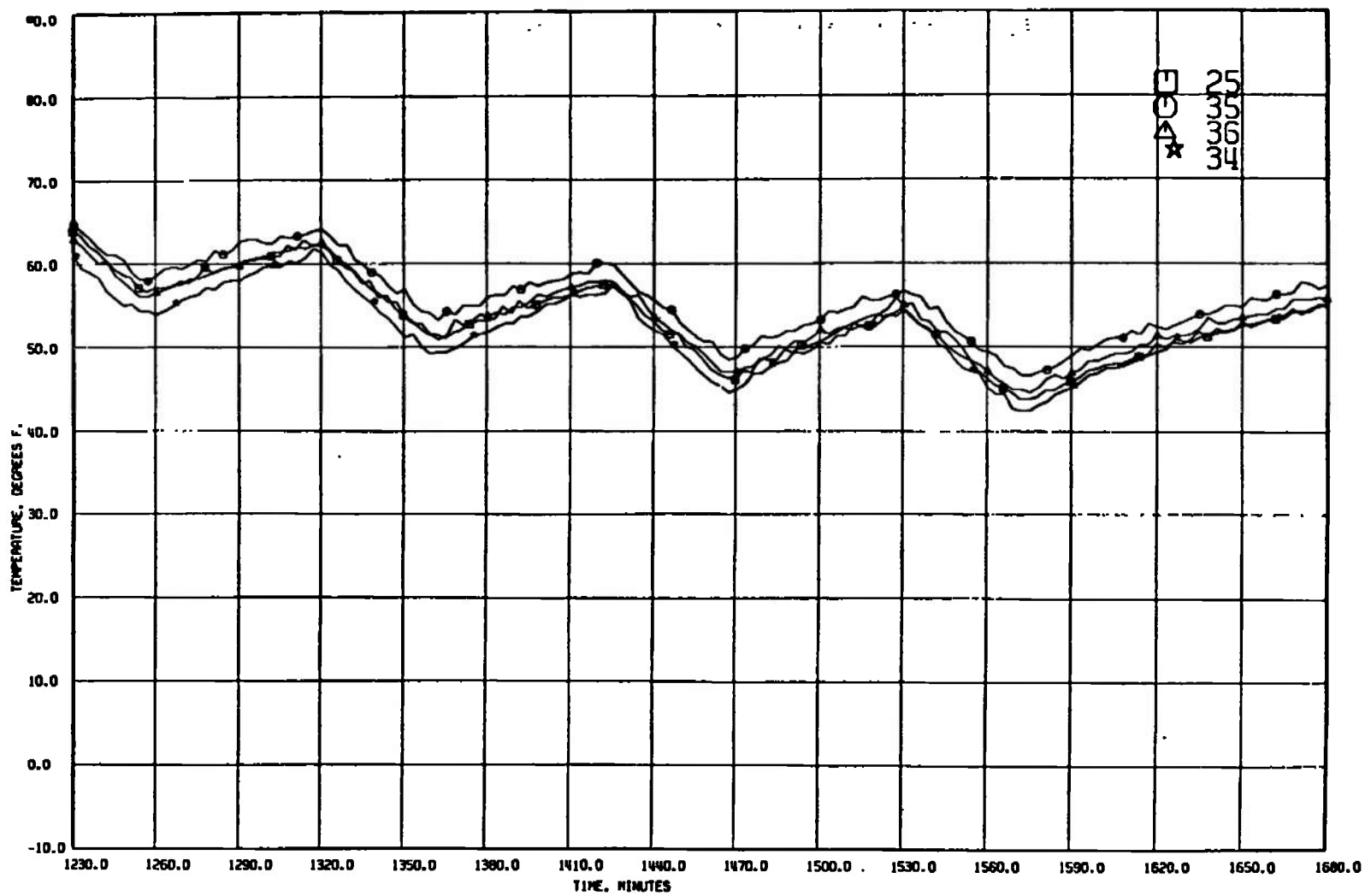


Fig. 17 Concluded

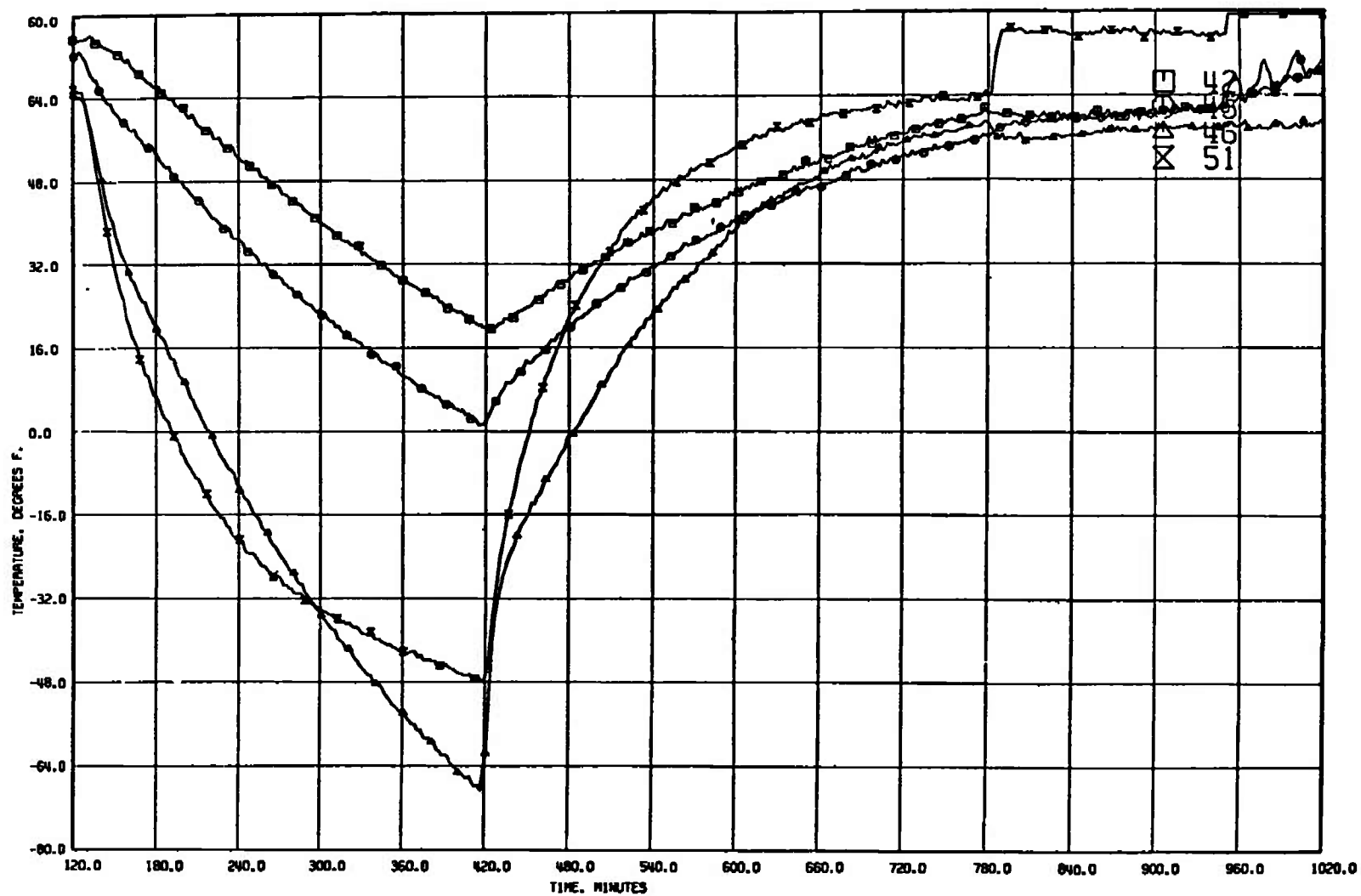


Fig. 18 Conduction through +Y Mounting Block

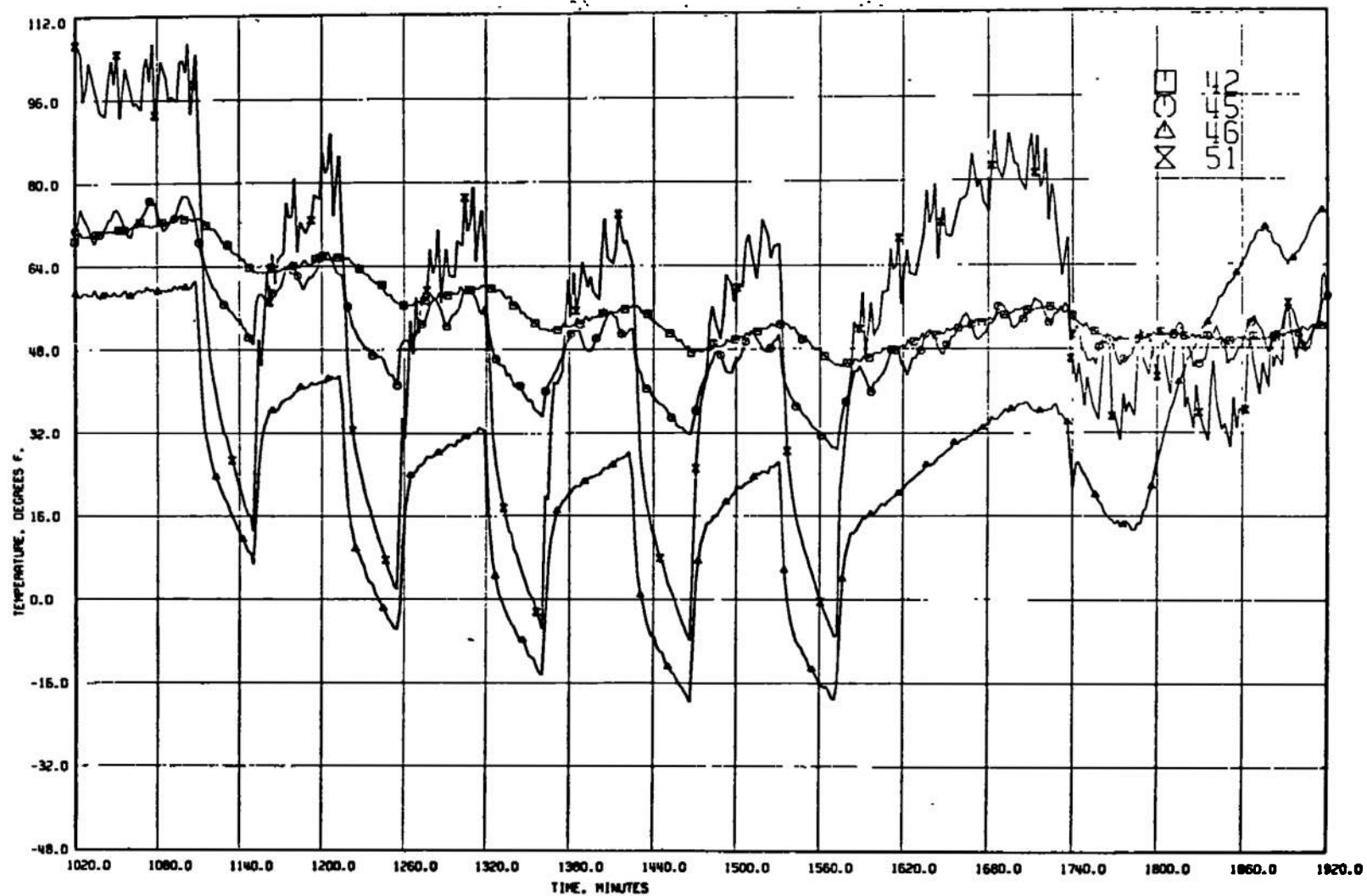


Fig. 18 Concluded

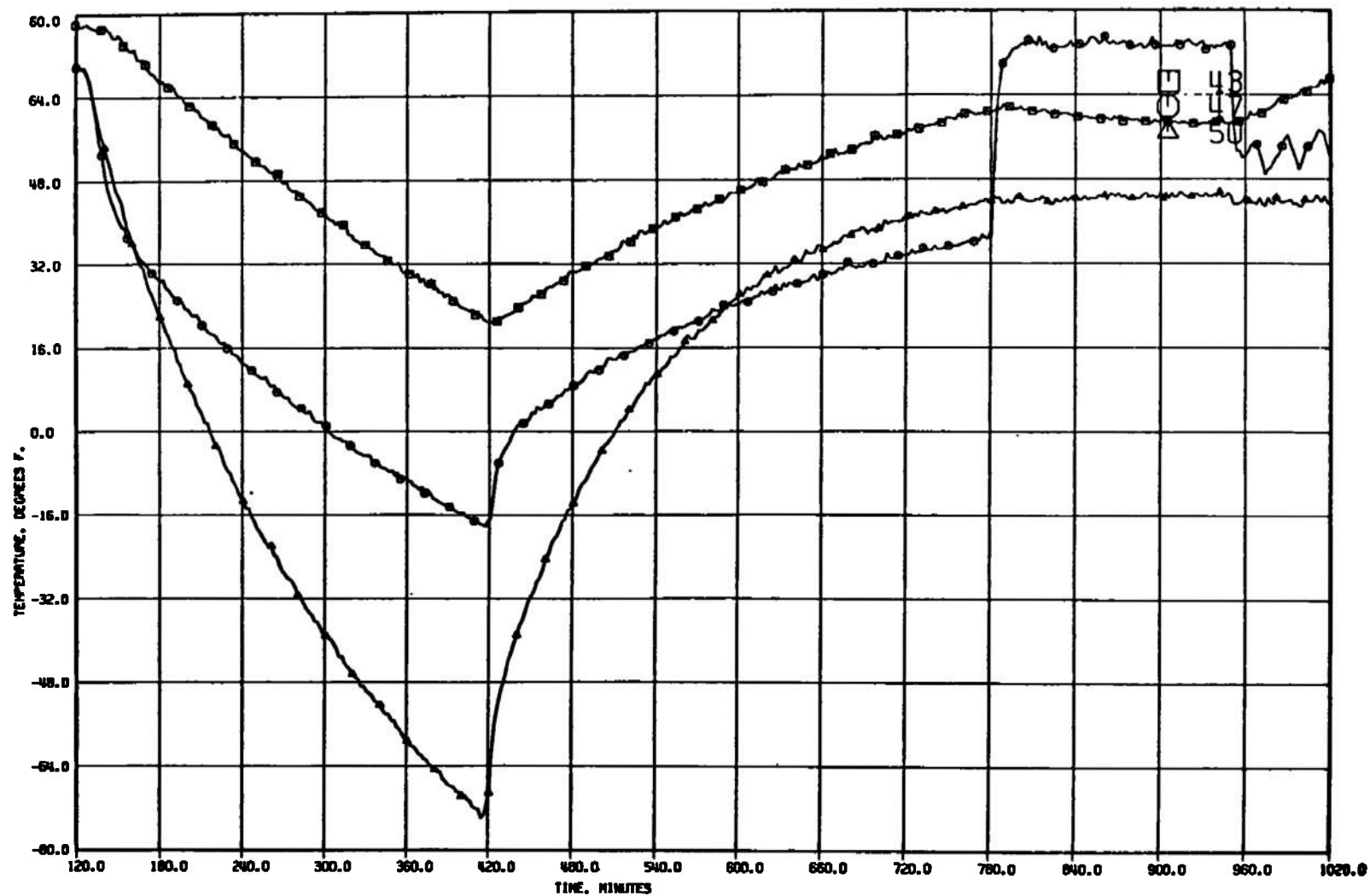


Fig. 19 Conduction through -Y Mounting Block

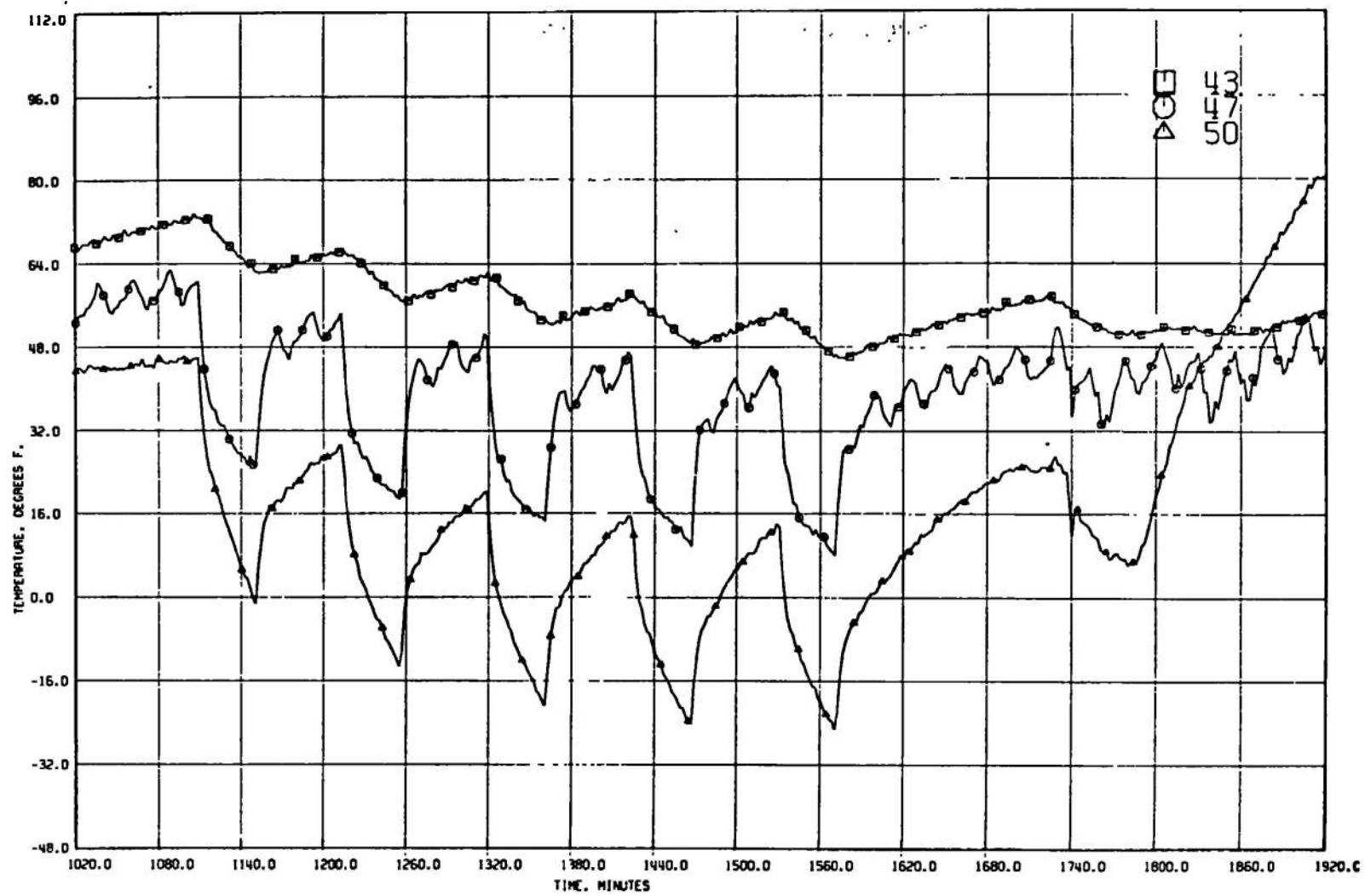


Fig. 19 Concluded

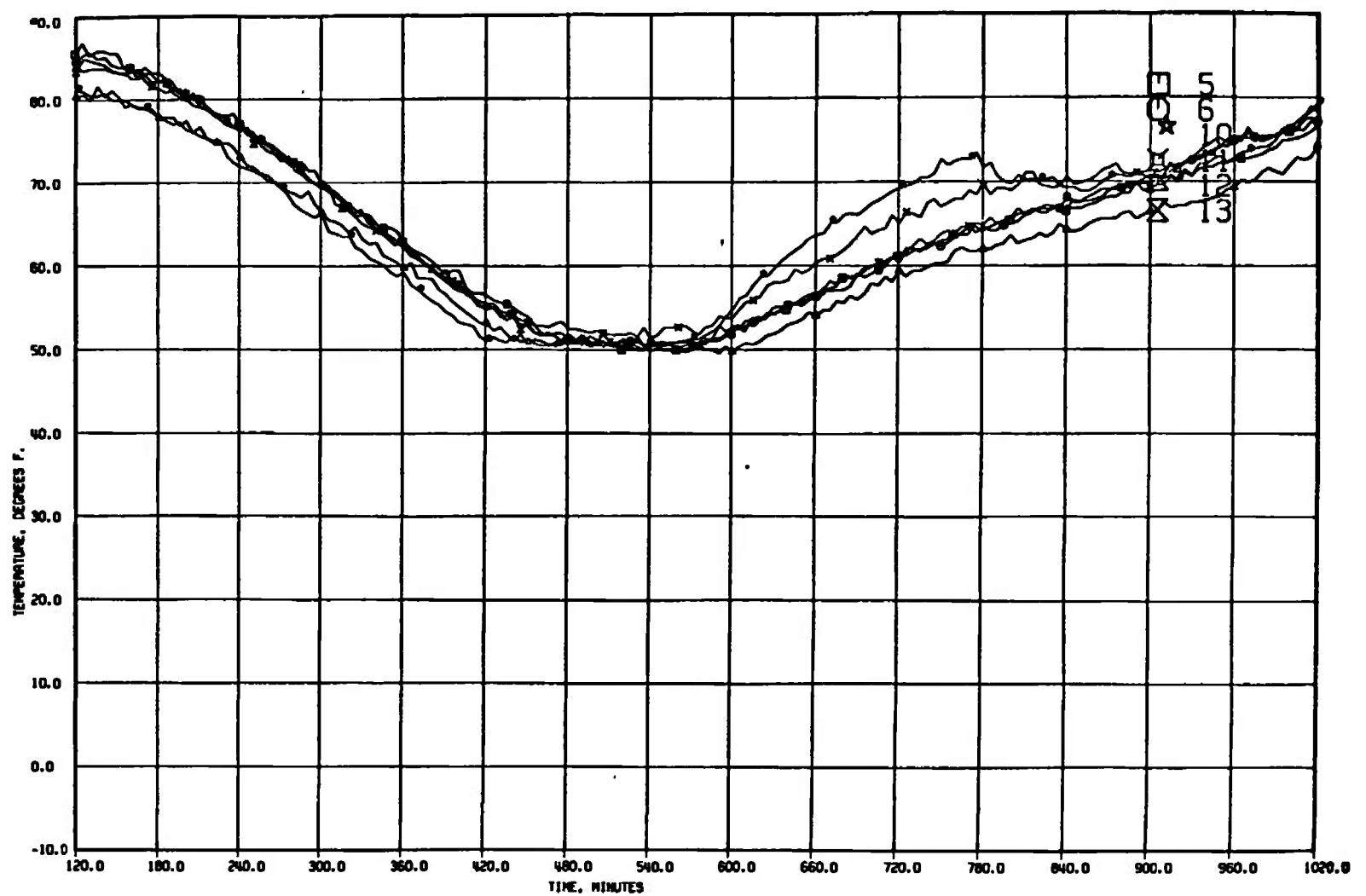


Fig. 20 Temperatures of North Deck Boxes

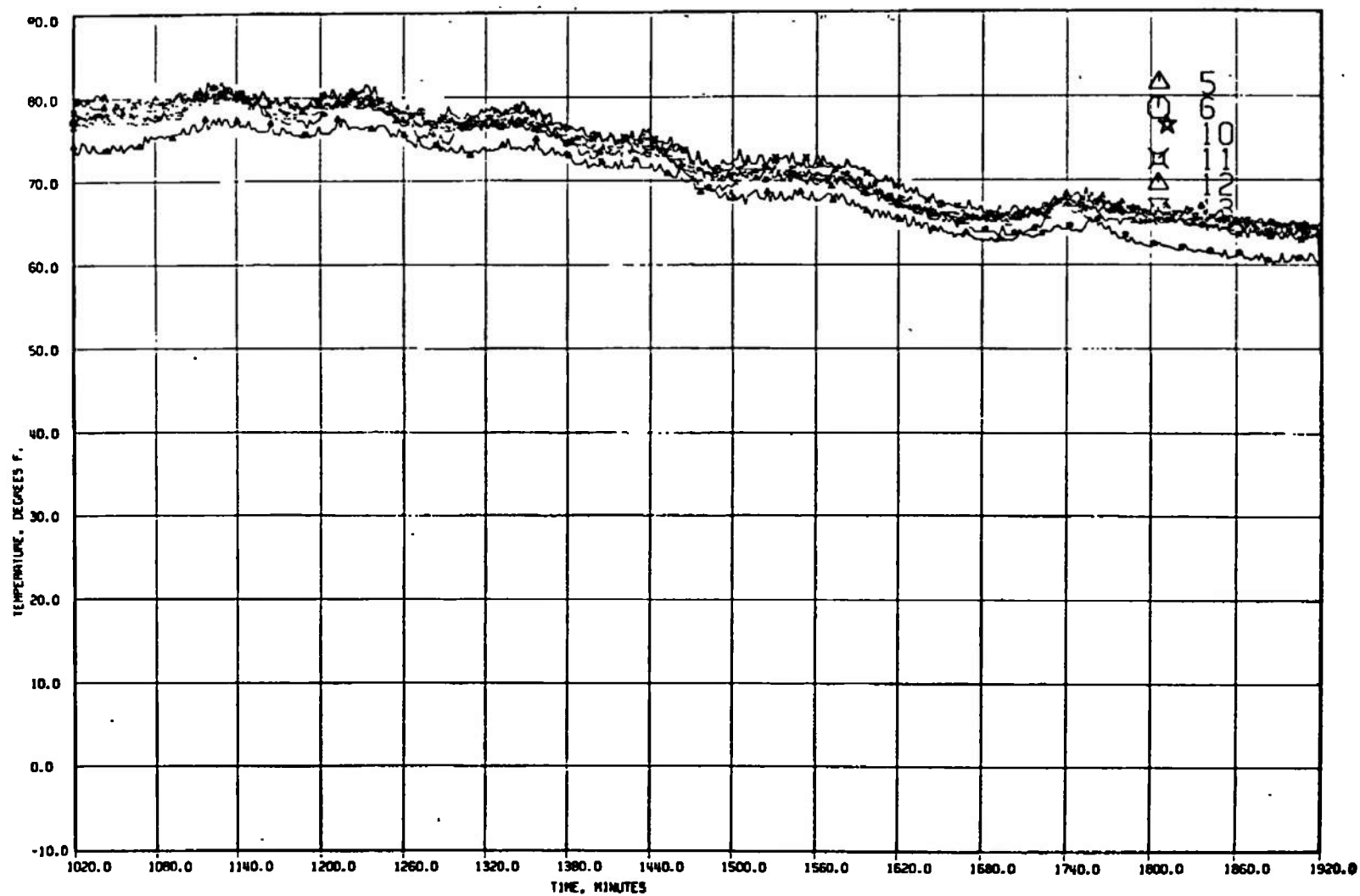


Fig. 20 Concluded

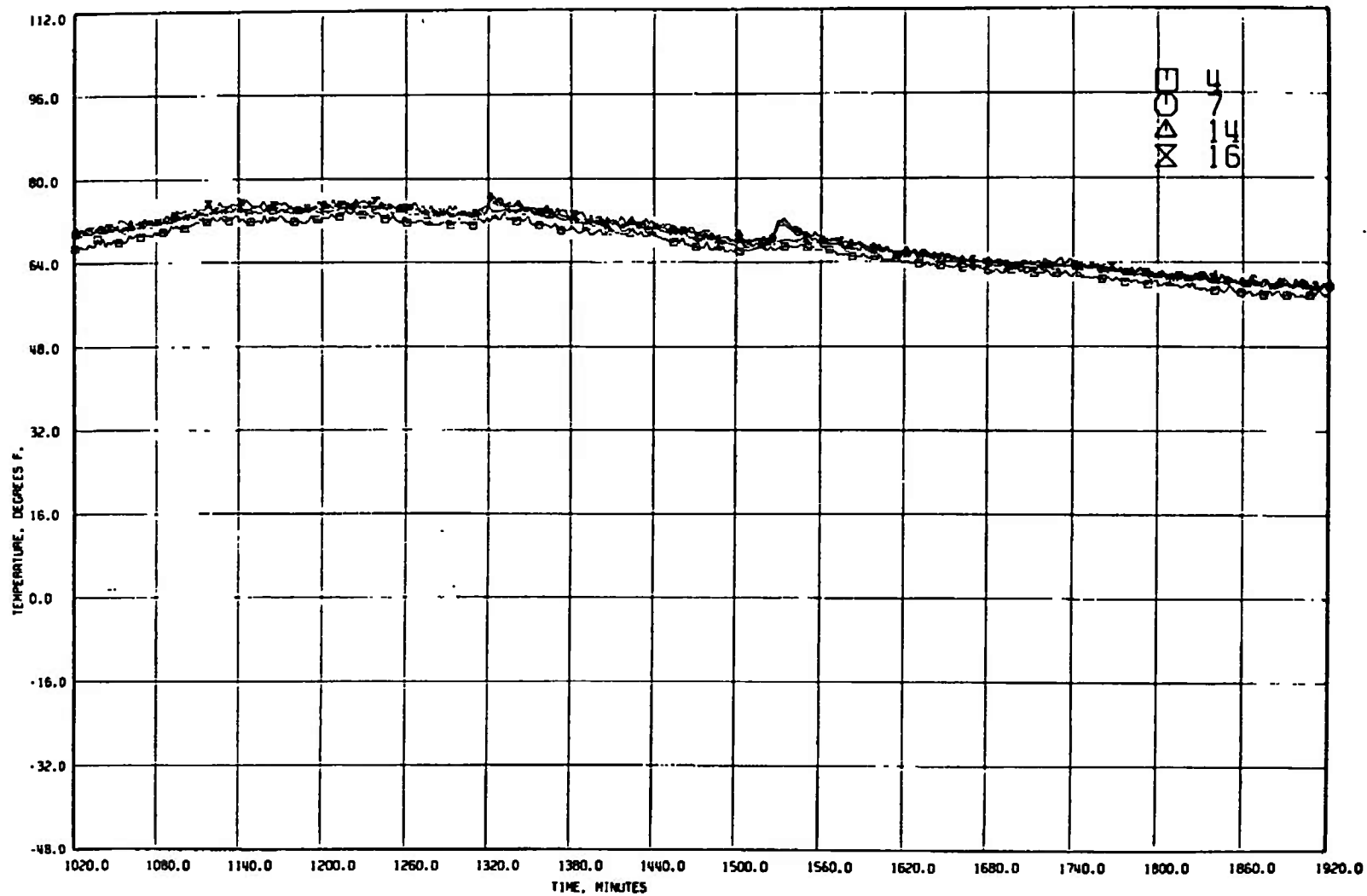


Fig. 21 Temperatures of South Deck Boxes

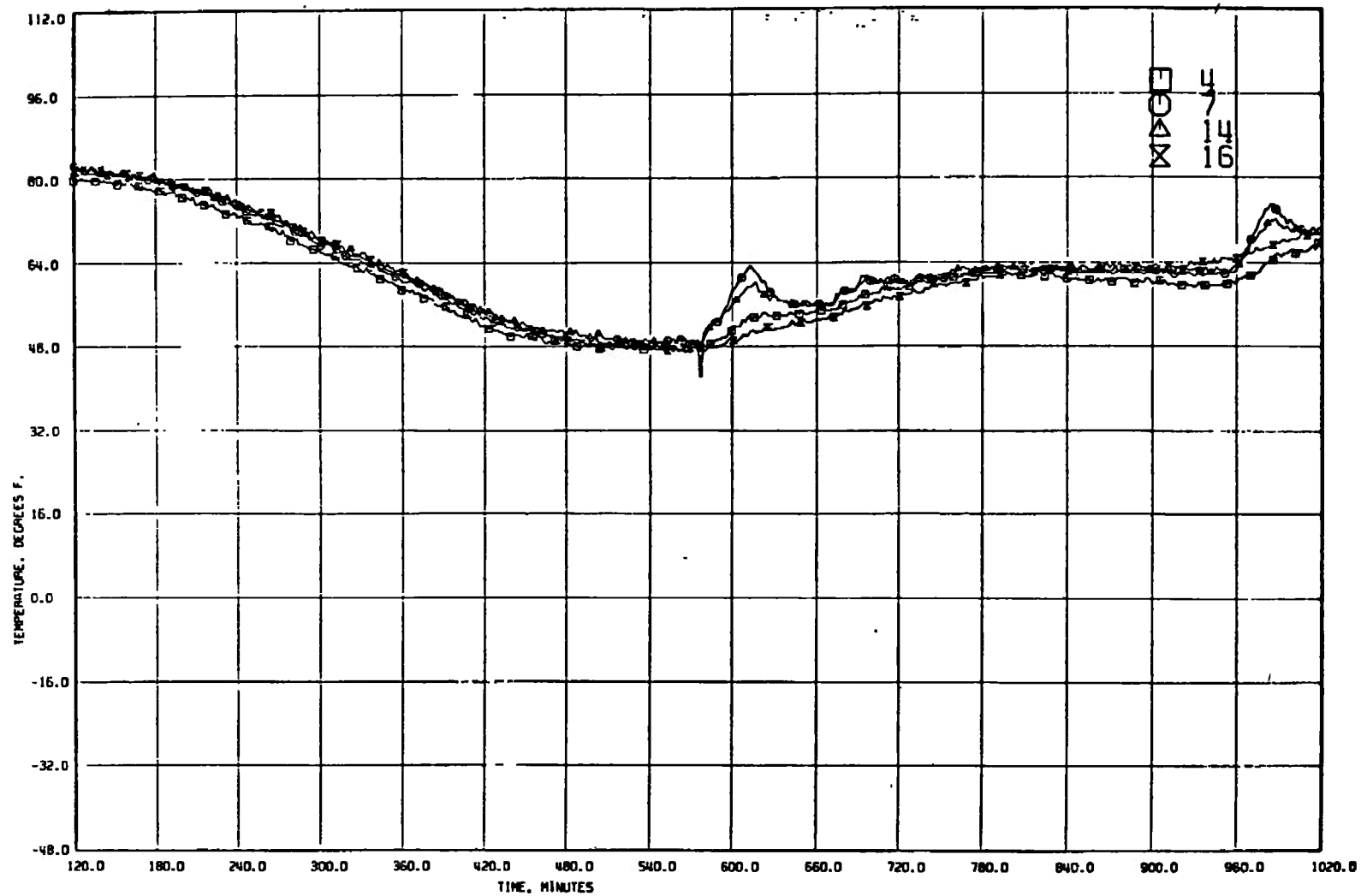


Fig. 21 Concluded

**TABLE I**  
**LN<sub>2</sub> CRYOWALL TEMPERATURES**

Data Point	Location of Thermocouple	Time and Reading in °F					
		19:05	01:27	04:03	11:05	11:46	14:00
1	View Port - West	-320	-320	-320	-320	-320	-320
2	View Port - East	-320	-320	-320	-320	-320	-320
3	Hy-Cal Shield	-320	-320	-320	-320	-320	-320
4	Solar Shield Panel 0°	-308	-276	-285	-281	-288	-278
5	Solar Shield Panel 90° (Est.)	-80	-80	-80	-80	-80	-80
6	Solar Shield Panel 180°	-307	-305	-308	-308	-307	-306
7(61)	Solar Shield Panel 270°	-80	-98	-78	-100	-93	-103
8	Cryopanel - North Left Back	-310	-312	-310	-311	-312	-307
9(55)	Cryopanel - North Right Back	-307	-305	-308	-300	-305	-299
10	Cryopanel - East Left Back	-318	-319	-315	-317	-316	-315
11	Cryopanel - East Right Back	-269	-272	-271	-275	-280	-273
12(56)	Cryopanel - Door	-306	-303	-310	-300	-304	-302
13(57)	Cryopanel - South Left Back	-291	-292	-295	-290	-293	-288
14	Cryopanel - Diff. Pump Vane	-240	-240	-240	-235	-235	-235
15	Cryopanel - West Left Bank	-320	-320	-320	-320	-320	-320
16(60)	Cryopanel - West Front Mid.	-307	-314	-310	-310	-312	-306
17	Cryopanel - Scavenger	-310	-308	-310	-307	-308	-305
18(54)	Cryopanel - Floor Ctn Fin	-281	-277	-280	-275	-306	-277
19	Cryopanel Floor Ring Hwd N. W.	-243	-243	-243	-244	-246	-244
20	Cryopanel Floor Ring Hwd S. E.	-244	-310	-312	-312	-310	-312
21	Shield Floor to Wall N. Side	-100	-108	-106	-108	-110	-110
22	Shield Floor to Wall N. Side	-102	-104	-104	-110	-111	-110
23	Shield Floor to Wall S. Side	-102	-106	-106	-108	-109	-107
24	Shield Floor to Wall E. Side	-95	-101	-101	-103	-104	-102
25	Cryopanel Floor N. Sec. W. Bot.	-308	-307	-307	-307	-316	-311
26	Cryopanel Floor N. Sec. E. Bot.	-314	-312	-315	-314	-308	-314
27	Cryopanel Floor N. Sec. Ctn Fin.	-307	-305	-307	-306	-300	-307
28	Cryopanel Floor N. Sec. E. Fin.	-302	-300	-320	-301	-298	-302
29	Cryopanel Floor N. Sec. W. Bot.	-306	-305	-306	-305	-311	-306
30	Cryopanel Floor S. Sec. W. Bot.	-308	-309	-308	-307	-318	-308
31	Cryopanel Floor S. Sec. E. Bot.	-309	-310	-308	-308	-319	-310
32	Cryopanel Floor S. Sec. E. Fin.	-303	-302	-303	-303	-310	-303
33	Cryopanel Floor S. Sec. W. Fin.	-288	-287	-288	-288	-304	-288
34	Solar Mirror	93	100	100	97	95	96
35	Solar Mirror	100	100	100	98	94	98

**TABLE II**  
**TEST STAND TEMPERATURES**

Data Point	Location of Thermocouple	Time and Reading in °F					
		19:05	01:27	04:03	11:05	11:46	14:00
36	Test Stand - E. Top	-3	31	32	-4	-24	12
37	Test Stand - S.E. Angle Brace	2	33	36	2	-34	16
38	Test Stand - S.E. Base	-3	31	35	-1	-31	13
39	Test Stand Cross Brace	-32	4	5	-26	-34	-15
40	Test Stand West Top	8	51	52	12	-7	26
41(45)	Test Stand - Drive Shaft Blk.	37	66	3	51	30	57
42(46)	Test Stand - Bearing Block	31	59	62	27	-20	38
43(47)	Test Stand Shaft Block	22	59	62	41	9	45
44(50)	Test Stand - Bearing Block	20	44	47	14	-25	26
45(51)	Main Drive Shaft	51	97	106	69	-7	85
SOLAR INTENSITY							
Data Point	Location of Calorimeter	Time and Reading in w/m <sup>2</sup>					
		19:05	01:27	04:04	11:05	11:46	14:00
46(3)	N. W. Rad. (Figs. 10 and 12)	1392	1407	1439	1344	0	1383
47	N. E. Rad. (Figs. 10 and 12)	Backup in Case of Loss of N.W. Rad.					
CHAMBER PRESSURE							
		Time and Reading in torr (x 10 <sup>-6</sup> )					
		2.2	3.0	3.0	1.8	1.8	3.0
48	Chamber - Top						

**TABLE III**  
**SATELLITE TEMPERATURES**

Data Point	Location of Thermocouple*	Time and Reading in °F					
		19:05	01:27	04:03	11:05	11:46	14:00
51(4)	Tape Recorder	48	60	73	68	67	63
52(5)	Battery Box	51	76	80	71	70	66
53(6)	C. W. Osc.	51	75	80	73	71	67
54(7)	Beacon	49	62	74	72	68	64
55(10)	Eng. Encoder	52	73	80	72	72	65
56(11)	Clock	53	75	80	73	73	66
57(12)	Battery Charge Cont'd	50	69	77	68	68	64
58(13)	N. Deck	51	73	79	72	70	66
59(14)	S. Deck	50	63	74	72	69	64
60(15)	Plate Com N. and S. Deck	50	65	76	69	68	63
61(16)	225° on Inside Rack	48	65	75	69	69	63
62(17)	+Z Inside	38	106	83	54	45	57
63(20)	+Z Outside	16	93	67	37	15	40
64(21)	45° in, +X+Z	53	97	81	53	44	56
65(22)	45° in, -X+Z	22	97	76	47	40	50
66(23)	45° in, -Y+Z	33	100	79	49	41	53
67(24)	45° in, +Y+Z	34	97	77	50	42	53
68(25)	+X in, +Z +X	63	87	81	55	44	58
69(26)	-Z Inside	37	40	66	52	47	55
70(27)	-Z Outside	18	26	55	43	23	48
71(30)	45° in, -Z+Y	37	41	65	52	43	54
72(31)	45° in, -Y-Z	34	38	65	49	41	52
73(32)	45° in, -Z-X	21	39	62	48	42	50
74(33)	37° in, -Z+X	47	37	66	51	43	54
75(34)	+X in, -Z+X	64	46	73	55	43	57
76(35)	+X Inside, N. Side	64	68	78	57	47	59
77(36)	+X Inside, S. Side	63	60	76	55	45	58
78(39)	-X Inside	20	54	66	49	41	50
79(40)	+X Outside	70	59	64	55	12	51
80(41)	-X Outside	9	45	62	36	25	42
81(42)	+Y Inside	44	63	74	54	46	56
82(43)	-Y Inside	43	60	74	55	47	58
83(44)	225° Outside	58	64	66	54	28	54

\*Furnished by user without further specification.

UNCLASSIFIED

Security Classification

## DOCUMENT CONTROL DATA - R &amp; D

(Security classification of title, body of abstract and indexing annotation must be entered when the overall report is classified)

## 1. ORIGINATING ACTIVITY (Corporate author)

Arnold Engineering Development Center  
Arnold Air Force Station, Tennessee 37389

## 2a. REPORT SECURITY CLASSIFICATION

UNCLASSIFIED

## 2b. GROUP

N/A

## 3. REPORT TITLE

OAR-901 SATELLITE THERMAL TEST

## 4. DESCRIPTIVE NOTES (Type of report and inclusive dates)

Final Report, April 20 through 22, 1971

## 5. AUTHOR(S) (First name, middle initial, last name)

N. C. Latture, ARO, Inc.

## 6. REPORT DATE

October 1971

## 7a. TOTAL NO. OF PAGES

124

## 7b. NO. OF REFS

1

## 8a. CONTRACT OR GRANT NO.

## b. PROJECT NO.

c. Program Element 63404F

## d.

## 9a. ORIGINATOR'S REPORT NUMBER(S)

AEDC-TR-71-157

## 9b. OTHER REPORT NO(S) (Any other numbers that may be assigned this report)

ARO-VKF-TR-71-133

## 10. DISTRIBUTION STATEMENT

Approved for public release; distribution unlimited.

## 11. SUPPLEMENTARY NOTES

Available in DDC.

## 12. SPONSORING MILITARY ACTIVITY

Air Force Cambridge Research Laboratory (SUOR), L. G. Hanscom Field,  
Bedford, Mass. 01730

## 13. ABSTRACT

The OAR-901 satellite flight is part of the continuing upper atmosphere experimental program. The satellite was tested in a vacuum chamber to establish equilibrium temperatures for three different orientations. Tests were successfully completed for two fixed orientations and with the satellite rotating  $\pm 270$  deg at 0.5 rpm. Solar simulation cycling was also performed to simulate earth shadowing. Simulated flight performances were accomplished satisfactorily. All facility equipment functioned satisfactorily throughout the test.

14.	KEY WORDS	LINK A		LINK B		LINK C	
		ROLE	WT	ROLE	WT	ROLE	WT
	OAR-901 artificial satellites scientific satellites space environment simulation cryogenics temperature measurements solar simulators						

AFSC  
Arnold AFB Tenn.